Molecular control of acute cystitis and potential new targets of treatment

Ph.D. Thesis

Károly Nagy M.D.

Doctoral School of Clinical Medicine,
Faculty of Medicine, University of Szeged

Supervisor: Prof. Péter Tenke M.D., Ph.D., DSc

Department of Urology, Jahn Ferenc South-Pest Hospital, Budapest
Department of Microbiology, Immunology and Glycobiology, Institute of Laboratory Medicine, Lund University, Lund, Sweden

Szeged
2020

Publications directly related to the Ph.D. thesis

I. Ambite I*, Puthia M*, Nagy K*, Cafaro C, Nadeem A, Butler DSC, Rydstrom G, Filenko N, Wullt B, Miethke T, Svanborg C; Molecular Basis of Acute Cystitis Reveals Susceptibility Genes and Immunotherapeutic Targets. PLOS PATHOGENS 12:10 Paper: e1005848 , 30 p. (2016) **IF: 6.608**
*These authors contributed equally to this work.

II. Butler DSC, Ambite I, Nagy K, Cafaro C, Ahmed A, Nadeem A, Filenko N, Tran TH, Andersson KE, Wullt B, Puthia M, Svanborg C; Neuroepithelial control of mucosal inflammation in acute cystitis. SCIENTIFIC REPORTS 8 Paper: 11015, 15 p. (2018) **IF: 4.122**

Publications related to the subject of the Ph.D. thesis

Full papers

III. Magyar A, Alidjanov J, Pilatz A, Nagy K, Arthanareeswaran VKA, Poth S, Becsi A, Wagenlehner FME, Naber KG, Tenke P, Köves B; The role of the Acute Cystitis Symptom Score questionnaire for research and antimicrobial stewardship. Validation of the Hungarian version. CENTRAL EUROPEAN JOURNAL OF UROLOGY 71:1 pp. 134-141. (2018)

IV. Magyar A, Dobák A, Bálint P, Arthanareeswaran VKA, Nagy K, Póth S, Bata A, Tenke P, Köves B; Húgyúti kórokozók spektrumának és antibiotikum-rezisztenciájának változása osztályunkon 2004 és 2017 között. MAGYAR UROLÓGIA 30:3 pp. 96-104. (2018)

V. Magyar A, Köves B, Nagy K, Dobak A, Arthanareeswaran VKA, Balint P, Wagenlehner F, Tenke P; Spectrum and antibiotic resistance of uropathogens between 2004 and 2015 in a tertiary care hospital in Hungary. JOURNAL OF MEDICAL MICROBIOLOGY 66:6 pp. 788-797. (2017) **IF: 2.122**

VI. Ambite I, Nagy K, Godaly G, Puthia M, Wullt B, Svanborg C; Susceptibility to Urinary Tract Infection: Benefits and Hazards of the Antibacterial Host Response. MICROBIOLOGY SPECTRUM 4:3 Paper: UNSP UTI-0019-2014, 23 p.(2016)

VII. Godaly G, Ambite I, Puthia M, Nadeem A, Ho J, Nagy K, Huang Y, Rydstrom G, Svanborg C; Urinary Tract Infection Molecular Mechanisms and Clinical Translation. PATHOGENS 5:1 e24, 9 p. (2016)

VIII. Tenke P. Köves B, Nagy K, Hultgren SJ, Mendling W, Wullt B, Grabe M, Wagenlehner FME, Cek M, Pickard R Botto H, Naber KG, Bjerklund Johansen TE; Update on biofilm infections in the urinary tract. WORLD JOURNAL OF UROLOGY 30:1 pp. 51-57. (2012) **IF: 2.888**

IX. Tenke P, Nagy K, Köves B, Németh Z, Howell AB, Botto H; A proanthocyanidin tartalmú tőzegáfonya szerepe a visszatérő húgyúti infekciók megelőzésében. MAGYAR UROLÓGIA 22:4 pp. 178-185. (2010)

X. Tenke P, Ludwig E, Szalka A, Köves B, Nagy K; Uroszepszis - az Európai Urológus Társaság (EAU) irányelve alapján. MAGYAR UROLÓGIA 20:3 pp. 156-164. (2008)

Book Chapters

XI. Köves B, Tenke P, Nagy K; The Prevention and Treatment of Penile Prosthesis Infections. In: Nikibakhsh A - Clinical Management of Complicated Urinary Tract Infection. Rijeka, Horvátország: pp. 239-246. (2011)

XII. Tenke P, Köves B, Nagy K, Uehara S, Kumon H, Hultgren SJ, Hung C, Mendling W; Biofilm and Urogenital Infections. In: Nikibakhsh A - Clinical Management of Complicated Urinary Tract Infection. Rijeka, Horvátország: pp. 145-158. (2011)

XIII. Köves B, Tenke P, Nagy K; Infections associated with penile prostheses. In: Naber KG, Schaeffer AJ, Heyns ChF, Matsumoto T, Shoskes D, Bjerklund Johansen TE (edit.) Urogenital Infections : International Consultation on Urogenital Infections. Arnheim, Hollandia: European Association of Urology (EAU), pp. 554-561. (2010)

XIV. Tenke P, Köves B, Nagy K; Urinary catheters and draigne systems: prevention and treatment of urinary tract infections. In: Naber KG, Schaeffer AJ, Heyns ChF, Matsumoto T, Shoskes D, Bjerklund Johansen TE (edit.) Urogenital Infections : International Consultation on Urogenital Infections. Arnheim, Hollandia: European Association of Urology (EAU), pp. 532-541. (2010)

Conference abstracts

XV. Magyar A, Arthanareeswaran VKA, Soós L, Nagy K, Dobák A, Szilágyi IM, Justh N, Chandra AR, Köves B, Tenke P; Does micropattern (sharklet) on urinary catheter surface reduce urinary tract infections? Results from phase I randomized open label interventional trial. EUROPEAN UROLOGY SUPPLEMENTS 16:3 pp.146-148. (2017)

XVI. Soós L, Magyar A, Adithyaaa VK, Nagy K, Arthanareeswaran VKA, Köves B, Tenke P; Comparison of bacterial cultures from urine and catheter surface in patients with indwelling urinary catheter. EUROPEAN UROLOGY SUPPLEMENTS 16:11 e2952 (2017)

XVII. Magyar A, Alidjanov J, Naber K, Wagenlehner FME, Köves B, Pilatz A, Adithyaa VK, Nagy K, Bécsi A, Tenke P; Translation and clinical validation of the Hungarian version of the Acute Cystitis Symptom Score (ACSS) questionnaire. EUROPEAN UROLOGY SUPPLEMENTS 15:11 e1442 (2016)

XVIII. Soós L, Magyar A, Adithyaa VK, Köves B, Nagy K, Bálint P, Dobák A, Tenke P; Spectrum and susceptibility of uropathogens between 2004 and 2015 in a tertiary care hospital in Hungary. EUROPEAN UROLOGY SUPPLEMENTS 15:11 e1436 (2016)

XIX. Nagy K, Köves B, Tenke P; The effectiveness of acoustic energy induced by uroshield device in the prevention of bacteriuria and the reduction of patients' complaints related to long-term indwelling urinary catheters. EUROPEAN UROLOGY SUPPLEMENTS 10: 2 pp. 163-164. (2011)

XX. Nagy K, Szabó I, Köves B, Tenke P; Az urophatogén kórokozók spektrumának és érzékenységének követése az elmúlt hét év során osztályunkon. UROONKOLÓGIA 7:4 pp. 126-127. (2010)

XXI. Tenke P, Köves B, Nagy K; Alacsony energiájú akusztikus hullámokat kibocsátó UroShield eszköz hatékonysága a katéterviselés mellett kialakuló bakteruria megelőzésében és a panaszok csökkentésében. MAGYAR UROLÓGIA 22:3 p. 42. (2010)

XXII. Köves B, Tenke P, Balint P, Nagy K, Bode I, Hagymasi N; Spectrum and antibiotic susceptibility of uropathogens in our department between 2004 and 2007. EUROPEAN UROLOGY SUPPLEMENTS 8:4 p. 230. (2009)

Table of Contents

List of Abbreviations

ABU	Asymptomatic bacteriuria
AP1	Activator protein 1
APN	Acute pyelonephritis
ASC/PYCARD	Apoptosis-associated speck-like protein containing A CARD
AU	Arbitrary unit
BSA	Serumalbumin
CFU	Colony forming units
CREB	cAMP response element-binding protein
CXCL	CXC-chemokine ligand
CXCR	Chemokine (C-X-C motif) receptor
CY	Acute cystitis
DMEM/F12	Dulbecco's Modified Eagle Medium: Nutrient Mixture F-12
DNA	Deoxyribonucleic acid
E. coli	Escherichia coli
ELISA	Enzyme-linked immunosorbent assay
FBS	Fetal bovine serum
GAPDH	Glyceraldehyde 3-phosphate dehydrogenase
H&E	Hematoxylin and eosin
IFNs	Interferons
Ig	Immunoglobulin
IL	Interleukin
IL-1RA	IL-1b receptor antagonist
IL-1α	Interleukin 1 alpha
IL-1β	Interleukin 1 beta
IRF	Interferon regulatory factor
LB	Luria-Bertani
LPS	Lipopolysaccharide
MIQE	Minimum Information for Publication of Quantitative Real-Time PCR Experiments
MMP	Matrix metalloproteinase enzyme
MMPI	Matrix metalloproteinase enzyme inhibitor
MyD88	Myeloid differentiation primary response 88
NeuN	Neuronal nuclei
NFDM	Non-fat drymilk
NFkB	Nuclear factor kappa-light-chain-enhancer of activated B cells

NK1R	Neurokinin-1 receptor
NLRP/NALP	Nucleotide-binding oligomerization domain, Leucine rich Repeat and Pyrin domain containing
PBS	Phosphate Buffered Saline
PCR	Polymerase chain reaction
PGE2	Prostaglandin E2
Ppt-A	Preprotachykinin A
PVDF	Polyvinylidene fluoride
qRT-PCR	quantitative RT-PCR
RIPA	Radioimmunoprecipitation assay
RNA	Ribonucleic acid
RPMI	Roswell Park Memorial Institute medium
RT	Room temperature
RT-PCR	Reverse transcription polymerase chain reaction
SEM	Standard error of mean
SP	Substance P
Tacr1	Tachykinin Receptor 1
TcpC	TIR containing protein C
TICAM	TIR Domain-Containing Adapter Molecule
TIRAP	TIR Domain Containing Adaptor Protein
TLR	Toll-like receptor
TNF	Tumor necrosis factor
TRAM	Translocation Associated Membrane Protein
TRIF	TIR-domain-containing adapter-inducing interferon-β
UPEC	Uropathogenic Escherichia coli
UTI	Urinary tract infection
WT	Wild type
DDT	Dichlorodiphenyltrichloroethane
FC	Fold Ch
i. p.	intraperitonally

1 INTRODUCTION

Urinary tract infections (UTIs) are common (1), dangerous, and interesting. It is estimated that 40–50% of women and 20% of men worldwide will develop symptomatic UTI at least once in their lifetime (2-4). As a consequence, UTIs are encountered at all levels of healthcare, whether primary or tertiary. They account for a majority of specialist referrals and hospitalizations, with substantial financial implications and significant consequences to morbidity, mortality, and antibiotic consumption (5). Fortunately, new insights are now making it possible to explore immune response modifiers as alternatives to antibiotics.

1.1 Urinary tract infections

UTIs differ in clinical presentation and severity, depending on the site of infection and molecular basis of disease (6-8). In patients with acute pyelonephritis (APN), bacteria reach the renal pelvis and triggers an intense mucosal inflammatory response with progression into the renal parenchyma. Symptoms include high fever, malaise, back pain, or even life-threatening septic shock (4).

In acute cystitis (CY), infection localized to the urinary bladder and cause a rapid and potent innate immune and inflammatory response in the bladder mucosa, clinical symptoms may include urgency, frequency, and supra-pubic pain, without systemic involvement (9-12).

Recurrent UTIs (rUTIs) are recurrences of UTIs, with a frequency of at least three UTIs/year or two UTIs in the last six months. Recurrent urinary tract infections are prevalent and pose significant clinical challenges (13). Patients with asymptomatic bacteriuria (ABU) may carry more than 10^5 cfu/ml of bacteria in their urine for months or years without developing symptoms or sequels (14).

While the clinical entities of acute cystitis and pyelonephritis usually are quite distinct, the molecular determinants of this difference in clinical presentation and severity are largely unknown. The bacterial interactions with the bladder mucosa have been shown to create inflammatory cascades (7, 15, 16), which also involve adjacent cells, such as mast cells, macrophages, (17-21) and the symptom profile indicates that the nervous system is also engaged in the pathogenesis of acute cystitis (22).

1.2 Uropathogenic *Escherichia coli* and its virulence factors

Mostly, UTIs are caused by Gram-negative bacteria from the intestinal flora. *Escherichia coli (E. coli)* is the most common source of UTIs (60-80%), and more than 90-95% of acute cystitis caused by *E. coli* infection. Uropathogenic *Escherichia coli* (UPEC) strains possess an arsenal of virulence factors that contribute their ability to cause diseases, including toxins, fimbrial adhesins, flagella, autotransporter protein, and iron-acquisition systems (23). Adhesins, including P and Type1 fimbriae, facilitate tissue attack and toxins perturb diverse cellular functions (24, 25). TcpC acts by inhibiting Toll-like receptor (TLR) signaling (26). Toxins, such as hemolysin and cytotoxic necrotizing factor, enhance uroepithelial damage, permeabilize and kill host cells, thereby disrupting the mucosal barrier and opening access to underlying tissues (27). Curli and cellulose support biofilm formation (28). The UPEC strains causing acute cystitis are an intermediary group with respect to O: K: H serotype diversity and virulence gene frequencies (24, 25, 29, 30).

1.3 Host response inductions

The defense of the urinary tract relies primarily on innate immunity (31), and pathogenesis begins with the bacterial attachment to superficial bladder epithelial cells, involving specific bacterial ligands and host cell receptors. Receptor perturbations alert the host cell to the presence of the pathogen, and different signaling pathways are activated, which leads to a cascade of innate immune response effectors. The activated epithelial cells secrete cytokines

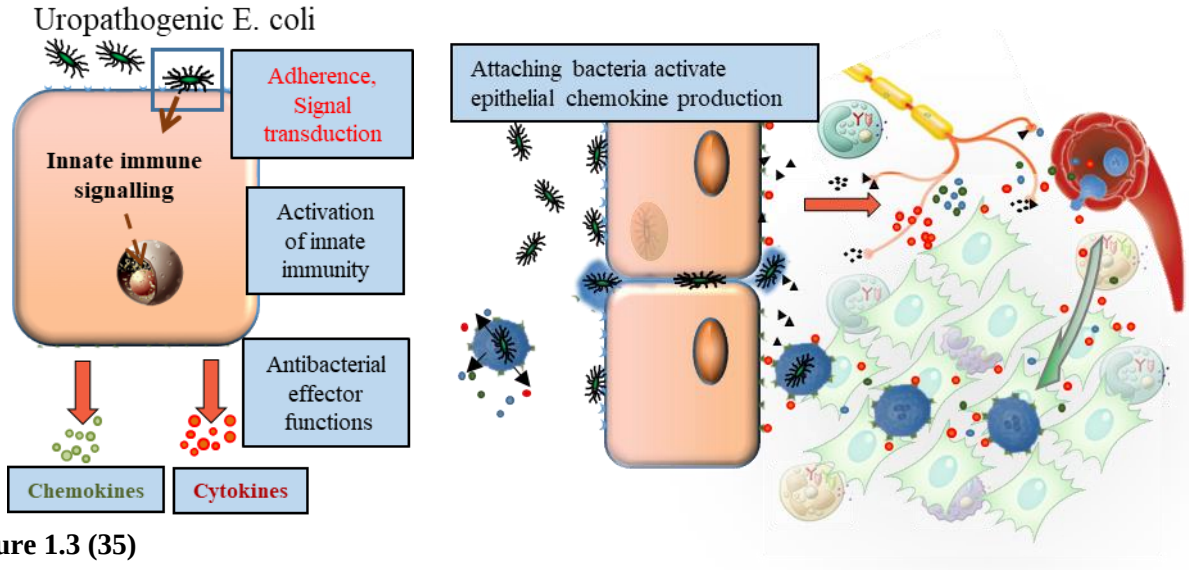

Figure 1.3 (35)

Initiation of the innate immune response by Uropathogenic E. coli.

and antimicrobial peptides (32-35) **(Figure 1.3)** . The local and systemic effects of these inflammatory mediators set the stage for defensive and damaging consequences of infection. Many of these cytokines are pleiotropic, causing a great number of different actions. Interleukin (IL)-1, tumor necrosis factor (TNF)-a, IL-6, and IL-8 are the major proinflammatory cytokines. They are the key inducers many of the symptoms, and signs accompanying the inflammatory disease and inducing events such as septic shock (36).

IL-1β is a pro-inflammatory cytokine that has been implicated in pain, inflammation and autoimmune conditions(37). Maturation and secretion of Il-1b is regulated by Inflammasomes, which are cytosolic multiprotein platforms of the innate immune system responsible for the activation of inflammatory responses(38). Inflammasomes contain NOD-like (nucleotide-binding oligomerization domain-like) receptors, such as the best-studied NLRP3, that acts as a sensor for microbial components and once activated it binds through the ASC (apoptosis-associated speck-like protein containing a CARD domain) adaptor protein. The activated ASC bind to pro-Caspase-1, causing proteolytic cleavage yielding activated Caspase- 1. The cleaved Caspase-1 can then process pro-IL-1β to its bioactive IL-1β form (39). IL-6 is a pyrogen and acute-phase response activator, and systemic levels of IL-6 have been shown to depend on disease severity and to predict the prognosis of infection. CXC-chemokine ligand (CXCL) 8 (also known as IL-8) is essential to amplify inflammation past the early phase by recruitment of neutrophils to the site of infection, ultimately, eliminating bacteria from the tissues (40). IL-6 and IL-8 found in the urine of patients with UTI (41-43). UPEC and IL-1α synergistically enhanced uroepithelial IL-6 and IL-8 response (44, 45). *In vitro* experimental infection of human uroepithelial cells with *E. coli* triggers the production of IL-6, IL-8, GRO-α, -β, -γ, ENA78, IP10, Mig, MCP1, RANTES, MIP-1α, -1β (46).

In contrast, in asymptomatic carriers, the mucosa remains relatively unresponsive despite the presence of large numbers of bacteria in the bladder lumen (47-50). Asymptomatic bacteriuria (ABU) strains are able to avoid the elimination the innate immune defense by inhibition of RNA polymerase II and host gene expression. This unresponsiveness is essential to protect the host from constant innate immune activation and to permit the symbiotic relationship between bacteria and host to develop into the commensal like and protective state of ABU (48, 51). It is therefore challenging to understand, at the molecular level, how a state of exaggerated mucosal inflammation can be generated specifically in acute cystitis patients.

1.4 Nerve cell activation and neuropeptides in bladder inflammation

The severe pain and irritative symptoms in acute cystitis indicate the direct involvement of the nervous system in the pathogenesis of bladder infection. The tachykinins, such as substance P (SP), are the most intensively studied neuropeptide families and participate in important physiological processes, including inflammation, nociception, smooth muscle contractility, epithelial secretion, and proliferation (52). SP is secreted by inflammatory (macrophages, eosinophils, lymphocytes, dendritic cells) and nerve cells, and mediate nociception and pain signaling through the stimulation of the neurokinin-1 receptor (NK1R) (53, 54). Furthermore, SP has proinflammatory effects and mediate interactions between neurons, epithelial cells, and immune cells, influences cytokine production and immune cell proliferation (55, 56). Furthermore, the nervous system senses the presence of microbes and actively involved in antimicrobial defense. As the bacterial virulence factors engage specific receptors on nerve cells, activate ion fluxes, leading to nerve cell activation (57), such interactions include recognition of Lipopolysaccharide (LPS) by Toll-like receptor-4 (TLR-4) and of Shiga toxin by glycolipid receptors (58, 59). Specific nerve cell activation products also modulate inflammation, suggesting broad relevance for many infection-induced disease states (60, 61). Interestingly, SP and their neurokinin receptors are expressed in the human urinary tract and involved in the peripheral and central regulation of urinary functions (62). Furthermore, NK1R and SP overactivation were found in patients with interstitial cystitis and experimental pelvic pain models (63-65). Some studies on bacterial toxin and sensory nerve cell activation suggest an important TLR4-independent link between LPS and transient receptor potential channel A1, as well as *E. coli* derived formyl peptides and formyl peptide receptor (63, 66). However, the involvement of nervous system and nerve specific ligands/receptors in acute cystitis has not been defined.

1.5 Genetics of UTIs

In the pathogenesis of acute pyelonephritis P fimbriated *E. coli* activate the pathogen-specific TLR4 response by ceramide release and phosphorylation of TICAM-1 (TRIF) and TICAM-2 (TRAM) adaptors (67), CREB-1, c-FOS, and c-JUN, resulting in IRF- and AP1- dependent transcription (68). MyD88, TIRAP, and NFkB are also involved in the process depends on the virulence repertoire of the infecting strain. The IRF3-dependent gene expression and mCXCR2-dependent neutrophil activation were identified in genetic studies in murine UTI model as

determinants of bacterial clearance and tissue homeostasis. Infected *Irf3*$^{-/-}$ or *mCxcr2*$^{-/-}$ mice develop severe APN and tissue damage after one week (69), and relevance for human APN susceptibility has been demonstrated through disease-associated IRF3 and CXCR1 polymorphisms in APN prone patients (40, 68, 70, 71). Genetic markers of APN susceptibility show no association to acute cystitis (32), emphasizing that major differences in pathogenesis and genetic control must exist (72). Stamey et al. demonstrated that uroepithelial cells from women with recurrent cystitis have an increased density of receptors for adhering bacteria; a concept confirmed by several groups (73-75). Bacterial persistence in intracellular communities has been studied as a reservoir of infection (76), but explanations for the symptomatology and tissue destruction in these patients have not been provided. The cause and genetics of acute cystitis susceptibility have not been determined.

2 AIMS

Our aim was to examine the molecular and genetic background of acute bladder infection and identify molecular markers and factors specific in cystitis (*in vitro*, *in vivo,* and human).

1. To evaluate IL-1β response in acute cystitis, *in vitro*. (Paper I)

2. To investigate the inflammasome function, the maturation of IL-1β, and the role of inflammasome constituents (ASC, NLRP-3) in experimential bladder infection, *in vivo*. (Paper I)

3. To address if acute cystitis strains activate a neuropeptide- and neuropeptide receptor (SP/NK1R) response in the urinary bladder (*in vivo* and *in vitro*), and investigate the mucosal- and neuronal cell interactions in acute cystitis, *in vivo*. (Paper II)

4. To assess the inhibition of IL-1 receptor, IL-1β processing and NK1R in acute bladder infection, *in vivo*. (Paper I, II)

5. To determine the human relevance of the IL-1β pathway and neuropeptides. (Paper I, II)

3 MATERIAL AND METHODS

3.1 The IL-1β response in acute cystitis, *in vitro*

In experiments addressing how a hyper-inflammatory state is generated in patients with acute cystitis, human bladder epithelial cells (HTB-9) and kidney epithelial cells (A-498) were infected with selected *E. coli* strains to cause acute cystitis (CY) or asymptomatic bacteriuria (ABU). CY and ABU strains were prospectively isolated during a prospective study of childhood UTI in Göteborg, Sweden (14). The uropathogenic strain *E. coli* CFT073 (23, 77) and the asymptomatic bacteriuria strain *E. coli* 83972 (ABU 83972) (14, 15, 78) were used for reference. Bacteria were cultured on tryptic soy agar (TSA, 16 h, 37˚C), harvested in PBS. For the *in vitro* infection, Cells were washed with phosphate-buffered saline (PBS, pH 7.2), and serum-free media were added prior to infection with appropriately diluted bacteria in PBS. To examine if the capacity to elicit an IL-1β response characterizes acute cystitis strains, epithelial cells were exposed to 10^8 colony- forming units (CFU)/ml of bacteria with gentamicin for 4 hours and secreted IL-1β was quantified in epithelial cell supernatants. In remaining experiments, cells were exposed to 10^4 or 10^5 CFU/ml for 1 hour or 4 hours without antibiotics to focus on the early response. For the appropriate dilution of bacteria please see the respective figure legend or find in the text. Immunostaining of epithelial cells was performed, and supernatants or cell lysates were collected for analysis (Immulite 1000, ELISA Western Blot) to evaluate induction and processing of IL-1β in acute bladder infection (*in vitro*). Cell viability was measured by PresoBlue assay (Invitrogen, A13262). For the experimental procedure description and the used antibodies, reagent please see section 3.6.

3.2 The inflammasome function, the maturation of IL-1β, and the role of the inflammasome constituents (ASC, NLRP-3), *in vivo*

To further address if the pathogenesis of acute cystitis involves *Il1b* and genes in the inflammasome pathway, the response to infection in C57BL/6 mice with intact inflammasome function was compared to mice lacking IL-1β (*Il1b*$^{-/-}$) (79), NLRP-3 (*Nlrp3*$^{-/-}$) (80), and ASC (*Asc*$^{-/-}$) (81). Mice under Isofluorane anesthesia were intravesically infected (10^8 CFU in 0.1 ml) through a soft polyethylene catheter (outer diameter 0.61 mm; Clay Adams). *E. coli* strains that triggered high IL-1β responses in human bladder epithelial cells, *in vitro* (CFT073, CY-17, or

CY-92) were used for infection. Bacterial strains were cultured in Luria-Bertani broth overnight. Urine samples were collected prior to and at regular times (6, 24 hours, 3 and 7 days) after infection and quantitatively cultured. Neutrophils in uncentrifuged urine were counted using a hemocytometer. IL-1β levels in urine were evaluated by ELISA or Western Blot. Animals were sacrificed at 24 hours or 7 days after infection under anesthesia; kidneys and bladders were aseptically removed, fixed with 4% paraformaldehyde or frozen for sectioning and RNA extraction. Bladder infection was evaluated by gross pathology and histopathology score. The pathology score was based on edema, hyperemia, and size, on a scale of 0–10, where 0 is unchanged compared to the uninfected controls and 10 is the most edematous, most hyperemic, and largest size. The histopathology score was assigned by two experienced researchers to each mouse. The score was based on neutrophil infiltration, tissue architecture, and epithelial thickness on a scale of 0–10, where 0 is unchanged compared to uninfected controls and 10 the highest neutrophil infiltration, most destroyed tissue architecture, and maximum epithelial thickness. Viable counts in homogenized tissues (Stomacher 80, Seward Medical) were determined on TSA (37°C, overnight). For sample sizes and the number of experiments, please see each figure legend.

To further characterize the molecular basis of bladder pathology, RNA purified from infected bladders was subjected to genome-wide transcriptomic analysis (*Asc*$^{-/-}$ and *Nlrp3*$^{-/-}$ mice with the highest pathology score after seven days, and C57BL/6 WT and *Il1b*$^{-/-}$ mice with low pathology scores, and from uninfected bladders.) Genes modified by infection were defined in comparison with uninfected tissues from mice of each genetic background (Fold Change (FC) > 1.41, and $P < 0.05$).

3.3 The neuropeptide- and neuropeptide receptor (SP/NK1R) activation in urinary bladder infection, *in vitro* and *in vivo*

To address if acute cystitis strains activate a neuropeptide- and neuropeptide receptor response in the urinary bladder mucosa, nerve cells (SH-SY5Y) and bladder epithelial cells (HTB-9) were infected with selected uropathogenic *E. coli* isolate to cause acute cystitis (CY-17). The well-characterized uropathogens CFT073 and the model ABU strain, *E. coli* 83972, were used for reference. Prior to infection, the SH-SY5Y nerve cells were differentiated by treatment with Retinoic Acid (1%) and serum starvation for 7 days and differentiation was confirmed by

staining for the neuronal markers βIII-tubulin and NeuN (**Figure 3.3**). The infection was performed as before (see 3.1). The well-studied neurokinin-1 receptor (NK1R) and its ligand Substance P (SP) expression were selected for analysis. Immunostaining of epithelial cells was performed, and supernatants or cell lysates were collected for analysis (ELISA, Western Blot,

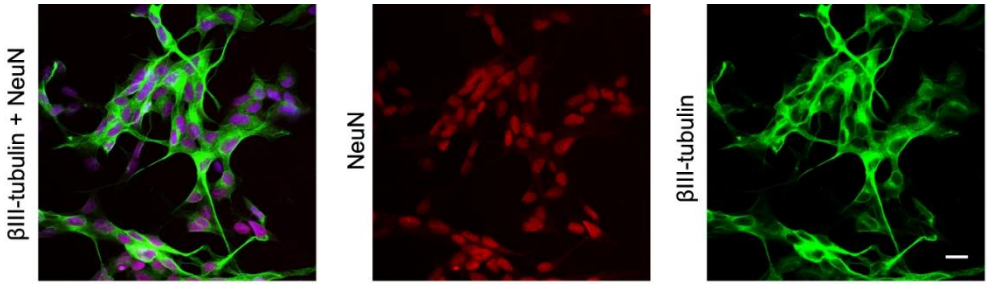

Figure 3.3
SH-SY5Y cells, differentiated using retinoic acid and serum starvation, showed characteristic morphology and staining for neuron-specific markers βIII-tubulin (green) and NeuN (red).

qRT-PCR) to evaluate the Neuro-epithelial response to *E. coli* infection, *in vitro.*

To examine the *in vivo* relevance of the neuro-epithelial activation in bladder infection, C57BL/6WT mice were intravesical infected with CY-17 (see 3.2). Urine samples for culture and immune response assessments were obtained after 6, 24 hours, 3 and 7 days. Symptoms were documented by video recording of the mice before and at defined times post-infection. Pain behavior (lack of rearing, lack of locomotion, and grooming behavior) was recorded for each mouse for 3 minutes in a clear cage at 24 hours and 7 days, modified from Rudick et al. (82). Bladder infection was evaluated at sacrifice at 24 hours or 7 days after infection. The severity of acute cystitis was quantified as the gross pathology score defined by size, edema, and hyperemia. Neuropeptide expression was evaluated by immunohistochemistry after staining with specific antibodies of frozen tissue sections, and by qRT-PCR of whole bladder RNA extracts, using primers specific for *Tacr1* and *Ppt-A.*

To address if resident nerve and epithelial cells or neutrophils and macrophages are the main source of NK1R and SP expression, tissue sections from infected C57BL/6WT- and *Nlrp3*$^{-/-}$ mice were stained for NK1R- and SP and counter-stained with neutrophil- or macrophage-specific antibodies.

3.4 The inhibition of IL-1 receptor, IL-1β processing and NK1R in acute bladder infection, *in vivo*

To address the effects of IL-1RA or NK1R inhibition *in vivo*, *Asc*$^{-/-}$ or *Nlrp3*$^{-/-}$ mice were treated with the IL-1 receptor antagonist Anakinra (IL-1RA) or the non-peptide NK1R antagonist SR140333. Anakinra (IL-1RA) were injected intraperitoneally (i.p.), 30 minutes before and daily after infection with *E. coli* CFT073 (1mg in 100 µl of PBS i.p. per mouse per day) for 7 days (**Figure 3.4. A**). SR140333 or vehicle were given intraperitoneally, one hour before infection or 30 minutes after infection with CY-17, mice were sacrificed after 24 h (**Figure 3.4. B**). The severity of acute cystitis was quantified as the gross pathology score and tissue pathology score after sacrificed.

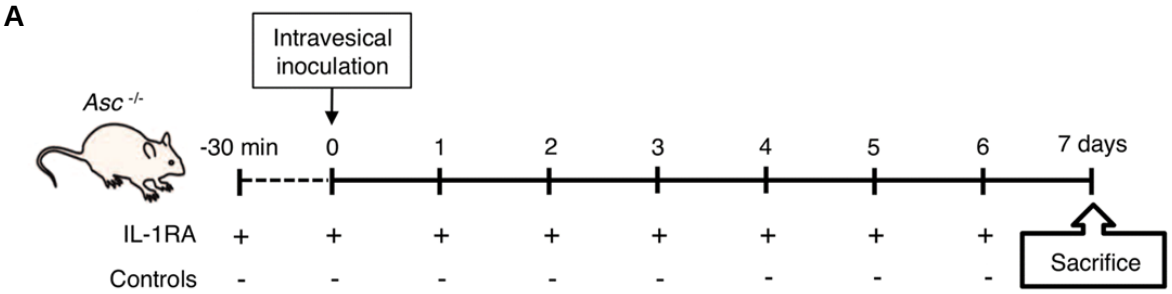

Figure 3.4 A

(**A**) *Asc*$^{-/-}$ mice were pre-treated with Anakinra (IL-1RA), 30 min before infection and daily after infection with *E. coli* CFT073 (1 mg in 100 µl of PBS i.p. per mouse) and sacrificed 7 days after infection. (*n* = 7 per treatment group, total of two experiments).

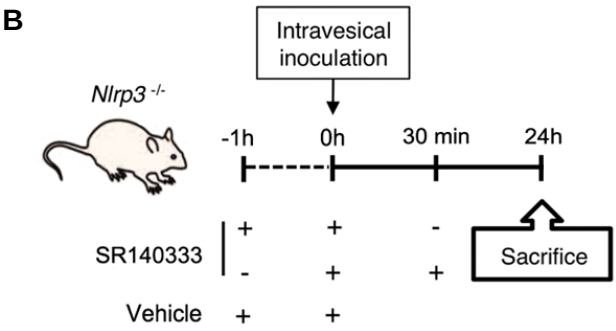

Figure 3.4 B

(**B**) *Nlrp3*$^{-/-}$ mice were either pre-treated with SR140333 or treated post-infection (1 mg/kg i.p. 30 minutes prior to, or 1 hour after infection) before being sacrificed after 24 hours. Infected, un-treated mice were used as controls (*n* = 10 mice per group, two repeats).

3.5 The human relevance of IL-1β and neuropeptides

Urine samples were collected from ambulatory patients with a diagnosis of acute cystitis and compared to samples from patients with long-term ABU. Urine IL-1β, MMP-7, and SP concentrations were quantified by ELISA.

Patients with acute cystitis were enrolled at two primary care clinics in Lund, Sweden. A diagnosis of acute cystitis was based on a urine dipstick analysis positive for bacteria and

symptoms from the lower urinary tract, including frequency, dysuria, and suprapubic pain. Midstream urine specimens were obtained at the time of diagnosis.

The control ABU samples were collected from patients with long-term ABU, who participated in a prospective placebo-controlled study. The patients with incomplete bladder emptying carried the prototype ABU strain *E. coli* 83972, following therapeutic inoculation (50). Urine samples were obtained monthly, and detailed symptom scores were registered for each sample.

3.6 Experimental procedures, Statistics, Ethics statement

3.6.1 *Escherichia coli* strains

For the characteristics of the *E. coli* strains used in the experiments, please refer to table 3.6.1.

Table 3.6.1 The *E. coli* strains for *in vivo* and *in vitro* experiments

CFT 073 (*E. coli* O6:K2:H1)	Uropathogenic *E. coli* strain isolated from the blood of a woman with acute pyelonephritis (77).
ABU 83972 (*E. coli* 83972) (*E. coli* OR:K5:H-)	The ABU *E. coli* strain 83972 was originally isolated from a girl who had carried it asymptomatically for 3 years. Strain 83972 is the prototypical asymptomatic bacteriuria (ABU) strain; patients with ABU may be infected for years (14). Strain 83972 has been extensively used for therapeutic urinary bladder colonization in patients with chronic urinary tract infections(50).
CY and ABU isolates: CY – 67 were randomly selected ABU – 62 were randomly selected	*E. coli* strains to cause acute cystitis (CY) or asymptomatic bacteriuria (ABU). CY and ABU strains were prospectively isolated during a prospective study of childhood UTI in Göteborg, Sweden (14, 83) .

3.6.2 Cell culture

For the characteristics of the cell culture used in the experiments, please refer to table 3.6.2. The HTB-9 and A-498 cells were grown to 70-80% confluency on 8-well glass chamber slides ($6x10^4$ cells/well), in 6-well plates ($6x10^5$ cells/well) or 96-well plates ($5x10^4$ cells/well) overnight in media supplemented with 10% FBS. SH-SY5Y cells were differentiated in 8-well chamber slides (2×10^4 cells/well) or 6 well plates (1.5×10^5 cells/well) using 1% Retinoic acid and serum starvation for 7 days (84).

Table 3.6.2 Cell Culture	
HTB-9 cells **5637, ATCC# HTB-9**	Human urinary bladder epithelial grade II carcinoma cells Origin: 68 years old Caucasian male https://www.lgcstandards-atcc.org/Products/All/HTB-9?
A-498 cells **ATCC# HTB-44**	Human kidney epithelial carcinoma cells Origin: 52 years old female https://www.lgcstandards-atcc.org/products/all/HTB-44.aspx?
SH-SY5Y **ATCC# CRL-2266**	Human bone marrow neuroblastoma cells Origin: 4 years old female https://www.lgcstandards-atcc.org/products/all/CRL-2266.aspx?

3.6.3 Mice for animal experiments

For the characteristics of the animals used in the experiments, please refer to table 3.6.3. Mice were bred and housed in the specific pathogen-free MIG animal facilities (Lund, Sweden) with free access to food and water. Female mice were used at 9-15 weeks of age. For the number of mice used, see respective figure legend.

Table 3.6.3 Mice for animal experiments	
C57BL/6 (B6/J)	Wild type mice
***Il1b*$^{-/-}$ (79)**	Genetic Background: C57BL/6 Carries a deletion of the *interleukin 1β* gene Purchased from the Iwakura lab, Laboratory Animal Research Center, Institute of Medical Science, University of Tokyo
***Nlrp3*$^{-/-}$ (80)**	*Genetic Background: C57BL/6* Carries a deletion of the *Nlrp3* gene Purchased from Jürg Tschopp's laboratory, Department of Biochemistry, University of Lausanne and Institute for Arthritis Research (aIAR)
***Asc*$^{-/-}$ (81)**	*Genetic Background: C57BL/6* Carries a deletion of the *Asc* gene Purchased from Jürg Tschopp's laboratory, Department of Biochemistry, University of Lausanne and Institute for Arthritis Research (aIAR)
***Mmp7*$^{-/-}$ (85)**	*Genetic Background: C57BL/6* Carries a deletion of the *Mmp7* gene Purchased from The Jackson Laboratories, USA

3.6.4 Cytokine measurements

Interleukin 1 beta (IL-1β) concentrations were determined by Immulite 1000 (Siemens, Deerfield, USA) and Human or Mouse Il-1β/IL-1F2 DuoSet ELISA kits (R&D Systems). Urine MMP-7 levels were quantified with Human total MMP-7 Immunoassay Quantikine ELISA (R&D Systems). SP in filtered supernatants was measured by Substance P parameter kit (R&D Systems). Urine SP levels were quantified by Human Substance-P ELISA kit (Abcam).

3.6.5 *In vitro* proteolysis of IL-1β by MMP-7

Recombinant human IL-1β (280 ng, H00003553-P02, Abnova) were incubated with recombinant active human MMP-7 (0.035U, #444270 Merck Millipore) in MMP reaction buffer (20 mM Tris, pH 7.6, 5 mM $CaCl_2$, 0.1 M NaCl) at 37°C until stopped with 100 mM diklór-difenil-triklóretán (DDT). Fragments were detected by Western blot using rabbit anti-IL-1 beta (1:2 000, ab9722, Abcam).

3.6.6 IL-1β activity assay

HTB-9 cells were treated with the products of the *in vitro* proteolysis of pro-IL-1β by MMP-7 at different concentrations or with pro-IL-1β or MMP-7 alone, serving as negative controls (86). Prostaglandin E2 (PGE2) concentrations were measured in filtered supernatants (Syringe Filter w/0.2 μm PES, VWR) by ELISA (R&D Systems).

3.6.7 Immunocytochemistry and Western blotting

After the *in vitro* infection, the cells were fixed and immunostaining (87) was performed. After nuclear staining (DRAQ5, Abcam), slides were mounted (Fluoromount, Sigma-Aldrich), imaged by laser-scanning confocal microscopy (LSM510 META confocal microscope, Carl Zeiss) and quantified by ImageJ 1.46r (NIH). For Western blot (88), cells were lysed and supernatants were filtered and concentrated by trichloroacetic acid precipitation, followed by acetone desiccation. Bands were quantified by ImageJ 1.46r (NIH). For the used primary and secondary antibodies please see **Table 3.6.6**.

3.6.8 Histology and immunohistochemistry

After infection animals were sacrificed at the selected time point; kidneys and bladders were aseptically removed, fixed with 4% paraformaldehyde or frozen for sectioning. Hematoxylin and eosin (H&E) or immunohistochemistry (86) were performed. For the used primary and secondary antibodies please see **Table 3.6.6.** Imaging was by fluorescence microscopy (AX60,

Olympus Optical). Richard-Allan Scientific Signature Series Hematoxylin 7211 and Eosin-Y 7111 (Thermo Scientific) were used to counterstain the tissue sections.

Table 3.6.6 Antibodies used for immunocytochemistry (ICC), Western blot (WB), Immunohistochemistry (IHC)

Antibodies	ICC	WB	IHC
Mouse anti-NK1R, sc-514453, Santa Cruz	1:50	1:100	1:50
Rabbit anti-MMP7, ab4044, Abcam	1:25	1:200	1:100
Rabbit anti-NK1R, sc-15323 , Santa Cruz	-	-	1:50
Rabbit anti-Substance P, ORB11399, Biorbyt	1:200	1:500	1:100
Mouse anti-NLRP-3, AG-20B-0014-C100, AdipoGene	1:200	1:1000	-
Rabbit anti-ASC, sc-22514, Santa Cruz	1:50	1:100	-
Rabbit anti-Il1b, ab9722, Abcam	1:100	1:2500	1:50
Mouse anti-bIII tubulin, MAB1195, R&D system	1:400	-	1:400
Rabbit anti-NeuN, mabn140, Millipore	1:200	-	-
Rat anti-neutrophil, ab2557, Abcam	-	-	1:200
Rat anti-macrophage, sc-101447, Santa cruz	-	-	1:50
Rabbit anti-*E. coli* antibody, NB200-579, Novus Biologicals	-	-	1:100
Mouse anti-b-actin, Sigma-Aldrich, A1978	-	1:4000	-
HRP-linked GAPDH, sc-25778, Santa Cruz	-	1:1000	-
Alexa488 labeled Goat anti-rabbit, A-11008, Thermo Fischer	1:400	-	1:200
Alexa488 labeled Goat anti-mouse, A-11001, Thermo Fischer	1:400	-	-
Alexa488 labeled Goat anti-rat, A-21210, Thermo Fischer	-	-	1:200
Alexa568 labeled Goat anti-rabbit, A-11011, Thermo Fischer	-	-	-
Alexa568 labeled Goat anti-mouse, A-11004, Thermo Fischer	1:400	-	1:200
Alexa568 labeled Goat anti-rat, A-11077, Thermo Fischer	-	-	1:200
HRP-linked Goat anti-rabbit , Cell signaling	-	1:4000	-
HRP-linked goat anti-mouse, Cell Signaling	-	1:4000	-

3.6.9 Global gene expression and *Quantitative* RT-PCR

Total RNA was extracted from murine bladders. After disruption in a tissue homogenizer (TissueLyser LT, Qiagen) using Precellys® Lysing kits (Bertin Technologies), with the RNeasy® Mini Kit (Qiagen), 100 ng of RNA was amplified using GeneChip 3′IVT Express Kit, 6 µg of fragmented and labeled RNA was hybridized onto Mouse Genome 430 PM array

strips and scanned using the Geneatlas system (all Affymetrix). Data were normalized using Robust Multi Average implemented in the Partek Express Software (Partek) (89, 90). Significantly altered genes were sorted by relative expression (2-way ANOVA model using Method of Moments, P values < 0.05 and absolute fold change > 1.41) (91) and analyzed by Ingenuity Pathway Analysis software (IPA, Ingenuity Systems, Qiagen) and ToppGene (92). Heat-maps were constructed by Gitools 2.1.1 software.

Quantitative RT-PCR was performed using primers pairs against *Mus Musculus Tacr1* and *Ppt-A* per the MIQE guidelines on a Rotor-Gene Q (Qiagen) (93). qRT-PCR reactions were run in technical duplicates and gene expression was analyzed based on *ΔΔ*CT comparison to *Mus Musculus Gapdh*.

3.6.10 Statistics

Unpaired t-tests and one-way ANOVA (Bonferroni for Post-Hoc analysis) were used for data determined to follow a normal distribution defined by D'agostino & Pearson normality test. Mann-Whitney U-tests, Wilcoxon signed ranked tests, and Kruskal Wallis tests (Dunn's test for Post-Hoc analysis) were used for non-parametric analyses. Welsh's t-test was used to determine statistics for kinetic responses. Significance was accepted at *P < 0.05, **P < 0.01 and ***P < 0.001. Data were examined using Prism (v. 6.02, GraphPad).

3.6.11 Ethics statement

Experimental infections were approved by the Malmö/Lund Animal Experimental Ethics Committee at the Lund District Court in Sweden (app. nr. M44-13). All animal care and protocols were governed by the European Parlement and Council Directive (2010/63 2016/63, EU), The Swedish Animal Welfare Act (Djurskyddslag 1988:534), the Swedish Animal Welfare Ordinance (Djurskyddsförordning 1988:539) and Institutional Animal Care and Use Committee (IACUC) guidelines. Experiments were reported according to the ARRIVE guidelines. The clinical studies were approved by the Human Ethics Committee at Lund University (app. nr. LU106-02, LU236-99, Dnr 298/2006; 463/2010 and Clin. Trial Reg. RTP-A2003, International Committee of Medical Journal Editors, www.clinicaltrials.gov). Patients gave their informed written consent, and all experiments were performed in accordance with the relevant guidelines and regulations.

4 RESULTS

4.1 The IL-1β response in acute cystitis, *in vitro*

4.1.1 IL-1β response to acute cystitis strains in epithelial cells

A rapid IL-1β response was detected following infection with acute cystitis (CY) strains CY-17, CY-92, and CY-132 (10^8 CFU/ml, 4 hours with gentamicin) ($P < 0.001$, compared to uninfected cells, two-tailed unpaired t-test) (**Figure 4.1.1 A**). *E. coli* CFT073 also triggered IL-1β secretion, but the response to the ABU 83972 strain was low, indicating a possible virulence-association. However, the kidney epithelial cells (A-498) did not secrete IL-1β in response to infection with the cystitis strains, indicating selectivity for a bladder infection (**Figure 4.1.1 B**).

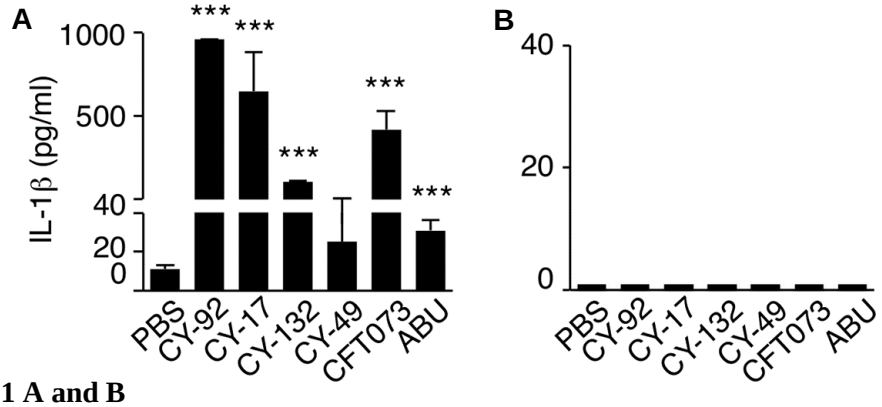

Figure 4.1.1 A and B

(**A**) IL-1β response in HTB-9 cells infected with acute cystitis strains (CY-92, CY-17, CY-132, CY-49) (4 h). CFT073 and ABU 83972 (ABU) were used as reference strains. (means± SEMs of 3 independent experiments, *** $P < 0.001$ compared to PBS, two-tailed unpaired t-test). (**B**) Lack of IL-1β secretion by infected human kidney epithelial cells (A-498), infected as in Fig. A.

4.1.2 Induction and processing of IL-1β

The IL-1β response to infection was further characterized by Western blots, using antibodies recognizing pro-IL-1β and mature IL-1β. Cells were infected with CY-17, CY-49, CY-92, and CY-132, representing high-, and intermediate IL-1β inducers, and the two reference strain (CFT073 and ABU 83972) (10^8 CFU/ml, 4 hours with gentamicin). An increase in pro-IL-1β and mature IL-1β was detected in supernatants suggesting that the acute cystitis strains activate *de novo* IL-1β synthesis and processing (**Figure 4.1.2 A**). A rapid increase in IL-1β staining intensity was observed by confocal microscopy, compared to uninfected controls. In this experiment, a clinically relevant concentration of bacteria was used (10^5 CFU/ml) and human

bladder cells were infected with each strain for 1 hour, without gentamicin (**Figure 4.1.2 B and C)**. The Western blot analysis of whole-cell extracts confirmed the increased cellular mature-IL-1β levels. Low levels of pro-IL-1β were detected at 1 hour (**Figure 4.1.2 D and E**). To address if the inflammatory cell death (pyroptosis) influences the IL-1β processing cell viability assay was performed. There was no significant reduction in cell viability after one (>= 95% viable) or 4 hours (>= 90% viable), as quantified by PrestoBlue staining and no evidence of pyroptosis after one hour, when the increase in cellular IL-1β levels was detected (**Figure 4.1.2 F and G**).

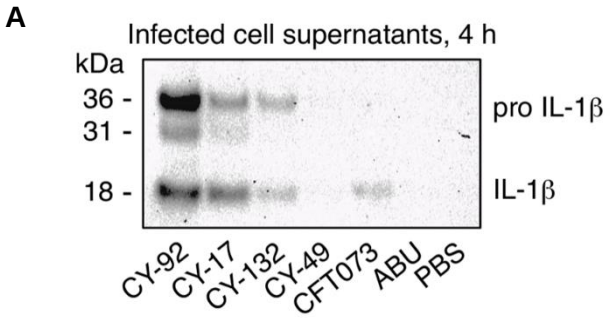

Figure 4.1.2 A
(**A**) Increased pro-IL-1β and mature IL-1β levels in HTB-9 cells infected with CY-92, CY-17 and CY-132 (Western blot analysis of cell supernatants, 4 hours, one representative experiment of several repeats).

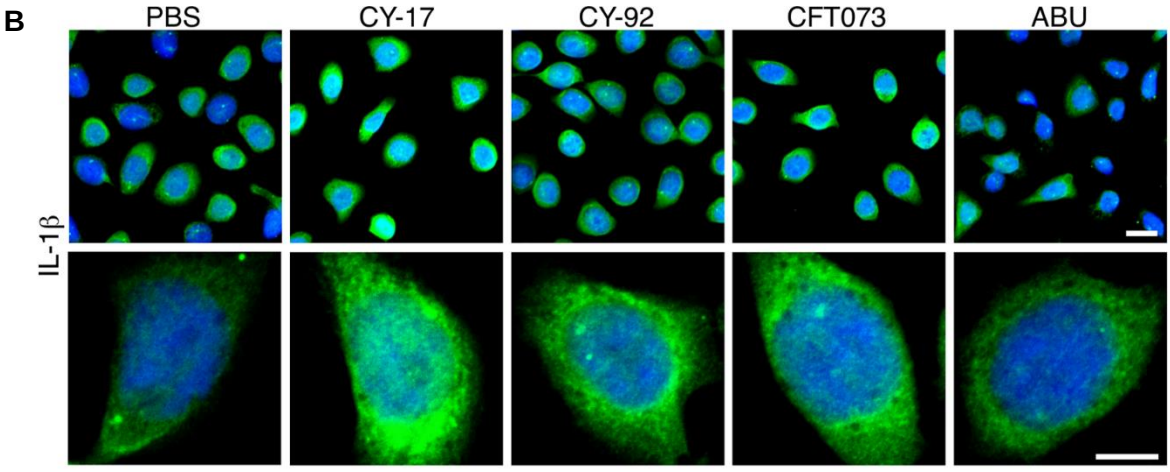

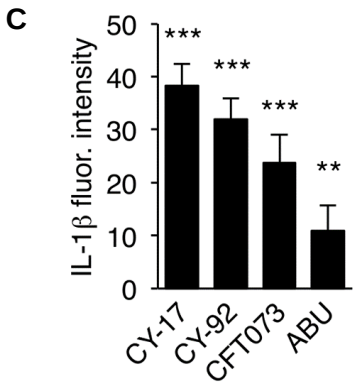

Figure 4.1.2 B and C
(**B**) IL-1β staining of HTB-9 cells infected with CY-17, CY-92, CFT073, or ABU 83972 (ABU) compared to the background in uninfected cells (PBS). Scale bars = 20 μm (upper panel) and 10 μm (lower panel). One representative experiment is shown. (**C**) Quantification of the cellular IL-1β response to infection. Increase in total fluorescence intensity (open pin-hole) after subtraction of the background staining in uninfected cells (PBS) (means ± SEMs of 50 cells per sample, ** $P < 0.01$ and *** $P < 0.001$ compared to PBS, two-tailed unpaired t-test).

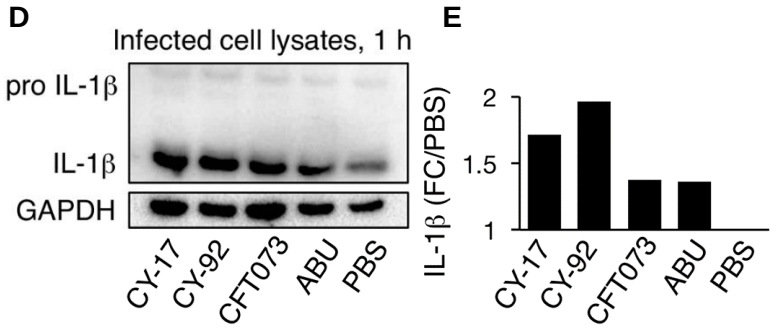

Figure 4.1.2 D and E
(**D**) IL-1β response to infection (1 hour) quantified by Western blot of whole cell extracts. (**E**) Quantification of integrated density relative to GAPDH normalized against the background of uninfected cells. One representative experiment of several repeats.

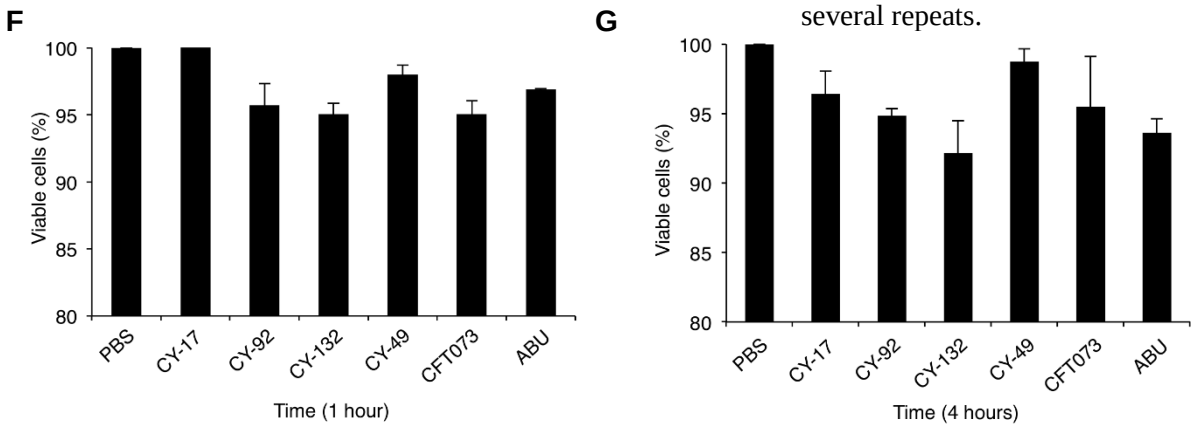

Figure 4.1.2 F and G
Cell viability was measured by PrestoBlue assay. (**F**) Cell viability was > 95% after 1 hour. (**G**) > 90% after 4 hours.

4.1.3 Epidemiologic association of IL-1β with acute cystitis

Most of the acute cystitis strains (85%) triggered an IL-1β response > 5 pg/ml (range 5 to >1000 pg/ml) (n=67, **Figure 4.1.3 A**). To further address if the IL-1β response is cystitis associated, the HTB-9 cells were infected with a collection of ABU strains from the same geographic area and background population as the CY strains (n=62, **Figure 4.1.3 B**) . Only 15% of the ABU strains triggered a high IL-1β response > 10pg/ml, compared to 64% of the CY strains ($P < 0.001$) and 61% were negative (< 5 pg/ml). The mean IL-1β response to infection was 121,8 pg/ml for the acute cystitis strains compared to 32,4 pg/ml for the ABU strains (**Figure 4.1.3 C**, $P < 0.001$). To address if the secretion of IL-1β was influenced by bacterial hemolysin , IL-1β concentrations were examined as a function of hemolytic activity in 40 CY and 38 ABU strains (**Figure 4.1.3 D**). There was no significant difference in IL-1β response between hemolysin positive and negative strains ($P = 0.07$, Mann Whitney unpaired test). The results suggest that the majority of acute cystitis strains activate an IL-1β response in human bladder epithelial cells.

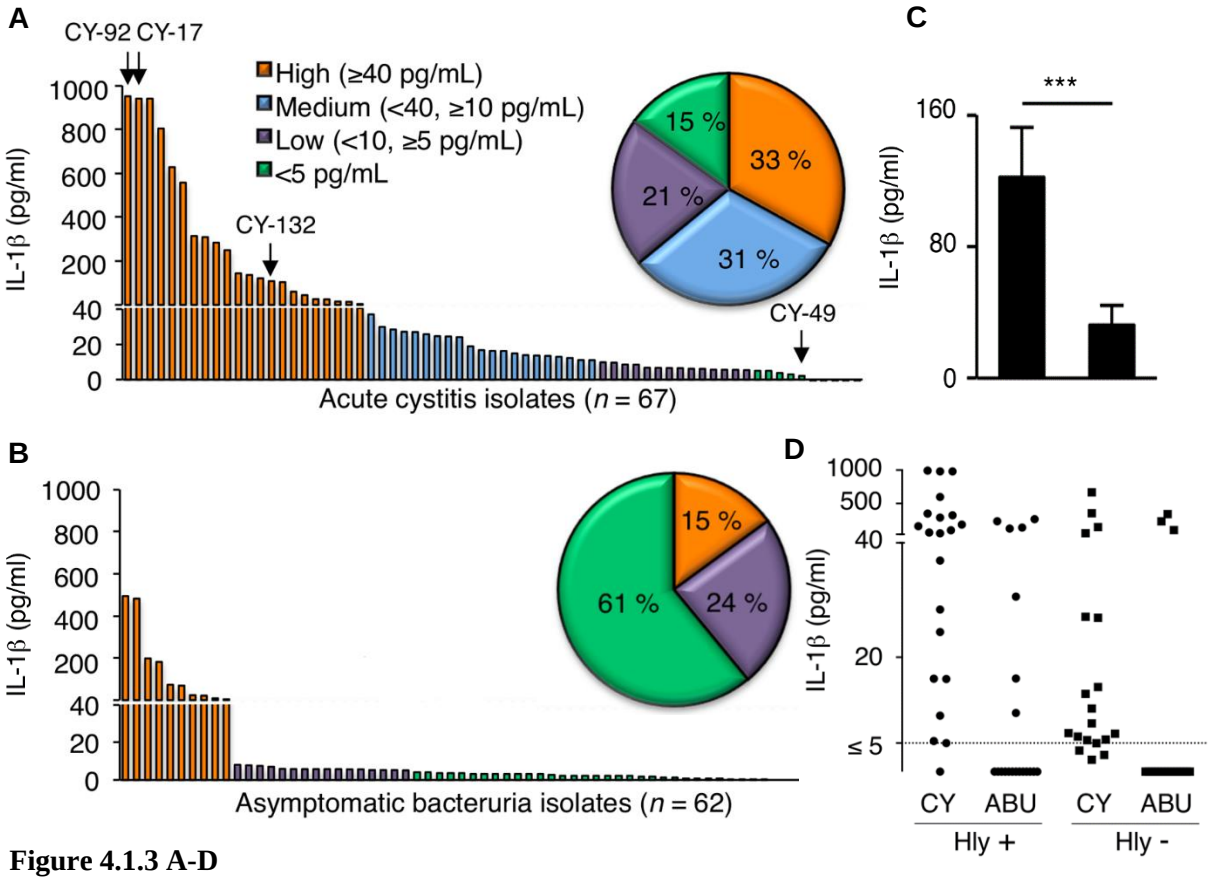

Figure 4.1.3 A-D

(**A**) IL-1β response to an epidemiologically defined collection of pediatric acute cystitis strains (n = 67) compared to (**B**) ABU strains (n = 62), obtained from children in the same geographic area. Pie chart depicting the frequency of bacterial strains activating IL-1β responses: high (orange), intermediate (blue), low (purple) or negative (green). (**C**) Histogram of the mean IL-1β response to CY versus ABU strains (means ± SEMs, *** $P < 0.001$, two-tailed Mann Whitney test). (**D**) IL-1β activation plotted against hemolytic activity in the collection of CY and ABU strains. No significant association was detected (n = 18-21, Hly+ versus Hly-, two-tailed Mann Whitney test).

4.2 The inflammasome function, the maturation of IL-1β, and the role of the inflammasome constituents (ASC, NLRP-3), *in vivo*

4.2.1 *In vivo* control of acute cystitis by *Il1b* and inflammasome genes

Major, genotype-specific differences in bladder pathology were detected 7 days after infection. Bladders from *Nlrp3*$^{-/-}$ and *Asc*$^{-/-}$ mice were severely inflamed; enlarged due to edema and hyperemia, with thickened bladder walls compared to bladders from control mice, which showed no macroscopic change. In H&E stained tissue sections, gross changes in bladder tissue structure were detected. Most bladders from *Asc*$^{-/-}$ mice showed extensive tissue destruction with edema, round cell infiltration, and hypertrophy of the bladder epithelium (10/14 mice,

71%). Similar but less extensive tissue destruction was observed in bladders from *Nlrp3*$^{-/-}$ mice (7/11 mice, 64%), (**Figure 4.2.1 A**). The mean gross bladder pathology score of infected *Asc*$^{-/-}$ and *Nlrp3*$^{-/-}$ mice was 7.9 and 7.2 (**Figure 4.2.1 B**). Bacteria and neutrophils were localized in tissue sections by immunohistochemistry, using specific antibodies (**Figure 4.2.1 C**).

In *Asc*$^{-/-}$ mice, bacterial staining was mainly epithelial, with extensive sloughing of mucosal cells into the lumen. Neutrophils accumulated in and under the epithelial barrier, forming

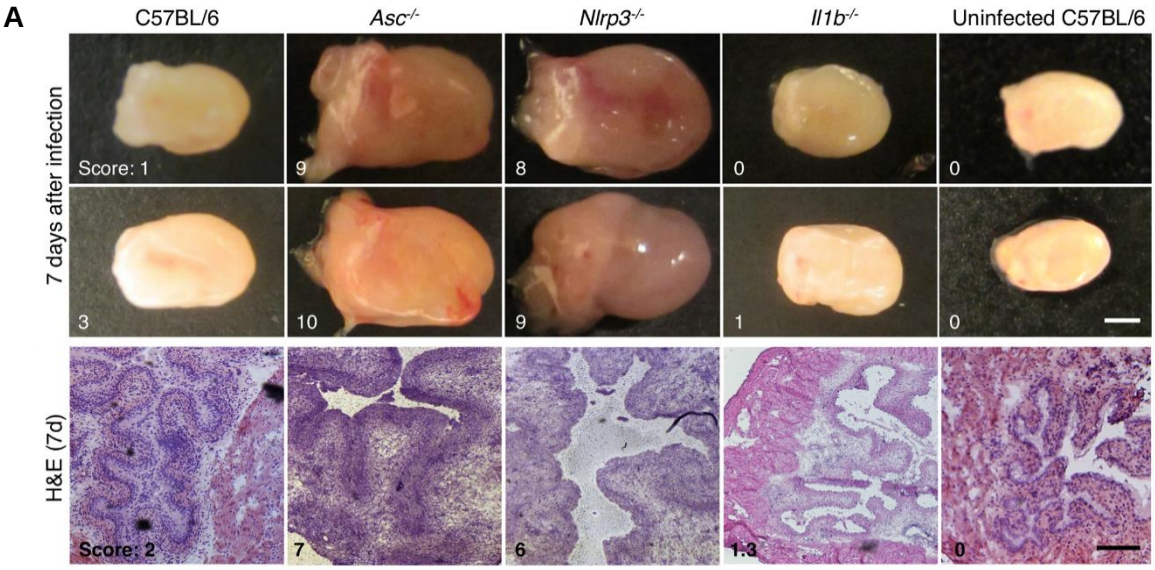

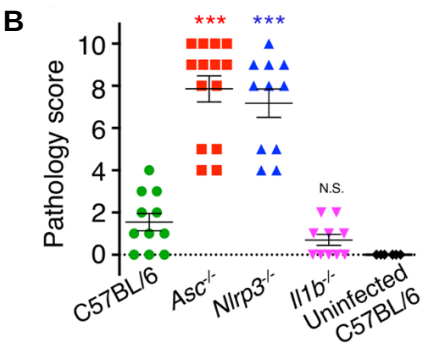

Figure 4.2.1 A and B

(**A**) Macroscopic evidence of acute cystitis in CFT073 infected mice, 7 days after infection. Scale bar = 1 mm. Two representative bladders are shown for each genotype. Bladder tissue structure in H&E-stained tissue sections. Scale bar = 200 µm. (**B**) Gross bladder pathology score in infected mice (7 days) and uninfected C57BL/6 WT controls (means ± SEMs of two experiments, *** P < 0.001, two-tailed unpaired t-test compared to WT mice). Experiments included 14 Asc$^{-/-}$, 11 *Nlrp3*$^{-/-}$, 11 C57BL/6 WT, 10 Il1b$^{-/-}$ mice.

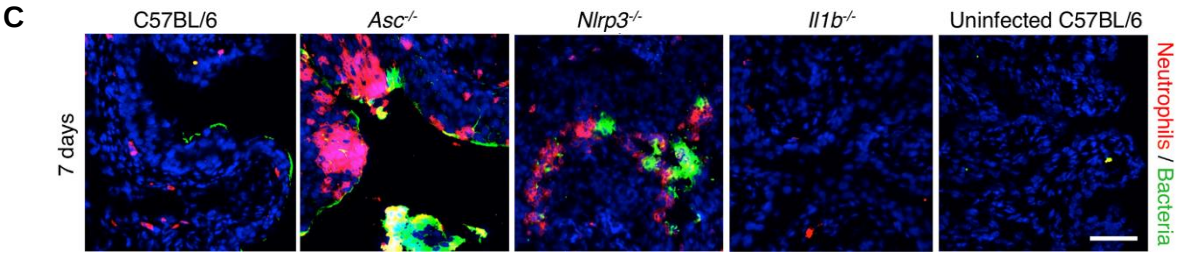

Figure 4.2.1 C

(**C**) Detection of neutrophils and bacteria in the mucosa of infected and control mice by immunohistochemistry. Scale bar = 50 µm.

aggregates or micro-abscesses all along the mucosa. In *Nlrp3*$^{-/-}$ mice, bacterial staining extended along the mucosa with less intense mucosal neutrophil accumulation than in *Asc*$^{-/-}$ mice. Neutrophils were present as individual cells or micro-abscesses (**Figure 4.2.1 C**). Pathology was accompanied by defective bacterial clearance from infected bladders. Bacterial numbers were elevated in bladders from *Nlrp3*$^{-/-}$ and *Asc*$^{-/-}$ mice compared to WT (P<0.01) or *Il1b*$^{-/-}$ mice (P < 0.001) (**Figure 4.2.1 F**). In the urine of *Asc*$^{-/-}$ mice, bacterial counts remained elevated from an initial peak after 6 hours until day 7 (**Figure 4.2.1 E**), (P < 0.001 compared to WT mice). In *Nlrp3*$^{-/-}$ mice, bacterial numbers in urine declined more rapidly, reaching similar numbers as the WT mice on day 7 (n.s.). Neutrophil counts in urine increased dramatically in *Asc*$^{-/-}$ and *Nlrp3*$^{-/-}$ mice compared to WT mice, with the highest numbers in *Asc*$^{-/-}$ mice (P < 0.001 compared to WT mice on day 7, **Figure 4.2.1 D**). In C57BL/6 wild-type (WT) mice, the bladder epithelium was clearly delineated, with little round cell infiltration, distinct sub-epithelial morphology and a small increase in size, edema, and hyperemia compared to uninfected controls (**Figure 4.2.1 A and B,** mean pathology score 1.5). The low level of macroscopic morphology was confirmed by histology, with no evidence of tissue damage **(Figure 4.2.1 A**). By immunohistochemistry, bacterial staining was weak and very few neutrophils were detected in the bladder mucosa (**Figure 4.2.1 C**). Infection was accompanied by an increase in urine neutrophil numbers (**Figure 4.2.1 D**) and bacterial numbers reached a peak after 24 hours and then declined (**Figure 4.2.1 E and F**). In contrast, *Il1b*$^{-/-}$ mice showed no macroscopic change of bladder morphology, compared to WT mice. There was no evidence of tissue pathology in bladder tissue sections (**Figure 4.2.1 A and B**, mean histopathology score 0.9, P=0.003 compared to WT mice). Remarkably, bacteria and neutrophils were not detected

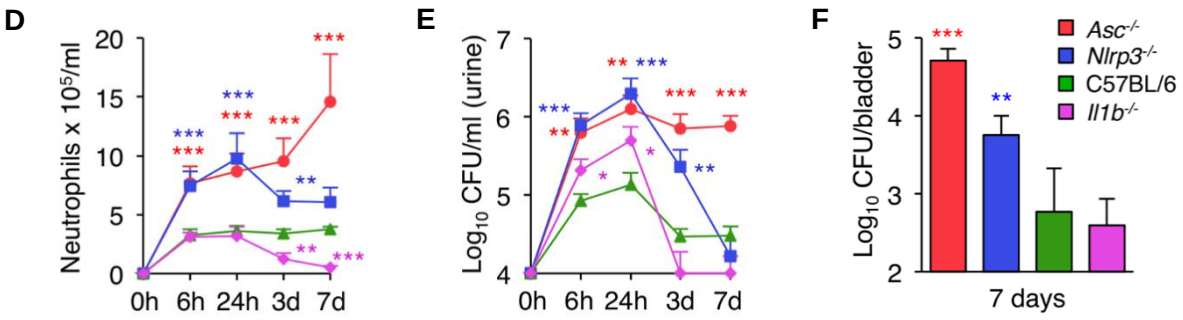

Figure 4.2.1 D-F

(**D**) Neutrophil counts in urine. (**E**) Bacterial counts in urine. (**F**) Bacterial counts in bladder tissues at 7d. (SEMs of two experiments, *** P < 0.001, ** P < 0.01, * P < 0.05, two-tailed unpaired t-test compared to WT mice).

in tissue sections, consistent with the low bacterial- and neutrophil numbers in the urine of these mice (**Figure 4.2.1 C-E**). Bacterial numbers in urine or bladder tissues did not differ between *Il1b*$^{-/-}$ mice and WT mice, and urine neutrophil numbers were lower in *Il1b*$^{-/-}$ mice on day 7 than in WT mice (**Figure 4.2.1 E and F**, n.s.). Infection was accompanied by intense mucosal IL-1β staining in bladder tissue sections in WT mice, *Asc*$^{-/-}$, and *Nlrp3*$^{-/-}$ mice after 24 hours **(Figure 4.2.1 G**). Staining was mainly epithelial and was not seen in *Il1b*$^{-/-}$ mice or uninfected WT mice. In parallel with the epithelial staining, IL-1β was detected by ELISA in the urine of infected Asc$^{-/-}$ and *Nlrp3*$^{-/-}$ mice, with lower levels in WT mice (**Figure 4.2.1 H**). By Western blot analysis, bands of approximately 36 and 18 kDa were detected (**Figure 4.2.1 I**).

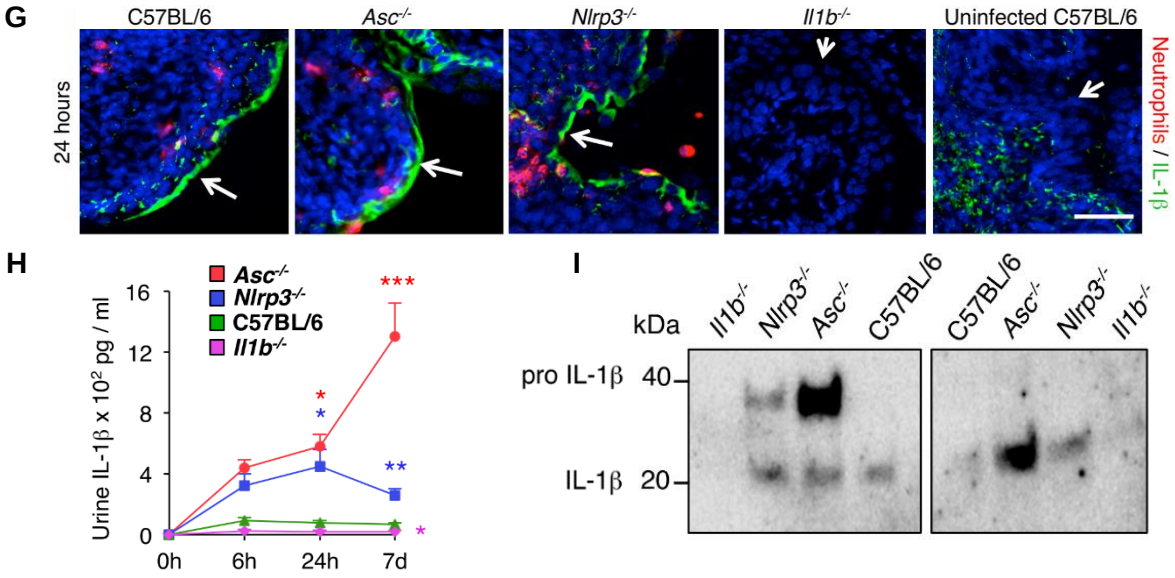

Figure 4.2.1 G-I

(**G**) Mucosal IL-1β staining in bladder tissue sections, obtained 24 hours after infection. Scale bar = 50 µm. Experiments included 4 Asc$^{-/-}$, 4 *Nlrp3*$^{-/-}$, 3 C57BL/6 WT. (**H**) Urine IL-1β concentrations, followed from 6 hours to 7 days after infection with CFT073, quantified by ELISA. (*n* = 6–7 mice per group, means ± SEMs, * $P < 0.05$, ** $P < 0.01$, *** $P < 0.001$, unpaired Mann Whitney test, compared to C57BL/6 WT mice) (**I**) Western blot of IL-1β in urine samples obtained after 7 days.

The results obtained with CFT073 were confirmed by infection of *Asc*$^{-/-}$ mice with CY-17 and CY-92 (high IL-1β responder CY strains *in vitro).* The mice developed macroscopic bladder pathology with a similar degree of enlargement, edema, hyperemia, and disruption of tissue structure as the CFT073 infected mice (**Figure 4.2.1 J-L**). In contrast, there was no disease phenotype in *Asc*$^{-/-}$ mice infected with the ABU strain (*E. coli* 83972) or in C57BL/6WTmice after 24 hours or 7 days (**Figure 4.2.1 M-N**). The results suggest that IL-1β, ASC, and NLRP-3 control the pathogenesis of acute cystitis. Remarkably, loss of NLRP-3 and ASC caused

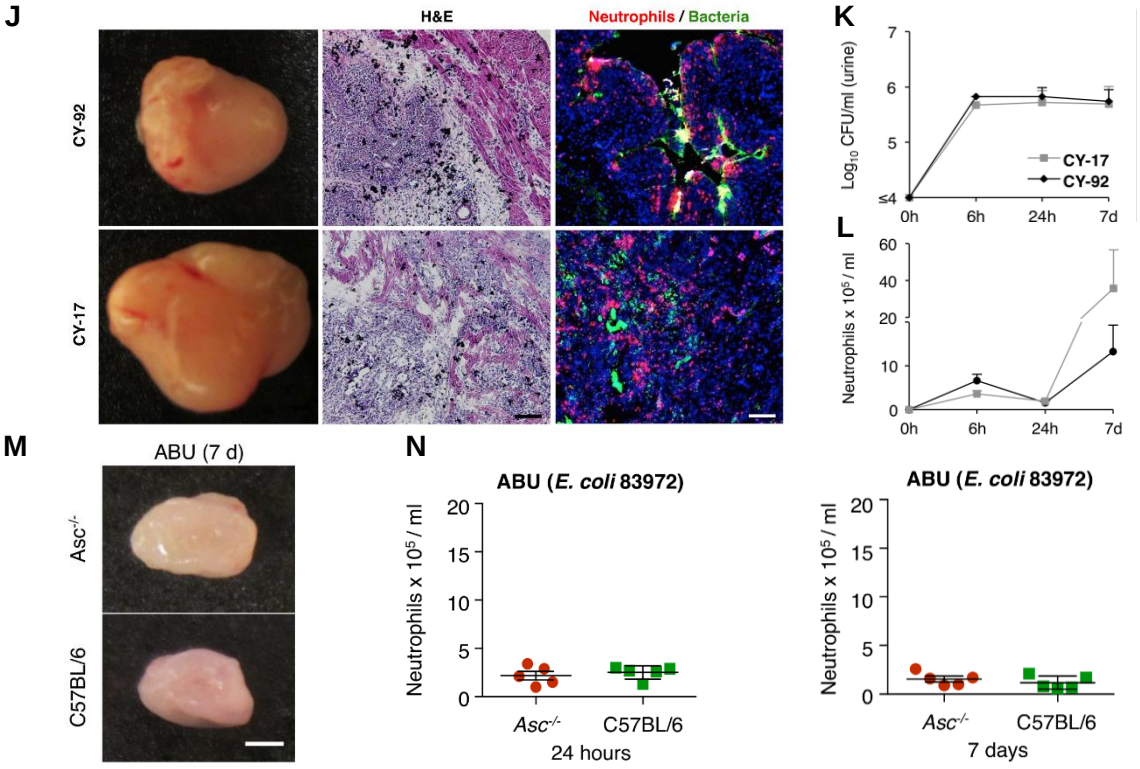

Figure 4.2.1 J-N
(**J**) Bladder pathology in *Asc*$^{-/-}$ mice infected with acute cystitis strains CY-17 or CY-92. H&E stained sections. Scale bar = 100 µm. Bacterial- and neutrophil staining detected by immunohistochemistry. Scale bar = 50 µm. (**K**) Bacterial and (**L**) neutrophil counts in urine (n = 4 mice per group, means ± SEMs). (**M**) Bladder pathology in *Asc*$^{-/-}$ or in WT mice infected with the ABU 83972, shown by gross bladder pathology and (**N**) neutrophil counts in urine after 24 hours and 7 days (n = 5 mice per group).

exaggerated pathology while the loss of IL-1β was protective, suggesting that IL-1β activation is required to initiate the host response and a functional inflammasome response is needed to avoid acute disease and pathology. These studies identify genetic determinants of host susceptibility to acute cystitis. *Asc* and *Nlrp3* were defined as key resistance determinants and IL-1β activation as a crucial step in the pathogenesis of acute cystitis.

4.2.2 Gene expression in infected bladders

About 2200 genes were altered exclusively in mice with the highest bladder pathology (heat map in **Figure 4.2.2 A**). Genes with an FC > 100 included metalloproteinase *Mmp7*, the neutrophil and monocyte chemoattractants *Cxcl6* and *Cxcl3*, the genes encoding calprotectin *S100a8* and *a9*, the *stefin* gene *Stfa1* (**Figure 4.2.2 B**). By top-scoring canonical pathway analysis, genes regulated in *Asc*$^{-/-}$ and *Nlrp3*$^{-/-}$ mice were shown to control granulocyte and

leucocyte diapedesis and signaling, acute phase responses including IL-6 and IL-1β signaling, IL-1R expression and NF-κB signaling, and dendritic cell maturation (**Figure 4.2.2 C**). These pathways were not significantly regulated in *Il1b*$^{-/-}$ and C57BL/6WT mice, suggesting a direct

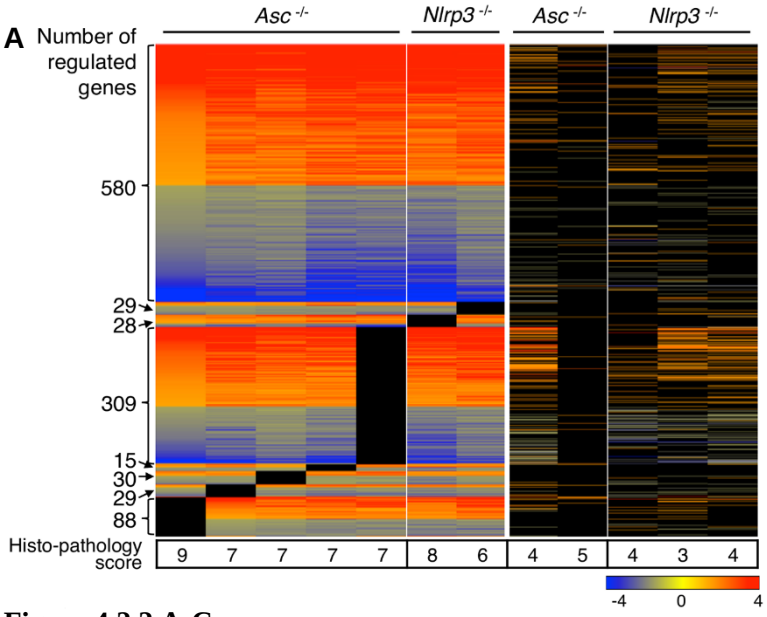

B

Top regulated genes, FC

Gene	*Asc*$^{-/-}$ #	*Nlrp3*$^{-/-}$ §
Cxcl6	**203** ±54	(**232**, **143**)
Cxcl3	**172** ±35	(**161**, **137**)
S100a8	**164** ±83	(**124**, **124**)
Mmp7	**134** ±33	(**259**, **62**)
Stfa1	**110** ±45	(**94**, **86**)
S100a9	**103** ±63	(**89**, **47**)
Ltf	**43** ±11	(**87**, **16**)
Aqp4	**39** ±13	(**56**, **25**)
Tnfrsf11b	**34** ±11	(**33**, **23**)
Fam3b	**31** ±3	(**28**, **22**)
Slc6a14	**31** ±8	(**23**, **20**)
C15orf48	**25** ±3	(**63**, **32**)
Olfm4	**25** ±8	(**32**, **3**)
Kcne3	**22** ±7	(**17**, **7**)
Gabrp	**21** ±8	(**31**, **7**)

mean±SEM of 5 mice in **A**
§ values for 2 mice in **A**

Figure 4.2.2 A-C

(**A**) Heatmap of regulated genes in *Asc*$^{-/-}$ and *Nlrp3*$^{-/-}$ mice with the highest bladder pathology score, defined by neutrophil infiltration, loss of tissue structure and epithelial thickness in H&E stained bladder tissue sections. Scale FC -4 to 4, red = upregulated, blue = downregulated. A distinct gene set distinguished the *Asc*$^{-/-}$ and *Nlrp3*$^{-/-}$ mice with a high histopathology score from WT mice or *Il1b*$^{-/-}$ mice without pathology. (**B**) Top upregulated genes in the pathology-associated gene set, compared to uninfected controls of each genotype. Means ± SEMs of 5 mice for *Asc*$^{-/-}$ mice and 2 *Nlrp3*$^{-/-}$ mice. (**C**) Top regulated pathways in mice with bladder pathology. Gene expression analysis comparing whole bladder RNA from *Asc*$^{-/-}$ and *Nlrp3*$^{-/-}$ mice with severe acute cystitis to protected *Il1b*$^{-/-}$ mice and 6 WT mice with mild bladder inflammation (Ingenuity Pathway Analysis). Bars show the -log(P-value) of the submitted gene list.

C

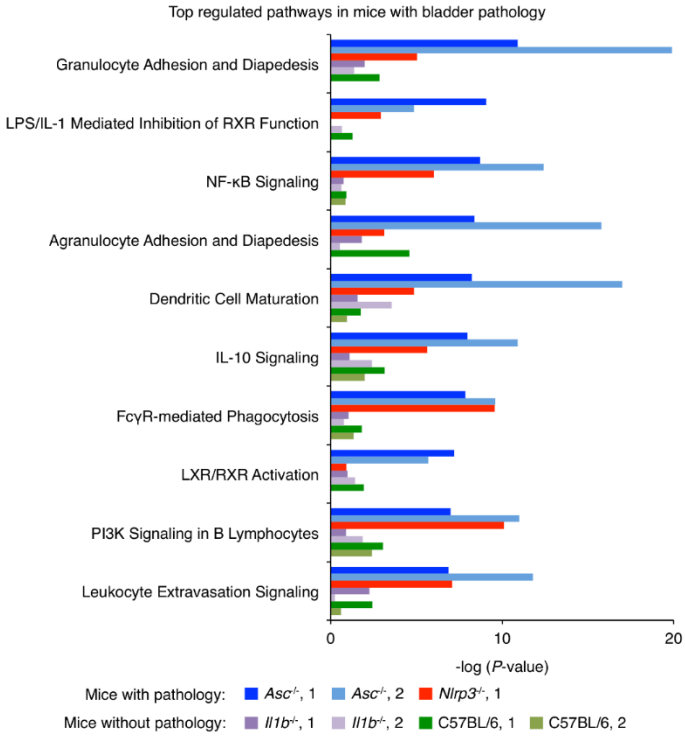

disease association. To address the role of IL-1β and the inflammasome for bladder pathology, genes encoding inflammasome complex constituents, inflammasome activators, or downstream effectors were selected for analysis (Qiagen's list of 84 key inflammasome genes). A marked difference was observed between mice with severe acute cystitis (*Asc*$^{-/-}$ *and Nlrp3*$^{-/-}$) and resistant mice (C57BL/6WT or *Il1b*$^{-/-}$) (**Figure 4.2.2 D**).

D

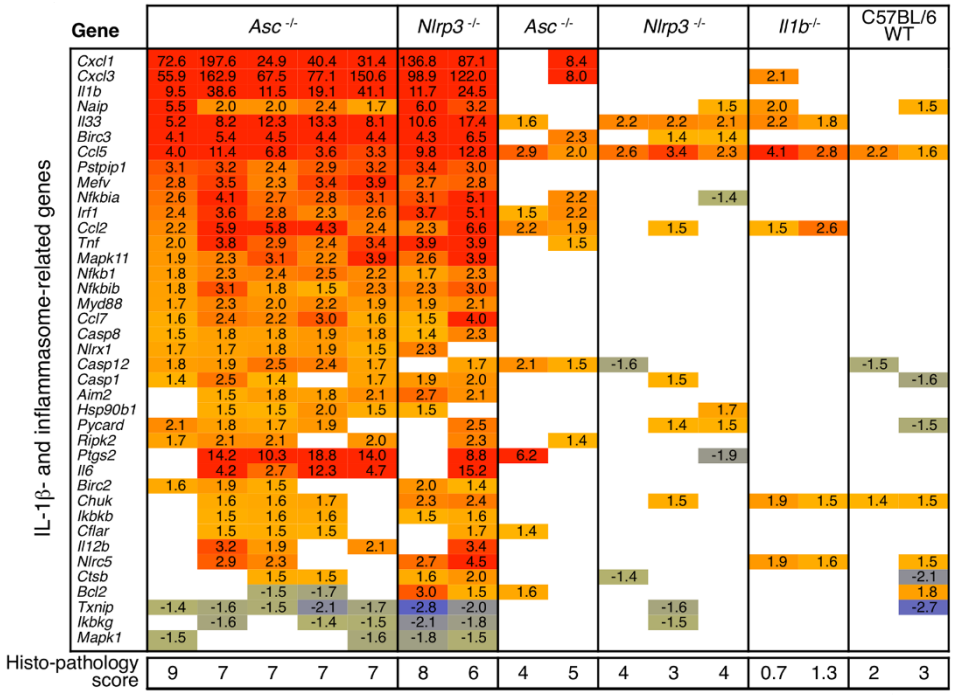

Figure 4.2.2 D

(**D**) Analysis of IL-1β, inflammasome activators and effectors in *Asc*$^{-/-}$ and *Nlrp3*$^{-/-}$ mice, detecting massive over-expression compared to *Il1b*$^{-/-}$ and WT mice. Red = upregulated, blue = suppressed. The data set included gene expression profiles from 7 *Asc*$^{-/-}$ and 5 *Nlrp3*$^{-/-}$ mice, and two each of the WT and *Il1b*$^{-/-}$ controls. Uninfected control RNA of each genotype were used to define significantly regulated genes (2 mice per genotype). Histopathology scores for individual mice showed below.

Pathology was associated with a drastic increase in overall gene expression in this family, and *Cxcl1*, *Cxcl3*, *Il1b*, and *Il33* expression were most strongly regulated (FC 5-200). *Il1a* expression was activated in *Asc*$^{-/-}$ and *Nlrp3*$^{-/-}$ mice with bladder pathology, but not among the 40 top-regulated genes (FC 1.6–8.7). *Il18*, *Casp11*, and inflammasome-related NLRP genes were not strongly regulated and a weak response was observed for genes encoding ASC (*Asc*) and Caspase-1. NF-κB constituents, *Mapk11*, *Myd88*, *Ccl -7*, *-5*, and *-2* were moderately enhanced (FC about 2). Importantly, inflammasome gene expression was virtually absent in *Il1b*$^{-/-}$ mice, further emphasizing that IL-1β is required to drive the response to a bladder infection.

4.2.3 Caspase-1 independent processing of IL-1β

The high Il-1β levels in the urine of *Asc*$^{-/-}$ and *Nlrp3*$^{-/-}$ mice with severe pathology and the presence of the mature IL-1β on WB suggest the IL-1β fragments were generated on caspase-1 independent manner. To address this question, human bladder epithelial cells were infected in presence of the Caspase-1 inhibitor, Z-VAD. Cells were preincubated with Z-VAD(OMe)- FMK (#BML-P416-0001, Enzo Life Sciences, 100 μM), 30 min before infection. CY-92 and CFT073 were selected for infection (10^5 CFU/ml for 4 hours, without gentamicin). Cell lysates and supernatants from infected cells were subjected to Western blot analysis, with antibodies specific for IL-1β. Partial inhibition of IL-1β processing was observed (about a 15-40% reduction, compared to cells without Z-VAD), suggesting that the majority of IL-1β processing in response to the acute cystitis strains is caspase-independent. This result was further supported by the presence of a mixture of pro-IL-1β, N-terminal pro-piece, and mature IL-1β in supernatants (**Figure 4.2.3 A and B).**

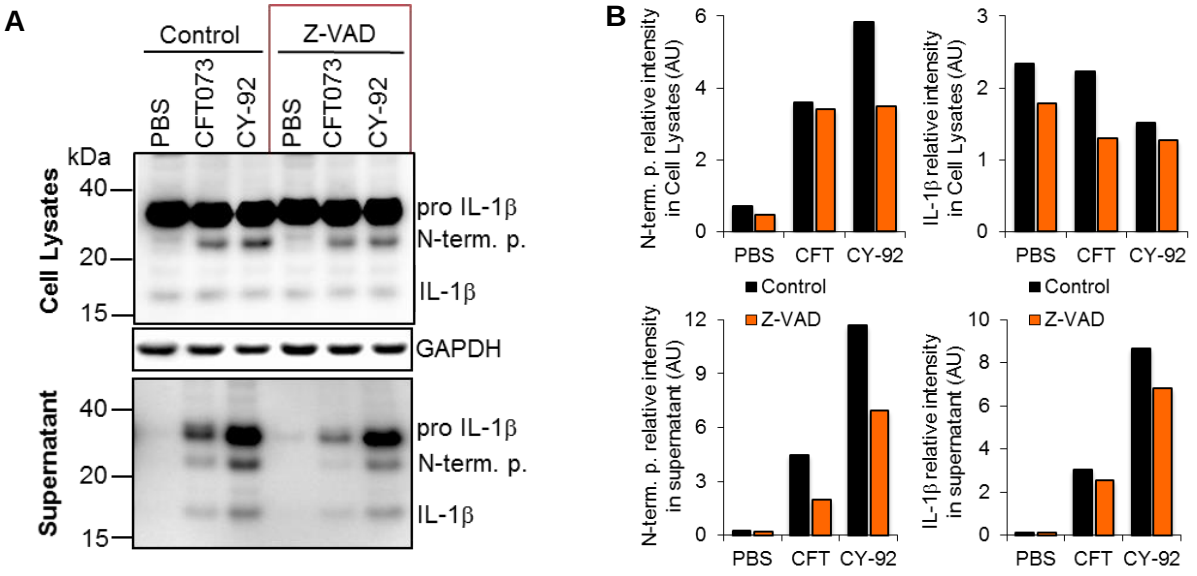

Figure 4.2.3 A and B

(**A**) Human bladder epithelial cells (HTB-9) were infected with CY-92 and CFT073 strains (10^5 CFU/ml, no gentamicin, 4 hours) in the presence of caspase-1 inhibitors (ZVAD, 100uM). Partial inhibition of IL-1β was observed by Z-VAD treatment. (**B**) The relative intensity of IL-1β in cell lysates and supernatant. (Western blot analysis of cell lysates and supernatants, one representative experiment of several repeats. AU- Arbitrary Unit)

4.2.4 Mechanism of atypical IL-1β processing

To identify caspase-independent mechanisms of IL-1β processing, genes regulated specifically in the mice that developed pathology were examined (**Figure 4.2.4 B**). *Mmp7* was identified as

the most strongly regulated gene in these mice (Asc$^{-/-}$ and *Nlrp3*$^{-/-}$), therefore MMP-7 expression was examined as a function of the histopathology score. In Asc$^{-/-}$ and *Nlrp3*$^{-/-}$mice, *Mmp7* expression showed a clear association with the overall bladder tissue pathology score and was not regulated in the *Il1b*$^{-/-}$ or C57BL/6WTmice (**Figure 4.2.4 A**). Strong epithelial MMP-7 staining was detected, by immunohistochemistry, in bladder tissue sections from Asc$^{-/-}$ and *Nlrp3*$^{-/-}$ mice with developed pathology, but not in resistant mice. Staining was exclusively epithelial and shedding of MMP-7 positive epithelial cell sheets was detected (**Figure 4.2.4 B**). Epithelial MMP-7 activation was detected 24 hours after infection and

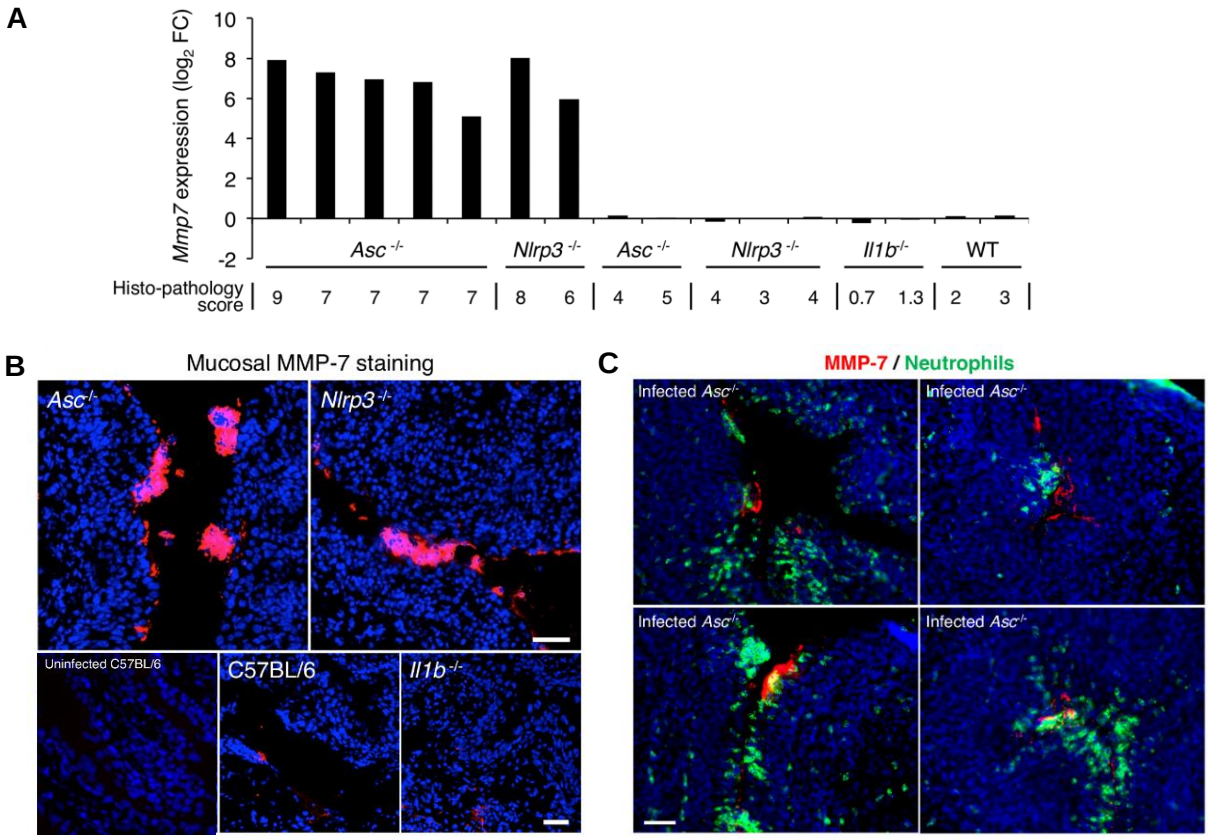

Figure 4.2.4 A-C

(**A**) Gene expression profiling identified *Mmp7* as one of the top upregulated gene in *Asc*$^{-/-}$ and *Nlrp3*$^{-/-}$ mice with bladder pathology (CFT073 infected mice, 7 days). Log_2 fold change of *Mmp7* expression levels in individual mice are shown relative to the H&E pathology score. (**B**) Strong epithelial MMP-7 staining in *Asc*$^{-/-}$ and *Nlrp3*$^{-/-}$ mice with bladder pathology. MMP-7 staining was very low in C57BL/6 WT, and *Il1b*$^{-/-}$ mice. Scale bars = 50 μm. (Infection with CFT073, 7d) (**C**) Separate MMP-7 and neutrophil staining in infected bladder tissue (24 h). Immunohistochemistry of bladder sections obtained 24 hours after infection of *Asc*$^{-/-}$ mice with CFT073. MMP-7 (red) was detected in the epithelium and recruited neutrophils (green) were present throughout with increased density towards the lumen. In most areas with recruited neutrophils, MMP-7 colocalization was not detected. Scale bar = 50 μm.

importantly, MMP-7 showed no detectable colocalization with neutrophils in the mucosa or submucosa (**Figure 4.2.4 C).** To further evaluate the involvement of MMP-7 in acute cystitis, *Mmp7*$^{-/-}$ (85) and *Asc*$^{-/-}$ mice were infected with CFT073 for 7 days. Consistent with their intact inflammasome function, *Mmp7*$^{-/-}$mice developed transient cystitis similar to C57BL/6WTmice. The bladder epithelium was clearly delineated, with little round cell infiltration, distinct sub-epithelial morphology (**Figure 4.2.4 D**). IL-1β levels in urine and IL-1β-dependent gene expression was comparable to that in WT mice, with the expression of *Ccl5*, *Nlrc5*, *Irf1*, *Ctsb*, *Birc3*, and *MyD88*. Thus, *Mmp7* did not drive pathology in mice with intact ASC or NLRP-3 function.

To address if MMP-7 degrades IL-1β, GST-tagged recombinant pro-IL-1β was incubated with the purified enzyme and proteolytic fragments were identified by Western blots using IL-1β specific antibodies. Kinetic analysis showed a time-dependent cleavage of IL-1β with a gradual reduction in full-length protein from 10 to 60 minutes. Using antibodies with a higher affinity for the mature IL-1β, a band of 18 kDa was detected corresponding in size to the recombinant, active, and mature IL-1β control. With increasing time, a band of 16 kDa was also observed **(Figure 4.2.4 E**).

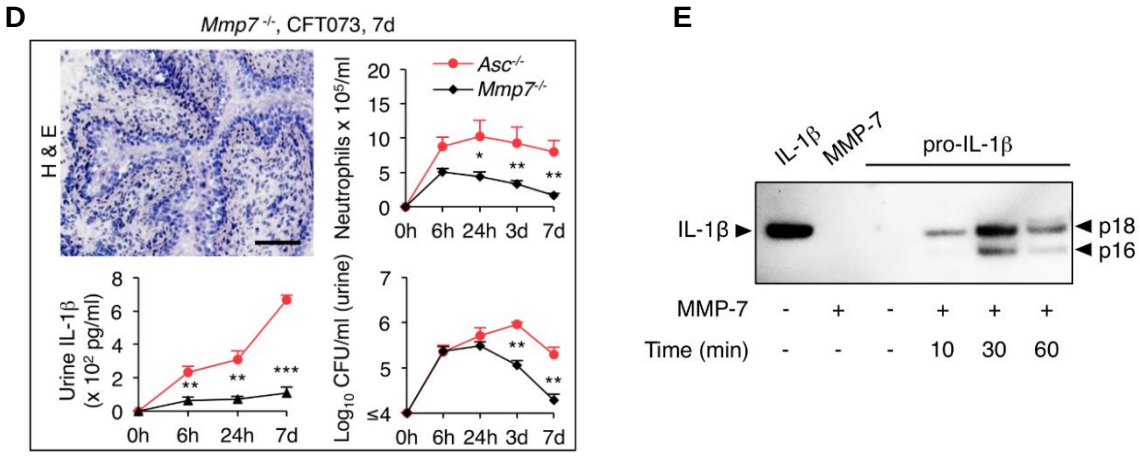

Figure 4.2.4 D and E

(**D**) Phenotype of *Mmp7*$^{-/-}$ mice, 7 days after infection with CFT073. Intact mucosal tissue structure with inflammatory cell infiltration. Low bacterial and neutrophil counts in urine compared to *Asc*$^{-/-}$ mice (n = 5 mice per group, means ± SEMs, **P < 0.01, *** P < 0.001, two-tailed unpaired t-test). Scale bar = 1 mm. IL-1β levels were elevated in the urine of *Asc*$^{-/-}$ mice but not in *Mmp7*$^{-/-}$ mice, as detected by ELISA. (**E**) Proteolytic cleavage of pro-IL-1β by MMP-7 *in vitro*, using purified enzyme and GST-tagged pro-IL-1β. The IL-1β fragments generated by proteolysis were 18 and 16 kDa, defined by Western blot using an antibody specific for the mature form of IL-1β. Recombinant mature IL-1β and GST-tagged pro-IL-1β were used as controls, as well as recombinant MMP-7.

To address if the cleaved IL-1β fragments were biologically active, reaction mixtures containing pro-IL-1β and MMP-7 were collected after 30 minutes, when the mature product was detected. Human bladder epithelial cells were stimulated with the reaction mixture for one hour, and IL-1β activity was quantified by measuring the prostaglandin E2 (PGE2) response . The cleaved products activated a dose-dependent PGE2 response. The recombinant MMP-7 and pro-IL-1β (280 and 840 ng/ml) alone had no effect (**Figure 4.2.4 F**). The results identify a new, MMP-7-dependent mechanism of pro-IL-1β processing in *Asc*$^{-/-}$ and *Nlrp3*$^{-/-}$ mice.

F

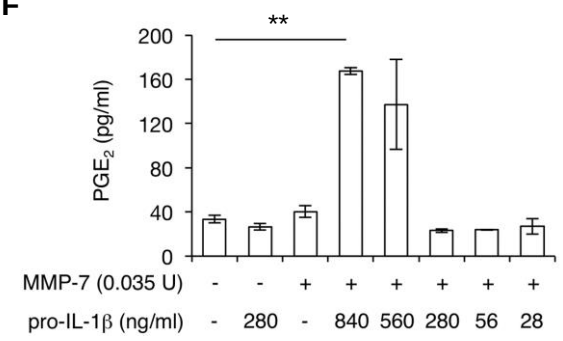

Figure 4.2.4 F
(**F**) Bioassay for IL-1β activity, measuring the PGE2 response of human bladder epithelial cells to the IL-1β fragments generated by MMP-7 proteolysis of GST-tagged pro-IL-1β. The cleaved products activated PGE2 but MMP-7 and pro-IL-1β had no effect (means ± SEMs of two experiments, ** P < 0.01, two-tailed Mann Whitney test).

4.3 The neuropeptide- and neuropeptide receptor (SP/NK1R) activation in urinary bladder infection, *in vitro* and in *vivo*

4.3.1 Neuro-epithelial response to *E. coli* infection, *in vitro*

CY-17 infection stimulated cellular NK1R and SP responses. An increase in NK1R and SP staining was observed after infection of differentiated nerve cells with the cystitis isolate (quantified by confocal imaging and western blot analysis) (**Figure 4.3.1 A-C**). Bladder epithelial cells showed a similar response to infection with CY-17 (10^4 CFU/ml, 4 hours) (**Figure 4.3.1 E-G)**. The APN strain (CFT073) actively induced SP expression in nerve cells, and NK1R/SP expression was also elevated in bladder epithelial cells ($P < 0.05$ compared to uninfected cells). In contrast, The ABU 83972 strain did not induce an SP or NK1R response (**Figure 4.3.1 A-C and E-G)**. In addition, SP levels in supernatants from infected bladder and nerve cells were measured by ELISA. CY-17 strongly stimulated the secretion of SP into the cell supernatants ($P < 0.05$), (**Figure 4.3.1 D and H**).

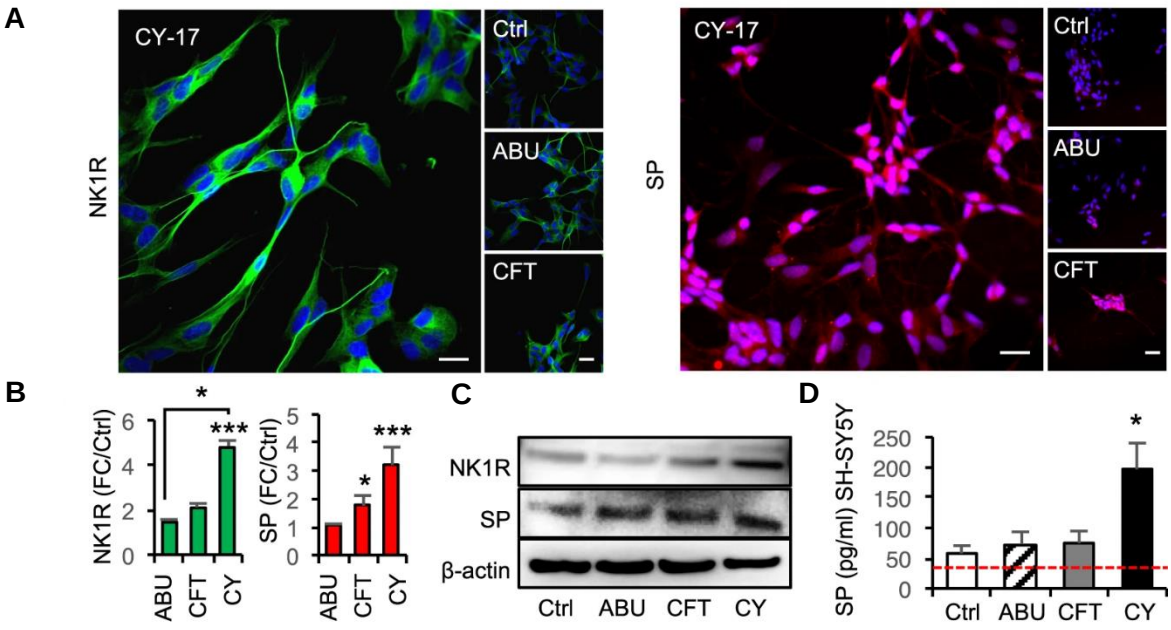

Figure 4.3.1 A-D

(**A**) Increase in NK1R (green) and SP (red) staining after infection of nerve cells with CY-17, CFT073, or ABU 83972 (10^4 CFU/ml, 4 h). (**B**) Quantification of fluorescence intensities in Fig. B, FC compared to uninfected cells ($n = 50$ cells, 4 repeats). (**C**) Western blot confirming of NK1R and SP protein levels in infected nerve cells (4 repeats). (**D**) Quantification of SP in supernatants from infected nerve cells compared to uninfected cells by ELISA ($n = 7$ samples, 2 repeats).

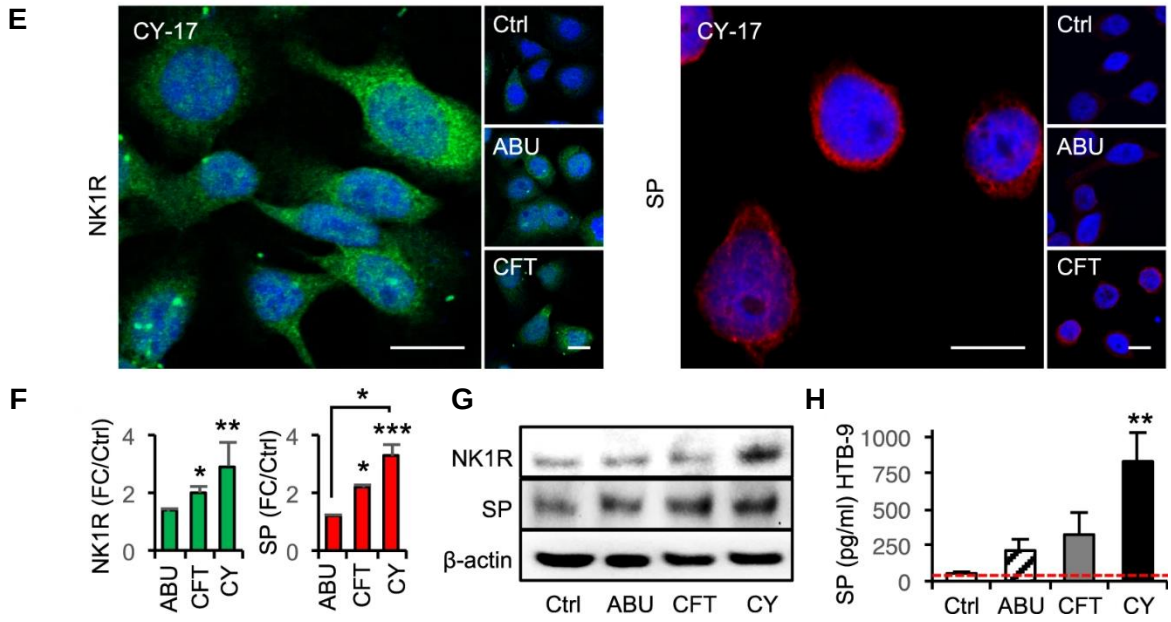

Figure 4.3.1 E-H

(**E**) Increase in NK1R (green) and SP (red) staining in bladder cells infected with CY-17, CFT073, or ABU 83972. (**F**) Quantification of fluorescence intensities in Fig. E, FC compared to uninfected cells, ($n = 50$ cells, 4 repeats). (**G**) Western blots of NK1R and SP protein levels in infected bladder cells (4 repeats). (**H**) Quantification of SP in supernatants from infected bladder cells compared to uninfected cells by ELISA, ($n = 6$, 2 repeats). **Fig. 4.3.1 A-H**: The data is presented as means + SEMs and analysed using Kruskal Wallis test, Dunn's correction. Scale bars = 20 μm. *$P < 0.05$, **$P < 0.01$, ***$P < 0.001$. Red line represents the detection limit of the ELISA.

4.3.2 Neuro-epithelial response to a bladder infection, *in vivo*

In infected mice, bladder pathology was observed with edema and hyperemia after 24 hours and at seven days (compared to uninfected, P < 0.05, both time points **Figure 4.3.2 A and B**). Urine neutrophil counts increased after 6 hours and remained elevated until day 7 (4-6×10^5 cells/ ml). Bacterial counts in urine showed similar kinetics and plateaued at 10^5 CFU/ml at 24h (P < 0.001, **Figure 4.3.2 C and D).** NK1R and SP staining intensity were

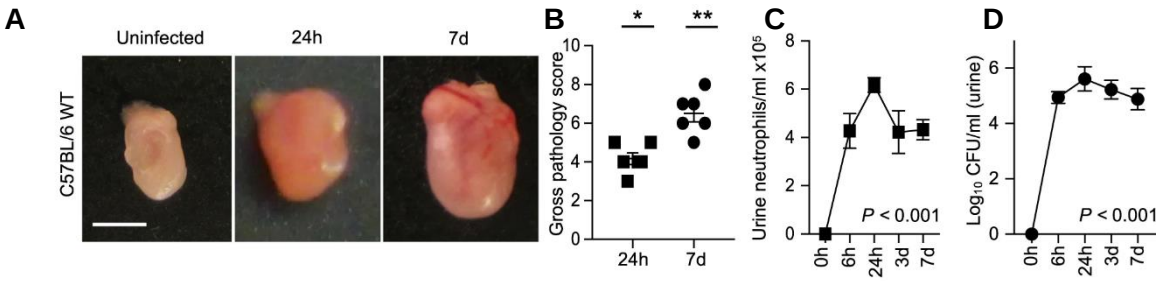

Figure 4.3.2 A-D

(**A**) Evidence of acute cystitis in C57BL/6WT mice infected with CY-17, defined by macroscopic inspection (Scale bar = 1 mm). (**B**) Gross pathology score of bladders from infected C57BL/6WT mice compared to uninfected controls. (**C**) Kinetics of the neutrophil response and (**D**) bacterial persistence, quantified in urine samples obtained 6 hours and 24 hours, 3 days and 7 days post infection. Data is represented as means ± SEMs from $n = 4–6$ mice per group, (two repeats) and analysed by Mann-Whitney U-test. $*P < 0.05$ $**P < 0.01$, $***P < 0.001$.

increased after infection with CY-17 (P = 0.004 and P = 0.02 compared to uninfected controls, **Figure 4.3.2 E and F**). NK1R was clearly visible in infected bladders, with a distinct staining pattern of the mucosal nerve plexus in the lamina propria. The colocalization of nerve cells with NK1R was confirmed by βIII tubulin immunostaining of tissues. SP was mainly observed in the epithelial layer of infected bladders. Colocalization with βIII tubulin was more restricted than for NK1R and only detected along the epithelial-nerve cell interface (**Figure 4.3.2 H and I**). The increase in NK1R and SP expression was confirmed by qRT-PCR of total bladder RNA (**Figure 4.3.2 G**). *Tacr1* and *Ppt-A* mRNA levels were increased, compared to uninfected mice (P = 0.02 and P = 0.008 for *Tacr1* and *Ppt-A*, respectively). Urine SP levels were elevated after 24 hours and 7 days in infected C57BL/6WT mice compared to uninfected controls (128 pg/ml and 217 pg/ml, respectively, compared to 43 pg/ml, P < 0.05, **Figure 4.3.2 J**).

A significant change in behavior was detected and quantified as a decrease in rearing and locomotion and an increase in grooming behavior (P < 0.05 for each of the three variables compared to uninfected controls, **Figure 4.3.2 J**). The results suggest that acute cystitis in

C57BL/6WT mice is accompanied by a mucosal neuropeptide response and symptoms from the site of infection.

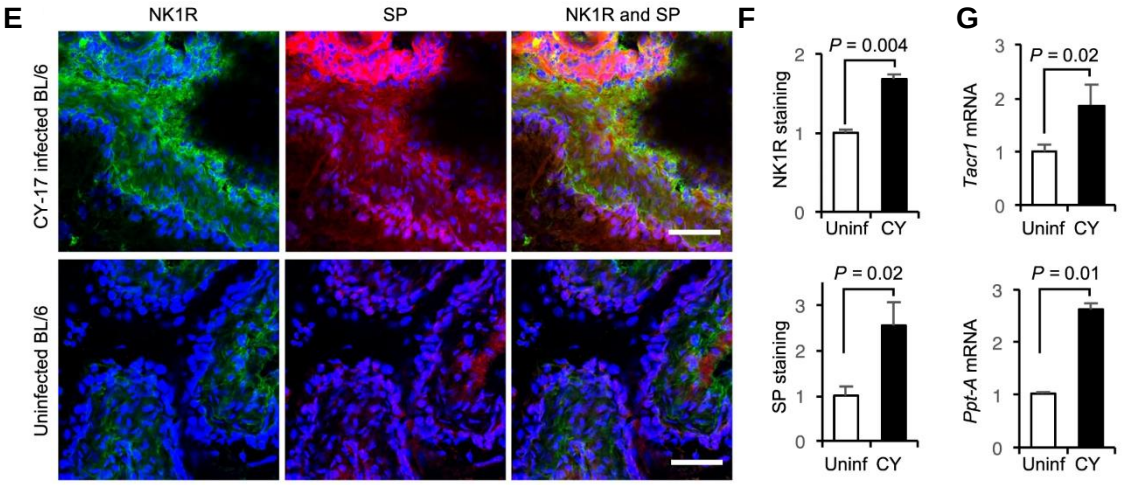

Figure 4.3.2 E-G

(**E**) NK1R and SP staining, quantified by immunohistochemistry of bladder sections. Mice were infected with CY-17 for 7 days. SP staining (red) was increased in the epithelium and NK1R (green) in the subepithelial compartment, compared to uninfected controls. (**F**) Quantification of NK1R and SP staining in Fig. E. (**G**) Increased expression of *Tacr1* and *Ppt-A* in bladders infected with CY-17 for 7 days, quantified by qRT-PCR.

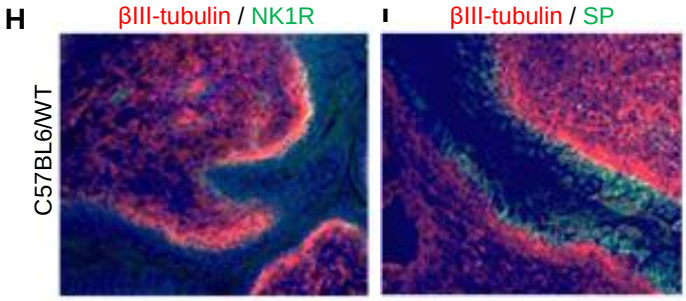

Figure 4.3.2 H and I

Tissue sections from C57BL/6 WT mice (n = 4 mice per group) were infected with CY-17 for 7 days and stained for NK1R or SP. The neutrophil marker were used. **(H)** Colocalization of NK1R (green) with βIII tubulin (red). (**I**) Colocalization of SP (green) with βIII tubulin (red).

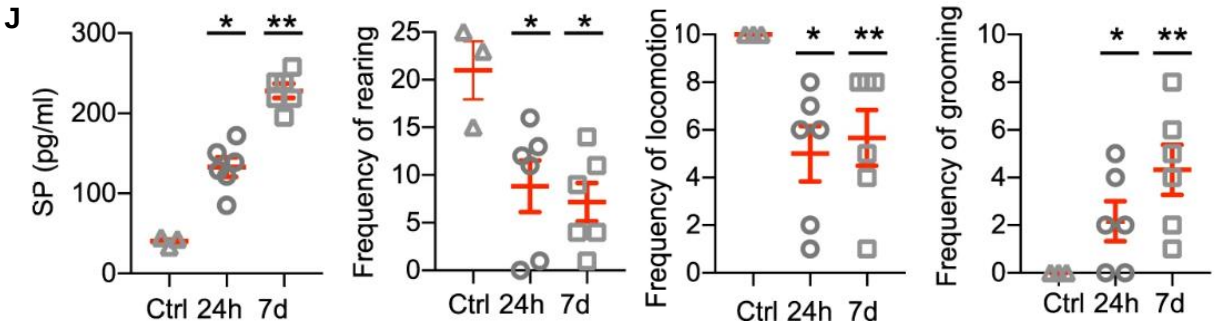

Figure 4.3.2 J

(**J**) Urine concentration of SP detected by ELISA and pain assessed in C57BL/6WT mice after 24 hours and 7 days of CY-17 infection. Mice behavior was recorded and scored according to locomotion, frequency of rearing and frequency of grooming compared to uninfected controls. Data is represented as means ± SEMs, analysed by Mann-Whitney U-test. *$P < 0.05$ **$P < 0.01$, ***$P < 0.001$.

4.3.3 Contributions of neutrophils and macrophages

Despite the massive neutrophil influx in the severely inflamed bladder, only minor evidence of colocalization was observed with NK1R and SP. The scattered resident macrophages in the infected bladder tissues didn't show colocalization with NK1R or SP (**Figure 4.3.3 A-D**). The results suggest that the resident nerve and epithelial cells are the main sources of NK1R and SP in the inflamed bladder mucosa.

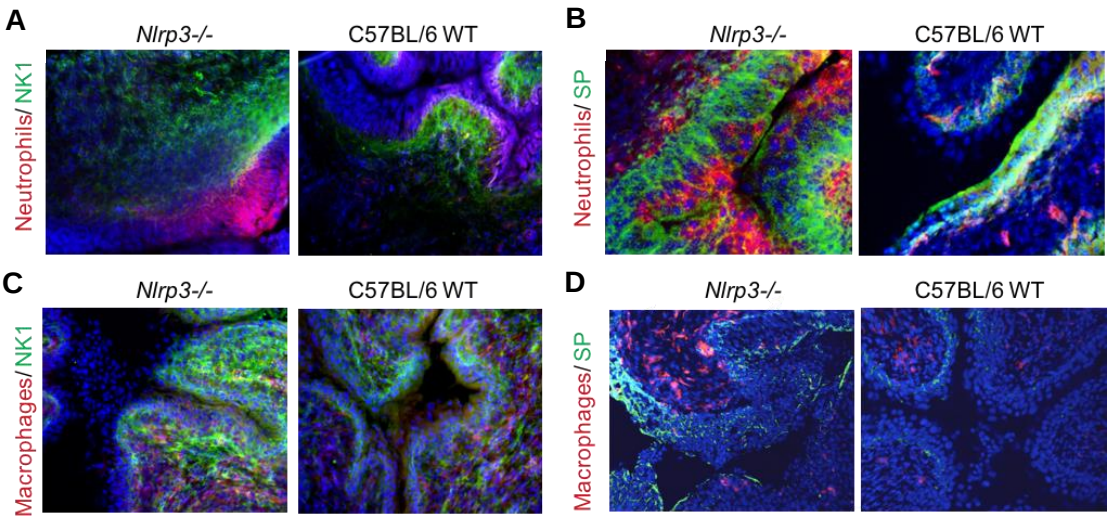

Figure 4.3.3 A-D
Tissue sections from *Nlrp3*$^{-/-}$ and C57BL/6 WT mice (n = 4 mice per group). Infected with CY-17 for 7 days and stained for NK1R or SP. The neutrophil marker LY6G or the macrophage marker RM0029-11H3, were used. (**A**) No colocalization of NK1R (green) with Neutrophils (red). (**B**) No colocalization of SP (green) with Neutrophils (red). (**C**) No colocalization of NK1R (green) with macrophages (red). (**D**) No colocalization of SP (green) with macrophages (red).

4.4 The inhibition of IL-1 receptor, IL-1β processing and NK1R in acute bladder infection, *in vivo*

4.4.1 Efficacy of the IL-1β receptor antagonist and MMP-7 inhibitor

The IL-1β receptor antagonist Anakinra (IL-1RA) treatment abrogated the macroscopic pathology, virtually removing bladder enlargement, edema, and hyperemia, resulting in a significantly lower pathology score ($P < 0.001$) compared to untreated *Asc*$^{-/-}$ mice (**Figure 4.4.1 A and B**). A marked reduction in pathology was also observed in bladder tissue sections (**Figure 4.4.1 C**). Tissue damage was not found and inflammatory cell infiltration was markedly reduced. Consistent with this reduction in inflammation, urine neutrophil numbers were low (**Figure 4.4.1 D**). As a control for unspecific effects of Anakinra on the bacteria, CFT073 was

grown in Luria-Bertani with or without 500 ng/ml of IL-1RA for 10 hours. No difference in bacterial growth rate was detected.

To further address the contribution of MMP-7, *Asc*$^{-/-}$ mice were also treated with an MMP inhibitor (Batimastat), 30 minutes before and daily (except day 4) after infection with *E. coli* CFT073 (0.5 mg in 100 µL of PBS i.p). At sacrifice (day 7), a dramatic difference in gross

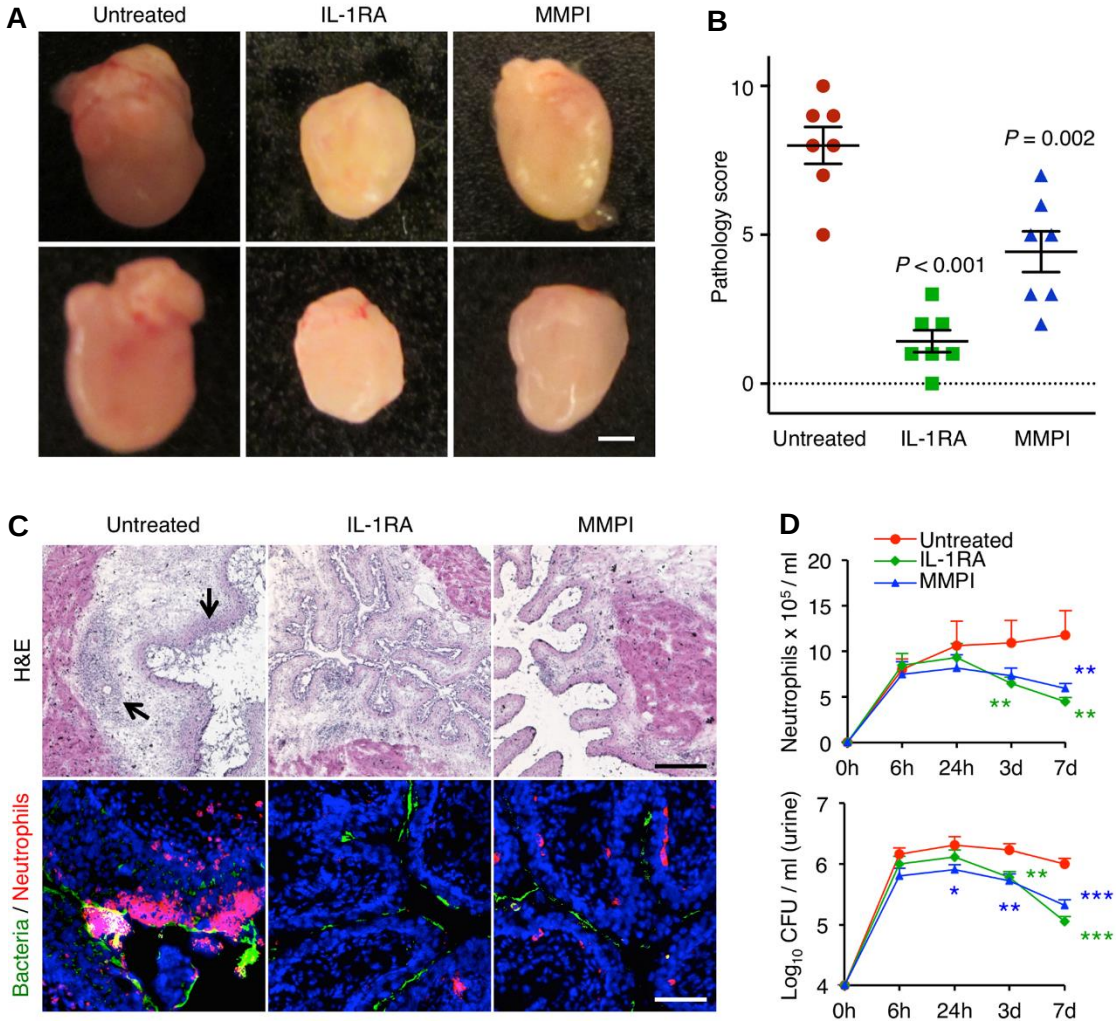

Figure 4.4.1 A-D

(**A**) Difference in gross bladder pathology between untreated controls and IL-1RA or MMPI treated mice. Scale bar = 1 mm. (**B**) Pathology scores from individual mice are shown. (P < 0.001, for IL-1RA compared to untreated *Asc*$^{-/-}$ mice and P = 0.002, for MMPI compared to untreated *Asc*$^{-/-}$ mice, means ± SEMs of two experiments, two-tailed Mann Whitney test). (**C**) Protection from bladder tissue pathology shown in H&E stained sections from treated versus control mice. Arrows indicate mucosal sloughing, edema and subepithelial abscesses in untreated mice. Scale bar = 200 µm (H&E) and 50 µm (immunofluorescence). (**D**) Kinetics of neutrophil recruitment and bacterial clearance in the urine of IL-1RA or MMPI treated *Asc*$^{-/-}$ mice, compared to untreated mice. (n = 7 mice per group, means ± SEMs, * P < 0.05, ** P < 0.01, *** P < 0.001, two-tailed unpaired t-test).

pathology was observed (**Figure 4.4.1 A**). Treatment reduced the enlargement, edema, and hyperemia, and a marked reduction in pathology was observed (P=0.002, **Figure 4.4.1 B**). The dramatic aggregation of neutrophils and bacteria in the mucosa of untreated *Asc*$^{-/-}$ mice was prevented in the treated mice and mucosal integrity was maintained (**Figure 4.4.1 C**). As in the IL-1RA-treated mice, bacterial numbers remained elevated (**Figure 4.4.1 D**). Batimastat (250 ng/ml) did not affect bacterial growth *in vitro* for up to 10 hours. The results demonstrate that IL-1β and MMP-7 are essential for the development of pathology in *Asc*$^{-/-}$ mice and confirmed the excessive IL-1β production in pathological bladders.

4.4.2 Effects of NK1R inhibition on mucosal inflammation

The SR140333 treatment abrogated the macroscopic pathology, removing edema and hyperemia, resulting in a significantly lower pathology ($P < 0.05$ for pre-and post-infection treatment), and tissue pathology score ($P = 0.005$ and $P = 0.03$ for pre-and post-infection treatment) **(Figure 4.4.2 A and B**). The urine neutrophil recruitment also was decreased ($P = 0.02$ and $P = 0.002$ for pre-and post-infection treatment). No significant change was observed in bacterial counts in urine ($P = 0.02$, **Figure 4.4.2 C**). SR140333 treatment inhibited NK1R staining in infected bladders and the reduction in NK1R expression was confirmed by qRT-PCR **(Figure 4.4.2 D and E**). The results identify NK1R as a potential therapeutic target in acute cystitis.

Figure 4.4.2 A
(**A**) Protective effect of SR140333 treatment, shown by macroscopic inspection of infected bladders. Scale bar = 1 mm.

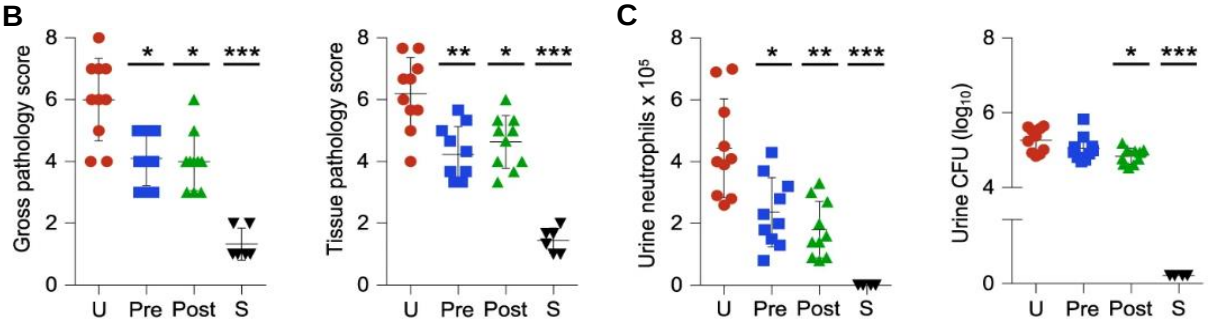

Figure 4.4.2 B-C
(**B**) Decrease by SR140333 treatment of gross bladder pathology score, tissue pathology score (defined by H&E staining). (**C**) Urine neutrophil and bacterial counts.

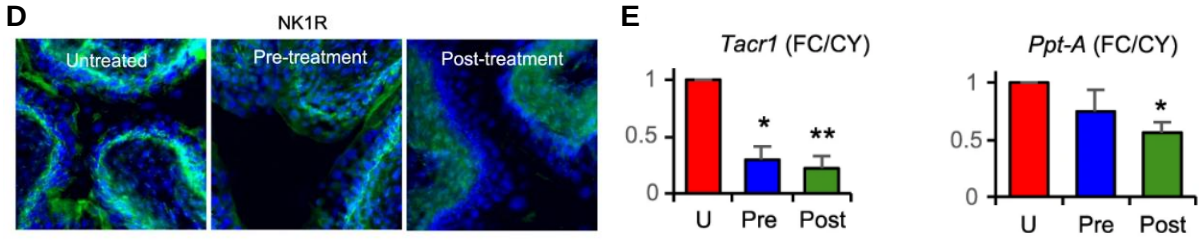

Figure 4.4.2 D and E

(**D**) Inhibition of NK1R (green) staining in SR140333 treated *Nlrp3*$^{-/-}$ mice compared to infected, untreated controls. (**E**) Reduced bladder *Tacr1* and *Ppt-A* expression in SR140333 treated *Nlrp3*$^{-/-}$ mice by qRT-PCR. (**Fig. B-E:** Data is presented as means ± SEMs $n = 10$ mice per group (two repeats). Data was analysed by Kruskal Wallis with Dunn's correction, *$P < 0.05$, **$P < 0.01$, ***$P < 0.001$.

To further understand the protective effect of NK1R inhibition, the expressed gene profile was analyzed in SR140333-treated *Nlrp3*$^{-/-}$ mice (**Figure 4.4.2 F**). Almost 50% of the regulated genes were suppressed, compared to infected untreated controls, including sensory perception of pain. Furthermore, the inflammasome and IL-1-superfamily genes were reduced by about 70%, including Il18, Il33, Il6, and ll1b (**Figure 4.4.2 G and H**). *Cxcl2* was the most strongly inhibited gene, consistent with the reduced number of neutrophils in treated mice.

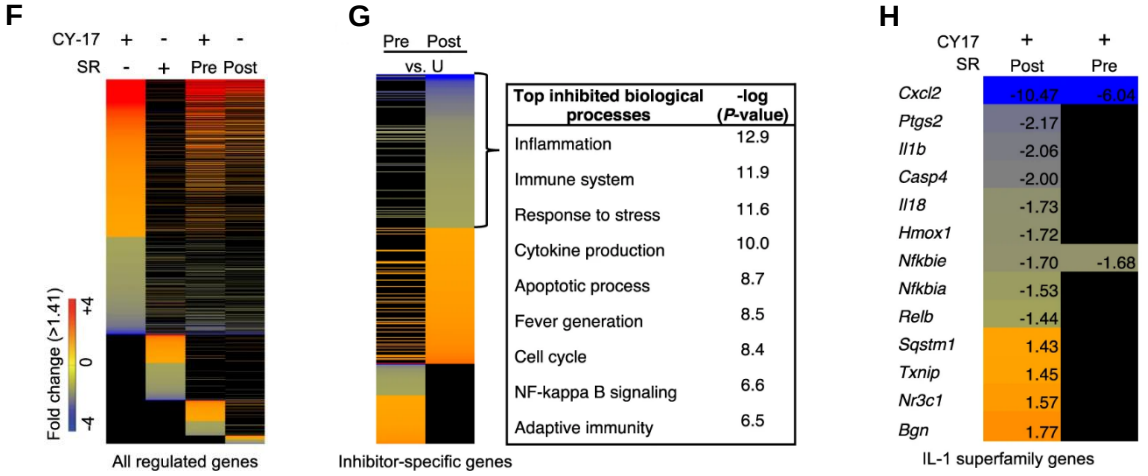

Figure 4.4.2 F-H

(**F**) Reduced gene expression in SR140333 treated mice compared to infected untreated controls defined by gene expression analysis of whole bladder mRNA ($n = 2$ mice per group, red = upregulated, blue = downregulated, $P < 0.05$, FC > 1.41, compared to uninfected controls). (**G**) Heat-map showing genes affected by SR treatment ($P < 0.05$, FC > 1.41 compared to infected untreated controls). Inhibited biological processes included inflammation and innate immune signaling. (**H**) Inhibition of inflammasome- and IL-1β related genes by SR140333 treatment, compared to untreated infected controls.

4.5 The human relevance of IL-1β and neuropeptides

Elevated concentrations of IL-1β were found in patients with acute cystitis (n = 9 samples from 9 patients) compared to the ABU patients (n = 161 samples from 20 patients). In 56% of urine samples from CY patients the Il- 1β levels were higher than 40 pg/ml, and in all cases were greater than 10 pg/ml. In contrast, 90% of the ABU samples were negative (<10 pg/ml) (**Figure 4.5 A-B**), resulting significantly higher mean IL-1β concentrations in CY patients than ABU group (264.5 pg/ml and 1.5 pg/ml, respectively, P < 0.001, **Figure 4.5 C**).

The MMP-7 levels also were quantified in the urine samples (9 urine in CY group, from 9 patients and 28 samples in the ABU group, from 20 patients). All the patients with acute cystitis had positive MMP-7 levels above the detection limit of 0.15 ng/ml, resulting in mean concentrations of 15.4 ng/ml. In contrast, the mean MMP-7 concentration was significantly (P<0.001) lower in the ABU group (4,3 ng/ml) (**Figure 4.5 D)**.

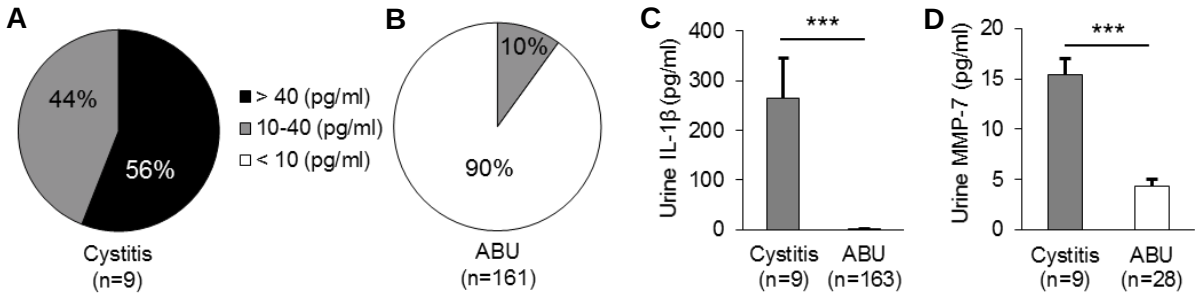

Figure 4.5 A-D

(**A**) Distribution of IL-1β concentrations in patients with acute cystitis (*n* = 9). (**B**) Distribution of IL-1β concentrations in patients with ABU, who were long-term asymptomatic carriers of *E. coli* 83972 (20 patients, 161 urine samples). (**C**) Histogram compares IL-1β concentrations between the two patient groups (means ± SEMs, *** P < 0.001, two-tailed Mann Whitney test). (**D**) MMP-7 concentrations were higher in urine samples from the patients with acute cystitis than in patients with long-term ABU (means ± SEMs, *** P < 0.001, two-tailed unpaired *t*-test).

In addition, SP levels of human urine samples were evaluated. Patients with acute cystitis (n=15 / 13 patients) had significantly higher urine SP (161,1 pg/ml), than patients with asymptomatic bacteriuria(n=42 / 20 patients) (69,7 pg/ml) (P < 0.001, **Figure 4.5 E)**.

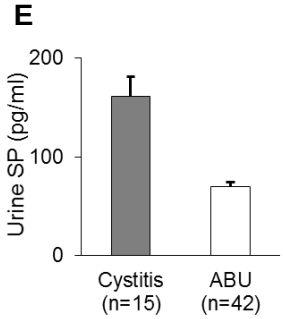

Figure 4.5 E

(**E**) Histogram shows elevated mean SP concentrations in patients with acute cystitis compared to ABU. The data is presented as means + SEMs, Mann-Whitney U-test ***P < 0.001.

5 DISCUSSION

The urinary bladder mucosa is often under microbial attack but rarely retaliates with full force. In asymptomatic carriers, the epithelium remains refractory despite bacterial numbers well above 10^5 CFU/ml (48, 50). Yet bacteria that cause acute cystitis create a state of exaggerated inflammation and the patients develop the characteristic symptoms of dysuria, frequency, pain as well as pyuria (2).

The results prove, that the cystitis is a hyperinflammatory disorder of the urinary bladder, driven by IL-1β in hosts with defective inflammasome function. In addition, the matrix metalloproteinase-7 was identified as a molecular player in mucosal inflammation, acting by proteolytically cleaving pro-IL-1β in susceptible hosts. The mucosal immune response in acute cystitis is regulated by direct bacterial effects on nerve cells and epithelial cells through the activation of neuropeptides- (SP) and neuropeptide receptors (NK1R). The importance of IL-1β, MMP-7, and NK1R/SP is further proven by the treatment of susceptible mice with IL-1 RA, MMP, or NK1R inhibitor. Elevated IL-1β levels were also detected in the urine of patients with acute cystitis compared to patients with ABU, and MMP-7, SP showed a similar pattern. These results are the first to provide a molecular context for acute cystitis, to reproduce the disease phenotype of acute cystitis patients in an animal model and to validate the IL-1β, MMP-7 and SP response in clinical studies. Furthermore, these findings suggest that IL-1β and MMP-7 may serve as targets for immunomodulatory therapy, or NK1R may be targeted therapeutically to alleviate symptoms associated with acute infection, complementing the increasingly problematic use of antibiotics in this patient group.

5.1 The IL-1β response in acute cystitis

The uropathogenic cystitis strains triggered a rapid IL-1β response in bladder epithelial cells, but not in kidney epithelial cells. The severity of acute cystitis was influenced by bacterial virulence as the acute cystitis strains activated IL-1β more efficiently than ABU strains. This comparison was especially valid, as the CY and ABU strains were isolated from the same pediatric population and geographic area (14, 83).

IL-1β is a powerful pro-inflammatory cytokine that initiates and amplifies innate immune responses (94, 95). The production increases in response to viral, bacterial, fungal, and parasitic infections and IL-1β is essential for the defense against microbial attack. IL-1β responses may

also be detrimental, however dysregulation of IL-1β has been observed in autoimmune and auto-inflammatory disorders, such as rheumatoid arthritis, multiple sclerosis, Crohn's disease or neurodegenerative disorders. This dichotomy was also apparent in the present study, where a controlled IL-1β response accompanied the clearance of infection in WT mice. The association of a dysregulated IL-1β response with disease suggested that acute cystitis is an infection-induced, hyper-inflammatory disorder of the urinary bladder. The protected phenotype in *Il1b*$^{-/-}$mice and the therapeutic efficacy of the IL-1R inhibitor identified IL-1β as the possible main effector principle in bladder pathology, linking acute cystitis to other hyper-inflammatory, IL-1β-driven disorders (96-98).

The mechanism of IL-1β activation by the acute cystitis strains remains unclear, however. Schaale et al. showed that UPEC strains CFT073 and UTI89 trigger inflammasome activation in human macrophages. The activation and secretion of IL-1β were hemolysin-dependent in murine model but not in human (21). Consistent with this, high IL-1β response was found in infections of virulent and hemolysin positive CY strains but the direct association with hemolysin production was not seen, suggesting that additional pathways must exist in the induction and secretion of IL-1β.

As *Il1b*$^{-/-}$ mice did not develop infection, and proinflammatory genes were not expressed, the IL-1β response may help render the bladder mucosa susceptible to infection, possibly by enhancing bacterial growth (99) or tissue invasion. The ability to activate IL-1β production in host cells may therefore be a key to bacterial virulence, as suggested by the epidemiologic survey of strains used in the present study.

5.2 The inflammasome function, the maturation of IL-1β, and the role of the inflammasome constituents (ASC, NLRP-3)

The dramatic disease phenotype in *Asc*$^{-/-}$ and *Nlrp3*$^{-/-}$ mice strongly suggested that a functional inflammasome response is required to maintain tissue homeostasis in infected bladders. The presence of large quantities of mature IL-1β in the urine of *Asc*$^{-/-}$ and *Nlrp3*$^{-/-}$ mice demonstrated that pro-IL-1β is processed in these mice. Yet, the effects of caspase inhibition were limited, suggesting that additional mechanisms must be involved.

These findings and the results of transcriptomic analysis (*Mmp7* was identified as the most strongly activated gene) add MMP-7 to the list of metalloproteinases (MMP-2, MMP-3, and MMP-9) that cleave pro-IL-1β or degrade IL-1β in other cell types (100). MMP-7 has also been

shown to process and modulate the activity of anti-bacterial peptides produced by the Paneth cells in the mouse small intestine (101), where cryptdins played a protective role during Salmonella typhimurium- (102) or Chlamydia trachomatis infections (103). In that model, the proinflammatory effects of MMP-7 were detected in the intestinal mucosa (104).

Importantly, the IL-1β response was largely restricted to the mucosa, where IL-1β accumulated in the epithelial lining of infected mice and was secreted into the urine. The excessive mucosal IL-1β response in *Asc*$^{-/-}$ and *Nlrp3*$^{-/-}$ mice coincided with an MMP-7 response, which was exclusively epithelial. The proximity of IL-1β and MMP-7 in epithelial cells may explain the efficiency of IL-1β processing and create the vicious cycle of IL-1β hyper-activation and tissue damage. Importantly, IL-1β and MMP-7 were not produced by recruited neutrophils, suggesting that bladder pathology is driven by an IL-1β and MMP-7 dependent epithelial response, with excessive release of IL-1β into the mucosa and into the urine, creating a paracrine activation loop involving IL-1 receptor-positive cells, not least the neutrophils, which may use IL-1β as a peripheral activation signal for degranulation and tissue toxicity. Interestingly, IL-18 and NLRPs other than NLRP3 were not regulated in contrast to Shigella and Salmonella infection models (105, 106), and the systemic susceptibility pattern in those mice was quite different from the mucosal response to UTI, described here. The proteolytic cleavage by MMP7 was identified as a potential mechanism of IL-1β activation, and evidence for IL-1β fragmentation by MMP-7 was obtained by direct cleavage of the purified components *in vitro, h*ighlighted, that the cleaved IL-1β fragments by MMP-7 were also biologically active. The results emphasize the difference in pathogenesis between acute cystitis and acute pyelonephritis. The mechanism used by acute cystitis strains to generate bladder pathology differ from the well-known acute pyelonephritis response caused by fimbriae-mediated activation of TLR4 signaling through the TICAM-1/2 (TRIF/TRAM) adaptors and activation of IRF-dependent transcription of type I interferons. This discrepancy was supported by transcriptomic analysis, where the acute cystitis strains were shown to activate MyD88-dependent *Il1b* and *Tnf* expression, potentially explaining the increase in the expression of IL-1β and IL-1β-dependent genes.

5.3 The neuropeptide- and neuropeptide receptor (SP/NK1R) activation in urinary bladder infection

The mucosal epithelial cells are important modulators of the nervous system and immune system, which are the main body sensory interfaces, and multidirectional interactions between the systems have been documented in autoimmune disease and inflammation (107, 108). The communication of these systems mediated by cytokines, chemokines, neuropeptides, and neurotrophins (109). Neurotransmitters and their receptors are expressed by immune cells, and neurons can sense and influence immune pathways (110). The bladder epithelium has the ability to sense changes in their extracellular environment and share key features with sensory neurons(111). They express a variety of receptors and ion channels, including the ability to express neuropeptides and neuropeptide receptors (112, 113). The uroepithelium actively influences the micturition reflex, either by a direct myogenic detrusor effect or by causing increased afferent activity and may participate in the regulation of pain (114, 115). The results showed that the pathogenesis of acute cystitis involves infected nerve cells. Furthermore, the epithelial cells resemble nerve cells and they express neuropeptide receptors and secrete neuropeptides in response to infection, suggesting that combined action of these two cell types may contribute significantly to pain at the site of infection and increased afferent and efferent CNS activity, which accompany mucosal infections. In addition, ligand release by each infected cell type was shown to trigger an amplification loop for coactivation of both cell types. It suggests that the symptoms of acute cystitis might be caused by the combined activation of the epithelial barrier and mucosal nerve cells (**Figure 5.3 A and B).** Triggered directly by infection, this response may increase afferent activity via C fibers, extending to the spinal cord and central nervous system, resulting in nociception as well as increased efferent activity, activating the lamina muscularis (116, 117). Additional cells in the lamina propria might play a role in this loop as well, including eosinophils and mast cells, which play an important role in acute cystitis and are known to produce and release SP in mice models and patients with interstitial cystitis/bladder pain syndrome (118-121).

SP-NK1R interaction is widely reported to regulate immune cell's function and the immunity to microbial infection (122). SP is also produced by immune cells and acts as an autocrine or paracrine fashion to regulate the function of immune cells, suggesting that neurocrine and

innate immune responses may converge (58, 123, 124). Furthermore, the NK-1R expression is upregulated by IL-1β (125).

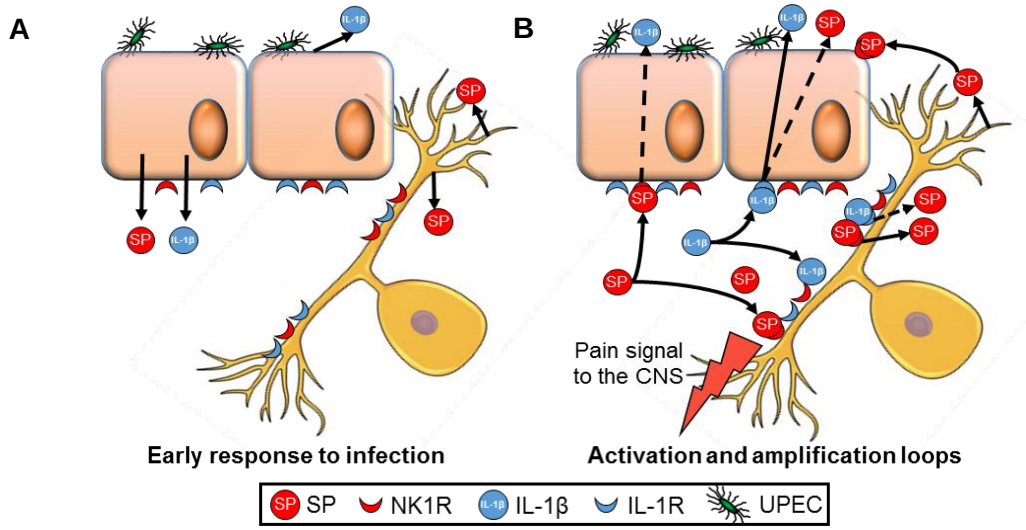

Figure 5.3 A and B
Model of the neuroepithelial response to *E. coli* infection – „the IL-1β - neurokinin loop". (**A**) *Early response*: Bacteria activate SP/NK1R expression in bladder epithelial cells, which are in parallel activated to produce IL-1R and to secrete IL-1β, creating an inflammatory response. (**B**) *Activation and amplification loops:* SP stimulates NK1R activation in nerve cells and activates IL-1β secretion in bladder epithelial cells, as shown by adding SP to uninfected cells. IL-1β then activates SP/NK1R expression in both nerve- and epithelial cells, which express IL-1R.

5.4 The inhibition of IL-1 receptor, IL-1β processing and NK1R in acute bladder infection

Recurrent or acute cystitis is a handicap, socially, professionally, and emotionally but despite its prevalence and importance for patients and society, acute cystitis is a poorly understood disease (22, 126, 127). Social and behavioral factors have been emphasized as a cause of recurrent infections and until recently, therapeutic options have included a variety of shorter or longer antibiotic regimens, many of which have been discontinued, due to resistance development. It therefore comes as no surprise, that this highly painful condition has been the focus of various interventions in addition to antibiotic therapy. Deliberate establishment of competitive microflora has shown promising clinical effects (48, 50), and anti-inflammatory agents are emerging as a novel therapeutic approach in acute cystitis, suppressing the symptoms while the host clears the infection (128), but novel therapeutic approaches are needed in this large patient group. The results showed that the pathology in acute cystitis is prevented by the

IL-1β receptor blockade and the Inhibition of MMP-7 was also protective, but with a less complete than mice receiving the IL-1RA. Furthermore, NK1R inhibition might constitute an interesting alternative approach to prevent inflammation and pathology in cystitis. Highlighted, IL-1RA (Anakinra) is in clinical use and NK1R antagonist treatment has proved effective in clinical studies of overactive bladder syndrome by reducing pain, urgency, and frequency (129-132). These findings suggest that the use of NK1R antagonist or short-term immunotherapy might be a realistic treatment option in patients with acute cystitis or recurrent UTIs, where antibiotic resistance is creating an urgent need for novel therapeutic alternatives.

5.5 The human relevance of IL-1β and neuropeptides

IL-1β is one of the first cytokines detected at the onset and elevation of urinary IL-1β was observed in patients with bacterial cystitis (133), and a correlation with pyuria was found by several groups (9). Consistent with these, the results show, patients with acute cystitis have more elevated concentrations of IL-1β in urine than patients with ABU. The MMP-7 levels also were elevated in urine samples from CY patients, proving the importance of Il-1β in acute bladder infection.

The importance of SP/NK1R in lower urinary tract symptoms, especially in bladder pain, has previously been documented in chronic pelvic pain, interstitial cystitis, and acute or chronic bladder inflammation (65). Numerous SP-reactive varicose nerve fibers have been observed in the lamina propria, in the submucosal layer or beneath the epithelium, and most of them ran freely in the connective tissue (134). Additionally, NK1R density was increased in bladder biopsies from cystitis patients (135). Furthermore, increased *Tac1* gene expression was detected after bladder infection in mice (136), and elevated urine SP concentrations were observed in patients with interstitial cystitis and in UTI (137-140). Consistent with these studies, elevated SP levels were found in patients with acute cystitis compared to patients with ABU.

The identified molecular determinants may also be helpful to address the unmet need for diagnostic tools in this patient group. The frequency of genetic variants, such as ASC mutations, and their relevance to disease would be an interesting focus of prospective clinical studies.

6 CONCLUSION

1. Acute cystitis is an Interleukin-1 beta-driven, hyper-inflammatory condition of the infected urinary bladder. (Paper I)
2. Disease severity was controlled by the mechanism of IL-1β processing, and mice with intact inflammasome function developed a moderate, self-limiting form of cystitis. The most severe form of acute cystitis was detected in mice lacking the inflammasome constituents ASC or NLRP-3, and IL-1β processing was hyperactive in these mice, due to a new, non-canonical mechanism involving the matrix metalloproteinase-7 (MMP-7). (Paper I)
3. The infection activates Neurokinin-1 receptor (NK1R) and Substance P (SP) expression in nerve cells and bladder epithelial cells *in vitro* and *in vivo* in the urinary bladder mucosa, and a neuro-epithelial activation loop was identified that participates in the control of mucosal inflammation and pain in acute cystitis. (Paper II)
4. The IL-1 receptor antagonist and NK1R inhibitors attenuated acute cystitis in susceptible mice, supporting a role in disease pathogenesis. Furthermore, the MMP inhibitor had a similar therapeutic effect. (Paper I, II)
5. Elevated levels of IL-1β, SP, and MMP-7 were detected in patients with acute cystitis, suggesting a potential role as biomarkers and potential therapeutic targets. (Paper I, II)

7 MAGYAR NYELVŰ ÖSSZEFOGLALÓ

Az elmúlt évtizedekben történt nagyarányú antibiotikum-felhasználásnak köszönhetően a kórokozók antibiotikummal szembeni rezisztenciája folyamatosan növekszik, ezzel megnehezítve a betegek kezelését. A megfelelő antibiotikum-politika és újabb antibiotikumok kifejlesztése mellett kimagaslóan fontos a fertőző betegségek hátterében végbemenő molekuláris folyamatok, genetikai faktorok megismerése, melyek segítségével csökkenthető a fertőzések kialakulásának esélye és a felesleges antibiotikum-felhasználás. Továbbá az eredmények segítséget nyújthatnak új terápiás lehetőségek kifejlesztéséhez. A fertőző betegségek csoportján belül a húgyúti infekciók jelentősége kiemelkedő, mind a fertőzéses esetek számát, mind az antibiotikum-felhasználást nézve.

A húgyúti fertőzések megjelenése és súlyossága széles skálán mozog, az egyszerű hólyaghuruttól a súlyos, életet veszélyeztető uroszepszisig. Az egyik leggyakoribb formája a cisztitisz, ezzel az orvoshoz fordulás és antibiotikum-felhasználás egyik leggyakoribb okát képezve. Lefolyása és az általa okozott panaszok súlyossága egyénenként széles skálán mozog, a visszatérési hajlama magas, különösen a betegek bizonyos csoportjánál. A fertőzés kialakulása esetén a veleszületett immunrendszer gyors és erős reakcióval válaszol a hólyag mucosa segítségével, ezzel hirtelen kialakuló erős fájdalmat, gyakori és sürgető vizelést, akár alvadékos vérvizelést okozva. Ezen tünetek hátterében zajló molekuláris folyamatok alapjai nem tisztázottak.

Jelen kutatásban az akut cisztitisz (CY) esetén végbemenő molekuláris folyamatokat, genetikai faktorokat és az ezeken alapuló lehetséges új terápiás lehetőségeket vizsgáltuk a kialakuló patológia és a tünetek terén.

A vizsgálat első felében az akut gyulladás során végbemenő mucosa választ és a háttérben zajló génaktiválódást vizsgáltuk. Az eredmények alapján a cisztitisz egy IL-1β által mediált, és az inflamasoma diszregulációval összefüggésbe hozható hiper-inflammatorikus betegség. Az *in vitro* körülmények között megfertőzött emberi húgyhólyag epithelsejtek (HTB-9) gyors IL-1β termeléssel reagáltak a cisztitiszes betegekből izolált *E. coli* törzsekkel történt infekciót követően. A fertőzést követően létrejövő fokozott IL-1β szintézist és aktiválódást az immun-hisztokémiai vizsgálatok és a sejt felülúszóban kimutatott pro- és érett IL-1β eredmények is igazolták. Az azonos epidemiológia csoportból származó CY és ABU izolátumok screening vizsgálata megerősítette az IL-1β hólyagfertőzésben betöltött specifikus szerepét. Az *in vivo*

(rágcsáló modell) vizsgálatokban bizonyos inflamasoma gének hiánya esetén (*Asc*$^{-/-}$ és *Nlrp3*$^{-/-}$) a fertőzést követően dramatikus gyulladásos patológiai kép alakult ki a hólyag ödémájával és a nyálkahártya bevérzésével, leválásával. Ezzel szemben az *Il1b*$^{-/-}$ fenotípus védettséget jelentett a fertőzéssel szemben. A súlyos patológiát mutató, fertőzött egyedek hólyag epithelsejtjeiben az *Il1b* gének expressziója, valamint a Mátrix- metaloproteáz-7 (MMP-7) transzkripciója erősen fokozott volt. Az *Asc*$^{-/-}$ és *Nlrp3*$^{-/-}$ egerek vizeletében mért magas IL-1β szintek, az érett IL-1β jelenléte a vizeletben, valamint az *in vitro* caspase-1 gátlás részleges eredményessége felvetette az IL-1β aktiválódás egy eddig nem ismert módját. Az egerekben kialakuló súlyos patológia egyértelmű összefüggést mutatott a MMP-7 expresszójával, valamint az immunhisztokémia során kifejezett epitheliális MMP-7 expresszió volt látható a fertőzött hólyagokban. Az *in vitro* végzett vizsgálatok igazolták a pro-IL-1β MMP-7 általi degradálódást, amely aktív IL-1β fragmentumokat eredményezett, ezzel igazolva az IL-1β egy eddig nem ismert, az inflammaszómától független, aktiválódási módját. A hólyag súlyos gyulladásának kialakulása megelőzhető volt IL-1β receptor, vagy MMP7 inhibitorral, bizonyítva a fent említett molekulák fontosságát betegség patomechanizmusában.

A vizsgálat második felében húgyúti fertőzés során kialakuló erős fájdalom hátterében végbemenő neuro-epitheliális kapcsolatot térképeztük fel. Az infekció során az ideg- és hólyaghámsejtekben (*in vitro*), valamint *in vivo* a húgyhólyag nyálkahártyájában aktiválódik a Neurokinin-1 receptor (NK1R) és Suptance P (SP) átíródása. A farmakológiai NK1R gátlók enyhítették az akut cisztitisz lefolyását a fogékony egerekben, ezzel támogatva az NK1R/SP patogenezisben betöltött szerepét. Fenti eredmények klinikai relevanciáját igazolta az akut cisztitiszben szenvedő betegek vizeletében mért emelkedett IL-1β, MMP-7 és SP szintek, összehasonlítva a tünetmentes bakteriuriás betegek vizeletében mért szintekkel, ezzel rámutatva az IL-1β, MMP-7 és NK1R/SP potenciális terápiás lehetőségére. Jelen vizsgálat elsőként nyújtott átfogó eredményeket az akut hólyaghurut molekuláris hátteréről, mely eredmények a jövőben segítséget jelentenek új kezelési módok, diagnosztikus eljárások kifejlesztésben.

8 ACKNOWLEDGMENT

First of all, I would like to thank everyone who contributed to this work, especially my fellow authors.

Most of all, I would like to thank my supervisor, Prof. Péter Tenke, who has been „driving me forward" uninterrupted, providing continued support in both work and science. He provided every opportunity for my advancement and development. You taught me that nothing is impossible and and most of all we do not stop. Thank you for everything!

Special thanks to Prof. Catharina Svanborg, who introduced me to the mysteries of molecular biology, the beauties of basic research, and helped me through its difficulties. Without you, this work could not have been developed. Thank you for your help and patience!

Thanks to Dr. Björn Wult, who helped me with important advice in my work and made me feel at home in Lund. Thank you for your support!

Many thanks to the UTI and HAMLET team of the lab for all the help. You taught me everything needed in the lab and in science : Ines, Manoj, Gustav, Aftab, Anna, Daniel, James, Jenny, Nataliya, Yun… Thanks for ALL!

Special thanks to Gustav Rydström and Deepak Raina for becoming my friends! You were all with me at work, in my spare time during my stay abroad!! You are always welcome in Hungary! - PS: Gustav, my first son's name is not HÁROM, but I have „3". ☺

I would like to thank my wife for always supporting me and reviewing my „strange worded work". Helping me with everything… Thank you;)

Thanks to our children who „have always given me great devotion as I work on my computer", especially to Apor Károly Nagy and „Guardians of the Galaxy".

Thanks to my parents who supported me to get this far.

To my colleagues and friends who have endured my „patient nature", especially if the weight of „science" has pushed my shoulders. Thanks to Béla Köves, Ildikó Bérczy and Katalin Szujer for their advice and help in my scientific work and the European Association of Urology and the Hungarian Urology Society for a research grant.

PS: Ezek után lehet NAGY-A-POR. És ha lesz NAGY-JELES. Csak a lányom NAGY-ZOLNA. (Hungarian word-play)

9 REFERENCES

1. Flores-Mireles AL, Walker JN, Caparon M, et al. Urinary tract infections: epidemiology, mechanisms of infection and treatment options. Nat Rev Microbiol. 2015;13(5):269-84.

2. Stamm WE, Hooton TM. Management of urinary tract infections in adults. N Engl J Med. 1993;329(18):1328-34.

3. Scholes D, Hawn TR, Roberts PL, et al. Family history and risk of recurrent cystitis and pyelonephritis in women. J Urol. 2010;184(2):564-9.

4. Kunin C. Urinary Tract Infections. Detection, Prevention and Management. 5th ed. Baltimore: Williams and Wilkins; 1997.

5. Foxman B, Barlow R, D'Arcy H, et al. Urinary tract infection: self-reported incidence and associated costs. Ann Epidemiol. 2000;10(8):509-15.

6. Svanborg C. Resistance to Urinary-Tract Infection. New England Journal of Medicine. 1993;329(11):802-3.

7. Ragnarsdottir B, Fischer H, Godaly G, et al. TLR- and CXCR1-dependent innate immunity: insights into the genetics of urinary tract infections. Eur J Clin Invest. 2008;38 Suppl 2:12-20.

8. Sivick KE, Mobley HL. Waging war against uropathogenic Escherichia coli: winning back the urinary tract. Infect Immun. 2010;78(2):568-85.

9. Candela JV, Park E, Gerspach JM, et al. Evaluation of urinary IL-1alpha and IL-1beta in gravid females and patients with bacterial cystitis and microscopic hematuria. Urol Res. 1998;26(3):175-80.

10. de Man P, van Kooten C, Aarden L, et al. Interleukin-6 induced at mucosal surfaces by gram-negative bacterial infection. Infect Immun. 1989;57(11):3383-8.

11. Kumar S, Dave A, Wolf B, et al. Urinary tract infections. Dis Mon. 2015;61(2):45-59.

12. Otto G, Burdick M, Strieter R, et al. Chemokine response to febrile urinary tract infection. Kidney Int. 2005;68(1):62-70.

13. Glover M, Moreira CG, Sperandio V, et al. Recurrent urinary tract infections in healthy and nonpregnant women. Urol Sci. 2014;25(1):1-8.

14. Lindberg U, Claesson I, Hanson LA, et al. Asymptomatic bacteriuria in schoolgirls. VIII. Clinical course during a 3-year follow-up. J Pediatr. 1978;92(2):194-9.

15. Agace WW, Hedges SR, Ceska M, et al. Interleukin-8 and the neutrophil response to mucosal gram-negative infection. J Clin Invest. 1993;92(2):780-5.

16. Frendeus B, Wachtler C, Hedlund M, et al. Escherichia coli P fimbriae utilize the Toll-like receptor 4 pathway for cell activation. Mol Microbiol. 2001;40(1):37-51.

17. Abraham SN, St John AL. Mast cell-orchestrated immunity to pathogens. Nat Rev Immunol. 2010;10(6):440-52.

18. De Man P, Jodal U, Van Kooten C, et al. Bacterial adherence as a virulence factor in urinary tract infection. APMIS. 1990;98(12):1053-60.

19. Ingersoll MA, Albert ML. From infection to immunotherapy: host immune responses to bacteria at the bladder mucosa. Mucosal Immunol. 2013;6(6):1041-53.

20. Nagamatsu K, Hannan TJ, Guest RL, et al. Dysregulation of Escherichia coli alpha-hemolysin expression alters the course of acute and persistent urinary tract infection. Proc Natl Acad Sci U S A. 2015;112(8):E871-80.

21. Schaale K, Peters KM, Murthy AM, et al. Strain- and host species-specific inflammasome activation, IL-1beta release, and cell death in macrophages infected with uropathogenic Escherichia coli. Mucosal Immunol. 2016;9(1):124-36.

22. Norinder BS, Koves B, Yadav M, et al. Do Escherichia coli strains causing acute cystitis have a distinct virulence repertoire? Microb Pathog. 2012;52(1):10-6.

23. Nielubowicz GR, Mobley HL. Host-pathogen interactions in urinary tract infection. Nat Rev Urol. 2010;7(8):430-41.

24. Johnson JR. Virulence factors in Escherichia coli urinary tract infection. Clin Microbiol Rev. 1991;4(1):80-128.

25. Orskov I, Orskov F, Birch-Andersen A, et al. O, K, H and fimbrial antigens in Escherichia coli serotypes associated with pyelonephritis and cystitis. Scand J Infect Dis Suppl. 1982;33:18-25.

26. Cirl C, Wieser A, Yadav M, et al. Subversion of Toll-like receptor signaling by a unique family of bacterial Toll/interleukin-1 receptor domain-containing proteins. Nat Med. 2008;14(4):399-406.

27. Smith YC, Rasmussen SB, Grande KK, et al. Hemolysin of uropathogenic Escherichia coli evokes extensive shedding of the uroepithelium and hemorrhage in bladder tissue within the first 24 hours after intraurethral inoculation of mice. Infect Immun. 2008;76(7):2978-90.

28. Bokranz W, Wang X, Tschape H, et al. Expression of cellulose and curli fimbriae by Escherichia coli isolated from the gastrointestinal tract. J Med Microbiol. 2005;54(Pt 12):1171-82.

29. Sandberg T, Kaijser B, Lidin-Janson G, et al. Virulence of Escherichia coli in relation to host factors in women with symptomatic urinary tract infection. J Clin Microbiol. 1988;26(8):1471-6.

30. Johnson JR, Russo TA, Brown JJ, et al. papG alleles of Escherichia coli strains causing first-episode or recurrent acute cystitis in adult women. J Infect Dis. 1998;177(1):97-101.

31. Wullt B, Bergsten G, Fischer H, et al. The host response to urinary tract infection. Infect Dis Clin North Am. 2003;17(2):279-301.

32. Ragnarsdottir B, Lutay N, Gronberg-Hernandez J, et al. Genetics of innate immunity and UTI susceptibility. Nat Rev Urol. 2011;8(8):449-68.

33. Fischer H, Yamamoto M, Akira S, et al. Mechanism of pathogen-specific TLR4 activation in the mucosa: fimbriae, recognition receptors and adaptor protein selection. Eur J Immunol. 2006;36(2):267-77.

34. Hagberg L, Briles DE, Eden CS. Evidence for separate genetic defects in C3H/HeJ and C3HeB/FeJ mice, that affect susceptibility to gram-negative infections. J Immunol. 1985;134(6):4118-22.

35. Ambite I, Nagy K, Godaly G, et al. Susceptibility to Urinary Tract Infection: Benefits and Hazards of the Antibacterial Host Response. Microbiol Spectr. 2016;4(3).

36. Dinarello CA. The proinflammatory cytokines interleukin-1 and tumor necrosis factor and treatment of the septic shock syndrome. J Infect Dis. 1991;163(6):1177-84.

37. Ren K, Torres R. Role of interleukin-1beta during pain and inflammation. Brain Res Rev. 2009;60(1):57-64.

38. Broz P, Dixit VM. Inflammasomes: mechanism of assembly, regulation and signalling. Nat Rev Immunol. 2016;16(7):407-20.

39. Agostini L, Martinon F, Burns K, et al. NALP3 forms an IL-1beta-processing inflammasome with increased activity in Muckle-Wells autoinflammatory disorder. Immunity. 2004;20(3):319-25.

40. Godaly G, Bergsten G, Hang L, et al. Neutrophil recruitment, chemokine receptors, and resistance to mucosal infection. J Leukoc Biol. 2001;69(6):899-906.

41. Benson M, Jodal U, Andreasson A, et al. Interleukin 6 response to urinary tract infection in childhood. Pediatr Infect Dis J. 1994;13(7):612-6.

42. Jantausch BA, O'Donnell R, Wiedermann BL. Urinary interleukin-6 and interleukin-8 in children with urinary tract infection. Pediatr Nephrol. 2000;15(3-4):236-40.

43. Ko YC, Mukaida N, Ishiyama S, et al. Elevated interleukin-8 levels in the urine of patients with urinary tract infections. Infect Immun. 1993;61(4):1307-14.

44. Hedges S, Svanborg C. The mucosal cytokine response to urinary tract infections. Int J Antimicrob Agents. 1994;4(2):89-93.

45. Barber SA, Perera PY, Vogel SN. Defective ceramide response in C3H/HeJ (Lpsd) macrophages. J Immunol. 1995;155(5):2303-5.

46. Agace W, Hedges S, Andersson U, et al. Selective cytokine production by epithelial cells following exposure to Escherichia coli. Infect Immun. 1993;61(2):602-9.

47. Gronberg-Hernandez J, Sunden F, Connolly J, et al. Genetic control of the variable innate immune response to asymptomatic bacteriuria. PLoS One. 2011;6(11):e28289.

48. Lutay N, Ambite I, Gronberg Hernandez J, et al. Bacterial control of host gene expression through RNA polymerase II. J Clin Invest. 2013;123(6):2366-79.

49. Nicolle LE. Asymptomatic bacteriuria. Curr Opin Infect Dis. 2014;27(1):90-6.

50. Sunden F, Hakansson L, Ljunggren E, et al. Escherichia coli 83972 bacteriuria protects against recurrent lower urinary tract infections in patients with incomplete bladder emptying. J Urol. 2010;184(1):179-85.

51. Zdziarski J, Brzuszkiewicz E, Wullt B, et al. Host imprints on bacterial genomes--rapid, divergent evolution in individual patients. PLoS Pathog. 2010;6(8):e1001078.

52. Steinhoff MS, von Mentzer B, Geppetti P, et al. Tachykinins and their receptors: contributions to physiological control and the mechanisms of disease. Physiol Rev. 2014;94(1):265-301.

53. Gautam M, Prasoon P, Kumar R, et al. Role of neurokinin type 1 receptor in nociception at the periphery and the spinal level in the rat. Spinal Cord. 2016;54(3):172-82.

54. Luccarini P, Henry M, Alvarez P, et al. Contribution of neurokinin 1 receptors in the cutaneous orofacial inflammatory pain. Naunyn Schmiedebergs Arch Pharmacol. 2003;368(4):320-3.

55. O'Connor TM, O'Connell J, O'Brien DI, et al. The role of substance P in inflammatory disease. J Cell Physiol. 2004;201(2):167-80.

56. Weinstock JV. Substance P and the regulation of inflammation in infections and inflammatory bowel disease. Acta Physiol (Oxf). 2015;213(2):453-61.

57. Chiu IM, Heesters BA, Ghasemlou N, et al. Bacteria activate sensory neurons that modulate pain and inflammation. Nature. 2013;501(7465):52-7.

58. Acosta C, Davies A. Bacterial lipopolysaccharide regulates nociceptin expression in sensory neurons. J Neurosci Res. 2008;86(5):1077-86.

59. Obata F, Hippler LM, Saha P, et al. Shiga toxin type-2 (Stx2) induces glutamate release via phosphoinositide 3-kinase (PI3K) pathway in murine neurons. Front Mol Neurosci. 2015;8:30.

60. Azzolina A, Bongiovanni A, Lampiasi N. Substance P induces TNF-alpha and IL-6 production through NF kappa B in peritoneal mast cells. Biochim Biophys Acta. 2003;1643(1-3):75-83.

61. Callsen-Cencic P, Mense S. Expression of neuropeptides and nitric oxide synthase in neurones innervating the inflamed rat urinary bladder. J Auton Nerv Syst. 1997;65(1):33-44.

62. Lecci A, Maggi CA. Tachykinins as modulators of the micturition reflex in the central and peripheral nervous system. Regul Pept. 2001;101(1-3):1-18.

63. Rudick CN, Berry RE, Johnson JR, et al. Uropathogenic Escherichia coli induces chronic pelvic pain. Infect Immun. 2011;79(2):628-35.

64. Rudick CN, Schaeffer AJ, Klumpp DJ. Pharmacologic attenuation of pelvic pain in a murine model of interstitial cystitis. BMC Urol. 2009;9:16.

65. Saban R, Saban MR, Nguyen NB, et al. Neurokinin-1 (NK-1) receptor is required in antigen-induced cystitis. Am J Pathol. 2000;156(3):775-80.

66. Meseguer V, Alpizar YA, Luis E, et al. TRPA1 channels mediate acute neurogenic inflammation and pain produced by bacterial endotoxins. Nat Commun. 2014;5:3125.

67. Fischer H, Ellstrom P, Ekstrom K, et al. Ceramide as a TLR4 agonist; a putative signalling intermediate between sphingolipid receptors for microbial ligands and TLR4. Cell Microbiol. 2007;9(5):1239-51.

68. Fischer H, Lutay N, Ragnarsdottir B, et al. Pathogen specific, IRF3-dependent signaling and innate resistance to human kidney infection. PLoS Pathog. 2010;6(9):e1001109.

69. Svensson M, Yadav M, Holmqvist B, et al. Acute pyelonephritis and renal scarring are caused by dysfunctional innate immunity in mCxcr2 heterozygous mice. Kidney Int. 2011;80(10):1064-72.

70. Frendeus B, Godaly G, Hang L, et al. Interleukin 8 receptor deficiency confers susceptibility to acute experimental pyelonephritis and may have a human counterpart. J Exp Med. 2000;192(6):881-90.

71. Lundstedt AC, McCarthy S, Gustafsson MC, et al. A genetic basis of susceptibility to acute pyelonephritis. PLoS One. 2007;2(9):e825.

72. Lundstedt AC, Leijonhufvud I, Ragnarsdottir B, et al. Inherited susceptibility to acute pyelonephritis: a family study of urinary tract infection. J Infect Dis. 2007;195(8):1227-34.

73. Szabo RJ, Shortliffe LM, Stamey TA. Adherence of Escherichia coli and Proteus mirabilis to human transitional cells. J Urol. 1987;137(4):793-7.

74. Lomberg H, Hanson L, Jacobsson B, et al. Correlation of P blood group phenotype, vesicoureteral reflux and bacterial attachment in patients with recurrent pyelonephritis. N Engl J Med. 1983;308:1189-92.

75. Stapleton A, Nudelman E, Clausen H, et al. Binding of uropathogenic *Escherichia coli* R45 to glycolipids extracted from vaginal epithelial cells is dependent on histo-blood group secretor status. J Clin Invest. 1992;90(3):965-72.

76. Mulvey MA, Schilling JD, Hultgren SJ. Establishment of a persistent Escherichia coli reservoir during the acute phase of a bladder infection. Infect Immun. 2001;69(7):4572-9.

77. Mobley HL, Green DM, Trifillis AL, et al. Pyelonephritogenic Escherichia coli and killing of cultured human renal proximal tubular epithelial cells: role of hemolysin in some strains. Infect Immun. 1990;58(5):1281-9.

78. Wullt B, Bergsten G, Connell H, et al. P fimbriae enhance the early establishment of Escherichia coli in the human urinary tract. Mol Microbiol. 2000;38(3):456-64.

79. Horai R, Asano M, Sudo K, et al. Production of mice deficient in genes for interleukin (IL)-1alpha, IL-1beta, IL-1alpha/beta, and IL-1 receptor antagonist shows that IL-1beta is crucial in turpentine-induced fever development and glucocorticoid secretion. J Exp Med. 1998;187(9):1463-75.

80. Mariathasan S, Weiss DS, Newton K, et al. Cryopyrin activates the inflammasome in response to toxins and ATP. Nature. 2006;440(7081):228-32.

81. Mariathasan S, Newton K, Monack DM, et al. Differential activation of the inflammasome by caspase-1 adaptors ASC and Ipaf. Nature. 2004;430(6996):213-8.

82. Rudick CN, Bryce PJ, Guichelaar LA, et al. Mast cell-derived histamine mediates cystitis pain. PLoS One. 2008;3(5):e2096.

83. Leffler H, Svanborg-Eden C. Glycolipid receptors for uropathogenic Escherichia coli on human erythrocytes and uroepithelial cells. Infect Immun. 1981;34(3):920-9.

84. Lopes FM, Schroder R, da Frota ML, Jr., et al. Comparison between proliferative and neuron-like SH-SY5Y cells as an in vitro model for Parkinson disease studies. Brain Res. 2010;1337:85-94.

85. Wilson CL, Heppner KJ, Labosky PA, et al. Intestinal tumorigenesis is suppressed in mice lacking the metalloproteinase matrilysin. Proc Natl Acad Sci U S A. 1997;94(4):1402-7.

86. Matsushita K, Takeoka M, Sagara J, et al. A splice variant of ASC regulates IL-1beta release and aggregates differently from intact ASC. Mediators Inflamm. 2009;2009:287387.

87. Burry RW. Controls for immunocytochemistry: an update. J Histochem Cytochem. 2011;59(1):6-12.

88. Mahmood T, Yang PC. Western blot: technique, theory, and trouble shooting. N Am J Med Sci. 2012;4(9):429-34.

89. Bolstad BM, Irizarry RA, Astrand M, et al. A comparison of normalization methods for high density oligonucleotide array data based on variance and bias. Bioinformatics. 2003;19(2):185-93.

90. Irizarry RA, Bolstad BM, Collin F, et al. Summaries of Affymetrix GeneChip probe level data. Nucleic Acids Res. 2003;31(4):e15.

91. Eisenhart C. The assumptions underlying the analysis of variance. Biometrics. 1947;3(1):1-21.

92. Chen J, Bardes EE, Aronow BJ, et al. ToppGene Suite for gene list enrichment analysis and candidate gene prioritization. Nucleic Acids Res. 2009;37(Web Server issue):W305-11.

93. Bustin SA, Benes V, Garson JA, et al. The MIQE guidelines: minimum information for publication of quantitative real-time PCR experiments. Clin Chem. 2009;55(4):611-22.

94. Dinarello CA. Interleukin-1beta and the autoinflammatory diseases. N Engl J Med. 2009;360(23):2467-70.

95. Dinarello CA. Immunological and inflammatory functions of the interleukin-1 family. Annu Rev Immunol. 2009;27:519-50.

96. Di Virgilio F. The therapeutic potential of modifying inflammasomes and NOD-like receptors. Pharmacol Rev. 2013;65(3):872-905.

97. Dinarello CA. Biologic basis for interleukin-1 in disease. Blood. 1996;87(6):2095-147.

98. Martinon F, Mayor A, Tschopp J. The inflammasomes: guardians of the body. Annu Rev Immunol. 2009;27:229-65.

99. Porat R, Clark BD, Wolff SM, et al. Enhancement of growth of virulent strains of Escherichia coli by interleukin-1. Science. 1991;254(5030):430-2.

100. Schonbeck U, Mach F, Libby P. Generation of biologically active IL-1 beta by matrix metalloproteinases: a novel caspase-1-independent pathway of IL-1 beta processing. J Immunol. 1998;161(7):3340-6.

101. Wilson CL, Ouellette AJ, Satchell DP, et al. Regulation of intestinal alpha-defensin activation by the metalloproteinase matrilysin in innate host defense. Science. 1999;286(5437):113-7.

102. Eisenhauer PB, Harwig SS, Lehrer RI. Cryptdins: antimicrobial defensins of the murine small intestine. Infect Immun. 1992;60(9):3556-65.

103. Pal S, Schmidt AP, Peterson EM, et al. Role of matrix metalloproteinase-7 in the modulation of a Chlamydia trachomatis infection. Immunology. 2006;117(2):213-9.

104. Vandenbroucke RE, Vanlaere I, Van Hauwermeiren F, et al. Pro-inflammatory effects of matrix metalloproteinase 7 in acute inflammation. Mucosal Immunol. 2014;7(3):579-88.

105. Raupach B, Peuschel SK, Monack DM, et al. Caspase-1-mediated activation of interleukin-1beta (IL-1beta) and IL-18 contributes to innate immune defenses against Salmonella enterica serovar Typhimurium infection. Infect Immun. 2006;74(8):4922-6.

106. Sansonetti PJ, Phalipon A, Arondel J, et al. Caspase-1 activation of IL-1beta and IL-18 are essential for Shigella flexneri-induced inflammation. Immunity. 2000;12(5):581-90.

107. Veiga-Fernandes H, Mucida D. Neuro-Immune Interactions at Barrier Surfaces. Cell. 2016;165(4):801-11.

108. Weitnauer M, Mijosek V, Dalpke AH. Control of local immunity by airway epithelial cells. Mucosal Immunol. 2016;9(2):287-98.

109. Ordovas-Montanes J, Rakoff-Nahoum S, Huang S, et al. The Regulation of Immunological Processes by Peripheral Neurons in Homeostasis and Disease. Trends Immunol. 2015;36(10):578-604.

110. Kioussis D, Pachnis V. Immune and nervous systems: more than just a superficial similarity? Immunity. 2009;31(5):705-10.

111. Birder L, Andersson KE. Urothelial signaling. Physiol Rev. 2013;93(2):653-80.

112. Girard BM, Malley SE, Braas KM, et al. PACAP/VIP and receptor characterization in micturition pathways in mice with overexpression of NGF in urothelium. J Mol Neurosci. 2010;42(3):378-89.

113. Heng YJ, Saunders CI, Kunde DA, et al. TRPV1, NK1 receptor and substance P immunoreactivity and gene expression in the rat lumbosacral spinal cord and urinary bladder after systemic, low dose vanilloid administration. Regul Pept. 2011;167(2-3):250-8.

114. Maggi CA, Santicioli P, Giuliani S, et al. Activation of micturition reflex by substance P and substance K: indirect evidence for the existence of multiple tachykinin receptors in the rat urinary bladder. J Pharmacol Exp Ther. 1986;238(1):259-66.

115. Chien CT, Yu HJ, Lin TB, et al. Substance P via NK1 receptor facilitates hyperactive bladder afferent signaling via action of ROS. Am J Physiol Renal Physiol. 2003;284(4):F840-51.

116. Dafny N, Dong WQ, Prieto-Gomez C, et al. Lateral hypothalamus: site involved in pain modulation. Neuroscience. 1996;70(2):449-60.

117. Fowler CJ, Griffiths D, de Groat WC. The neural control of micturition. Nat Rev Neurosci. 2008;9(6):453-66.

118. Abraham SN, Miao Y. The nature of immune responses to urinary tract infections. Nat Rev Immunol. 2015;15(10):655-63.

119. Pang X, Boucher W, Triadafilopoulos G, et al. Mast cell and substance P-positive nerve involvement in a patient with both irritable bowel syndrome and interstitial cystitis. Urology. 1996;47(3):436-8.

120. Saban R, Gerard NP, Saban MR, et al. Mast cells mediate substance P-induced bladder inflammation through an NK(1) receptor-independent mechanism. Am J Physiol Renal Physiol. 2002;283(4):F616-29.

121. Wang X, Liu W, O'Donnell M, et al. Evidence for the Role of Mast Cells in Cystitis-Associated Lower Urinary Tract Dysfunction: A Multidisciplinary Approach to the Study of Chronic Pelvic Pain Research Network Animal Model Study. PLoS One. 2016;11(12):e0168772.

122. Suvas S. Role of Substance P Neuropeptide in Inflammation, Wound Healing, and Tissue Homeostasis. J Immunol. 2017;199(5):1543-52.

123. Chiu IM, von Hehn CA, Woolf CJ. Neurogenic inflammation and the peripheral nervous system in host defense and immunopathology. Nat Neurosci. 2012;15(8):1063-7.

124. Xu J, Xu F, Lin Y. Cigarette smoke synergizes lipopolysaccharide-induced interleukin-1beta and tumor necrosis factor-alpha secretion from macrophages via substance P-mediated nuclear factor-kappaB activation. Am J Respir Cell Mol Biol. 2011;44(3):302-8.

125. Guo CJ, Douglas SD, Gao Z, et al. Interleukin-1beta upregulates functional expression of neurokinin-1 receptor (NK-1R) via NF-kappaB in astrocytes. Glia. 2004;48(3):259-66.

126. Hooton TM. Recurrent urinary tract infection in women. Int J Antimicrob Agents. 2001;17(4):259-68.

127. Stamm WE. Urinary tract infections. Infect Dis Clin North Am. 2003;17(2):xiii-xiv.

128. Vik I, Bollestad M, Grude N, et al. Ibuprofen versus mecillinam for uncomplicated cystitis--a randomized controlled trial study protocol. BMC Infect Dis. 2014;14:693.

129. Frenkl TL, Zhu H, Reiss T, et al. A multicenter, double-blind, randomized, placebo controlled trial of a neurokinin-1 receptor antagonist for overactive bladder. J Urol. 2010;184(2):616-22.

130. Green SA, Alon A, Ianus J, et al. Efficacy and safety of a neurokinin-1 receptor antagonist in postmenopausal women with overactive bladder with urge urinary incontinence. J Urol. 2006;176(6 Pt 1):2535-40; discussion 40.

131. Haab F, Braticevici B, Krivoborodov G, et al. Efficacy and safety of repeated dosing of netupitant, a neurokinin-1 receptor antagonist, in treating overactive bladder. Neurourol Urodyn. 2014;33(3):335-40.

132. Tillisch K, Labus J, Nam B, et al. Neurokinin-1-receptor antagonism decreases anxiety and emotional arousal circuit response to noxious visceral distension in women with irritable bowel syndrome: a pilot study. Aliment Pharmacol Ther. 2012;35(3):360-7.

133. Martins SM, Darlin DJ, Lad PM, et al. Interleukin-1B: a clinically relevant urinary marker. J Urol. 1994;151(5):1198-201.

134. Wakabayashi Y, Tomoyoshi T, Fujimiya M, et al. Substance P-containing axon terminals in the mucosa of the human urinary bladder: pre-embedding immunohistochemistry using cryostat sections for electron microscopy. Histochemistry. 1993;100(6):401-7.

135. Marchand JE, Sant GR, Kream RM. Increased expression of substance P receptor-encoding mRNA in bladder biopsies from patients with interstitial cystitis. Br J Urol. 1998;81(2):224-8.

136. Duell BL, Carey AJ, Tan CK, et al. Innate transcriptional networks activated in bladder in response to uropathogenic Escherichia coli drive diverse biological pathways and rapid synthesis of IL-10 for defense against bacterial urinary tract infection. J Immunol. 2012;188(2):781-92.

137. Altuntas SC, Ipekci T, Yakupoglu G, et al. Changes in urine levels of substance P, vasoactive intestinal peptide and calcitonin-gene-related peptide in patients with urinary tract infections. Peptides. 2014;56:151-5.

138. Campbell DJ, Tenis N, Rosamilia A, et al. Urinary levels of substance P and its metabolites are not increased in interstitial cystitis. BJU Int. 2001;87(1):35-8.

139. Kushner L, Chiu PY, Brettschneider N, et al. Urinary substance P concentration correlates with urinary frequency and urgency in interstitial cystitis patients treated with intravesical dimethyl sulfoxide and not intravesical anesthetic cocktail. Urology. 2001;57(6 Suppl 1):129.

140. Pennycuff JF, Schutte SC, Hudson CO, et al. Urinary neurotrophic peptides in postmenopausal women with and without overactive bladder. Neurourol Urodyn. 2017;36(3):740-4.

I.

PLOS | PATHOGENS

RESEARCH ARTICLE

Molecular Basis of Acute Cystitis Reveals Susceptibility Genes and Immunotherapeutic Targets

Ines Ambite[1☯], Manoj Puthia[1☯], Karoly Nagy[1☯], Caterina Cafaro[1], Aftab Nadeem[1], Daniel S. C. Butler[1], Gustav Rydström[1], Nina A. Filenko[1], Björn Wullt[1], Thomas Miethke[2], Catharina Svanborg[1]*

1 Division of Microbiology, Immunology and Glycobiology, Department of Laboratory Medicine, Lund University, Lund, Sweden, **2** Institute of Medical Microbiology and Hygiene, Medical Faculty of Mannheim, University of Heidelberg, Mannheim, Germany

☯ These authors contributed equally to this work.
* catharina.svanborg@med.lu.se

Citation: Ambite I, Puthia M, Nagy K, Cafaro C, Nadeem A, Butler DSC, et al. (2016) Molecular Basis of Acute Cystitis Reveals Susceptibility Genes and Immunotherapeutic Targets. PLoS Pathog 12(10): e1005848. doi:10.1371/journal.ppat.1005848

Editor: Dana J. Philpott, University of Toronto, CANADA

Received: April 22, 2016

Accepted: August 6, 2016

Published: October 12, 2016

Data Availability Statement: All microarray data files are available from the NCBI's Gene Expression Omnibus database (accession number GSE86096).

Funding: We gratefully acknowledge the support of the Swedish Research Council, Medical Faculty (Lund University), Swedish Cancer Society, the Sharon D Lund, Söderberg and Österlund Foundations, the Anna-Lisa and Sven-Erik Lundgren-, Maggie Stephens-, Inga-Britt and Arne Lundberg- and HJ Forssman Foundations, the Royal Physiographic Society and the Network of Excellence: EuroPathoGenomics. KN was

Abstract

Tissue damage is usually regarded as a necessary price to pay for successful elimination of pathogens by the innate immune defense. Yet, it is possible to distinguish protective from destructive effects of innate immune activation and selectively attenuate molecular nodes that create pathology. Here, we identify acute cystitis as an Interleukin-1 beta (IL-1β)-driven, hyper-inflammatory condition of the infected urinary bladder and IL-1 receptor blockade as a novel therapeutic strategy. Disease severity was controlled by the mechanism of IL-1β processing and mice with intact inflammasome function developed a moderate, self-limiting form of cystitis. The most severe form of acute cystitis was detected in mice lacking the inflammasome constituents ASC or NLRP-3. IL-1β processing was hyperactive in these mice, due to a new, non-canonical mechanism involving the matrix metalloproteinase 7- (MMP-7). ASC and NLRP-3 served as transcriptional repressors of *MMP7* and as a result, *Mmp7* was markedly overexpressed in the bladder epithelium of *Asc*$^{-/-}$ and *Nlrp3*$^{-/-}$ mice. The resulting IL-1β hyper-activation loop included a large number of IL-1β-dependent pro-inflammatory genes and the IL-1 receptor antagonist Anakinra inhibited their expression and rescued susceptible *Asc*$^{-/-}$ mice from bladder pathology. An MMP inhibitor had a similar therapeutic effect. Finally, elevated levels of IL-1β and MMP-7 were detected in patients with acute cystitis, suggesting a potential role as biomarkers and immunotherapeutic targets. The results reproduce important aspects of human acute cystitis in the murine model and provide a comprehensive molecular framework for the pathogenesis and immunotherapy of acute cystitis, one of the most common infections in man.

Trial Registration

The clinical studies were approved by the Human Ethics Committee at Lund University (approval numbers LU106-02, LU236-99 and Clinical Trial Registration RTP-A2003, International Committee of Medical Journal Editors, www.clinicaltrials.gov).

supported by the European Urological Scholarship Program (EUSP/Scholarship S-03-2013). TM was supported by Deutsche Forschungsgemeinschaft, Grant MI471/6-1. The funders had no role in study design, data collection and analysis, decision to publish, or preparation of the manuscript.

Competing Interests: The authors have declared that no competing interests exist.

Author Summary

Infections continue to threaten human health as pathogenic organisms outsmart available therapies with remarkable genetic versatility. Fortunately, microbial versatility is matched by the flexibility of the host immune system which provide a rich source of novel therapeutic concepts. Emerging therapeutic solutions include substances that strengthen the immune system rather than killing the bacteria directly. Selectivity is a concern, however, as boosting of the antibacterial immune response may cause collateral tissue damage. This study addresses how the host response to urinary bladder infection causes acute cystitis and how this response can be attenuated in patients who suffer from this very common condition. We identify the cytokine Interleukin-1 beta (IL-1β) as a key immune response determinant in acute cystitis and successfully treat mice with severe acute cystitis by inhibiting IL-1β or the enzyme MMP-7 that processes IL-1β to its active form. Finally, we detect elevated levels of these molecules in urine samples from patients with cystitis, suggesting clinical relevance and a potential role of IL-1β and MMP-7 both as therapeutic targets and as biomarkers of infection. These findings provide a much needed, molecular framework for the pathogenesis and treatment of acute cystitis.

Introduction

Acute cystitis is rapidly becoming a therapeutic enigma, as antibiotic resistance is reducing the options to a minimum [1–4]. Fortunately, new insights are now making it possible to explore immune response modifiers as alternatives to antibiotics. Acute cystitis occurs predominantly in girls and women with normal urinary tracts and at least 60% of all females will report an episode during their lifetime [5–7]. The recurrence rate is high, especially in a subset of patients, where severe, often recurrent cystitis episodes may cause chronic tissue damage and negatively impact the quality of life [8]. In addition, acute cystitis patients pose a highly significant challenge to the health care system. This study addresses if immunotherapy might be a relevant complement to antibiotics, in this patient group.

The urinary bladder mucosa is often exposed to bacteria but does not always retaliate with full force. In patients with acute cystitis, infection triggers a rapid and potent innate immune and inflammatory response in the bladder mucosa and clinical symptoms include pain, urgency and frequency of urination [9–12]. The molecular basis of these symptoms is not well understood, but bacterial interactions with the bladder epithelium have been shown to create inflammatory cascades [13–15], which also involve adjacent mucosal cells, such as mast cells and macrophages [16–20]. In asymptomatic carriers, the mucosa is exposed to bacteria of lower virulence and the mucosa remains fairly unresponsive, despite the presence of large numbers of bacteria in the lumen [21–24]. Asymptomatic bacteriuria (ABU) strains have evolved a mechanism to avoid elimination by the innate immune defense, through effects on RNA polymerase II and inhibition of host gene expression [22, 25]. It is therefore challenging to understand, at the molecular level, how a state of exaggerated mucosal inflammation can be generated specifically in acute cystitis patients. The specific molecular interactions that drive the transition from a homeostatic innate immune response to bladder disease remain unclear.

This study examined how innate immune response genes influence the outcome of bladder infection and the pathogenesis of acute cystitis. We identify acute cystitis as an IL-1β-driven, hyper-inflammatory disease [26, 27], possibly related to other hyper-inflammatory disorders [28, 29]. Consistent with such a role, *Il1b*$^{-/-}$ mice were protected from infection and pathology. In contrast *Asc*$^{-/-}$ and *Nlrp3*$^{-/-}$ mice developed progressive IL-1β-driven bladder inflammation

and severe pathology, caused by a new, non-canonical IL-1β processing mechanism, involving the metalloproteinase MMP-7. We also identified the inflammasome constituents ASC (Apoptosis-associated speck-like protein containing a CARD) and NLRP-3 (NACHT, LRR and PYD domains-containing protein 3) as negative regulators of *MMP7*, explaining why MMP-7 is overexpressed in the mucosa of *Asc*$^{-/-}$ and *Nlrp3*$^{-/-}$ mice and the resulting state of IL-1β hyper-activation. Using IL-1β and MMP-7 as targets for immunotherapy, we succeeded in protecting susceptible *Asc*$^{-/-}$ mice against acute cystitis, confirming the potential of immunotherapy for this indication.

Results

Acute cystitis strains elicit an IL-1β response in human bladder epithelial cells

To address how infection creates a hyper-inflammatory state in patients with acute cystitis, we first infected the human bladder epithelial cell line HTB-9 *in vitro* and quantified inflammatory mediators in cell supernatants. We detected an increase in IL-1β secretion, four hours after infection with acute cystitis (CY) strains CY-17, CY-92, CY-132 or the uropathogenic *Escherichia coli* strain CFT073 ($P < 0.001$, compared to uninfected cells, two-tailed unpaired *t*-test). In contrast, the IL-1β response was low in cells infected with the ABU strain *E. coli* 83972, indicating a virulence-association (Fig 1A). IL-1β secretion was not detected in kidney epithelial cell supernatants after infection with the same strains, suggesting specificity for the bladder epithelium (Fig 1B). Western blot analysis confirmed that mature IL-1β was present in the supernatants of the infected HTB-9 cells (4 hours), as well as unprocessed pro-IL-1β and N-terminal fragment (Fig 1C). A rapid increase in IL-1β staining intensity was observed by confocal microscopy, in cells infected for one hour with 10^5 CFU/ml of CY-17, CY-92 and CFT073 compared to uninfected cells or cells infected with the ABU strain (Fig 1D and 1E, two-tailed unpaired *t*-test). This increase in cellular IL-1β levels was confirmed by Western blot analysis of whole cell extracts (Fig 1F and 1G). At this time (1 hour), low levels of pro-IL-1β were detected. There was no significant reduction in cell viability after one ($\geq$ 95% viable) or four hours ($\geq$ 90% viable), as quantified by PrestoBlue staining and no evidence of pyroptosis after one hour, when the increase in cellular IL-1β levels was detected (S1 Fig). The presence of unprocessed pro-IL-1β in the 4 hour supernatant might be due to secretion of unprocessed IL-1β *via* exosomes [30].

To address if IL-1β activation is a characteristic of acute cystitis strains, we infected human bladder epithelial cells with an epidemiologically defined collection of pediatric acute cystitis isolates ($n = 67$, [31, 32]). The majority of these strains (85%) triggered an IL-1β response > 5 pg/ml and 64% of those triggered a high response (40–1,000 pg/ml, Fig 1H). We also examined a collection of pediatric ABU strains ($n = 62$, [31, 33]), which was obtained by screening infants and children in the same geographic area for bacteriuria in the absence of urinary tract infection (UTI) symptoms. In contrast to the CY strains, most of the ABU strains did not trigger a strong IL-1β response (61% < 5 pg/ml), resulting in significantly higher mean IL-1β concentrations in supernatants of bladder cells infected with the CY strains than the ABU strains (121.8 and 32.4 pg/ml respectively, $P < 0.001$, Fig 1H). To address if the secretion of IL-1β was influenced by bacterial hemolysin [19, 20], IL-1β concentrations were examined as a function of hemolytic activity in 40 CY and 38 ABU strains (Fig 1I). There was no significant difference in IL-1β response between hemolysin positive and negative strains ($P = 0.07$, Mann Whitney unpaired test). In the cystitis subset, a significant difference between hemolysin positive and negative strains was observed, however ($P = 0.01$, Mann Whitney unpaired test), suggesting that hemolytic cell lysis may contribute to the IL-1β activating virulent phenotype of the acute

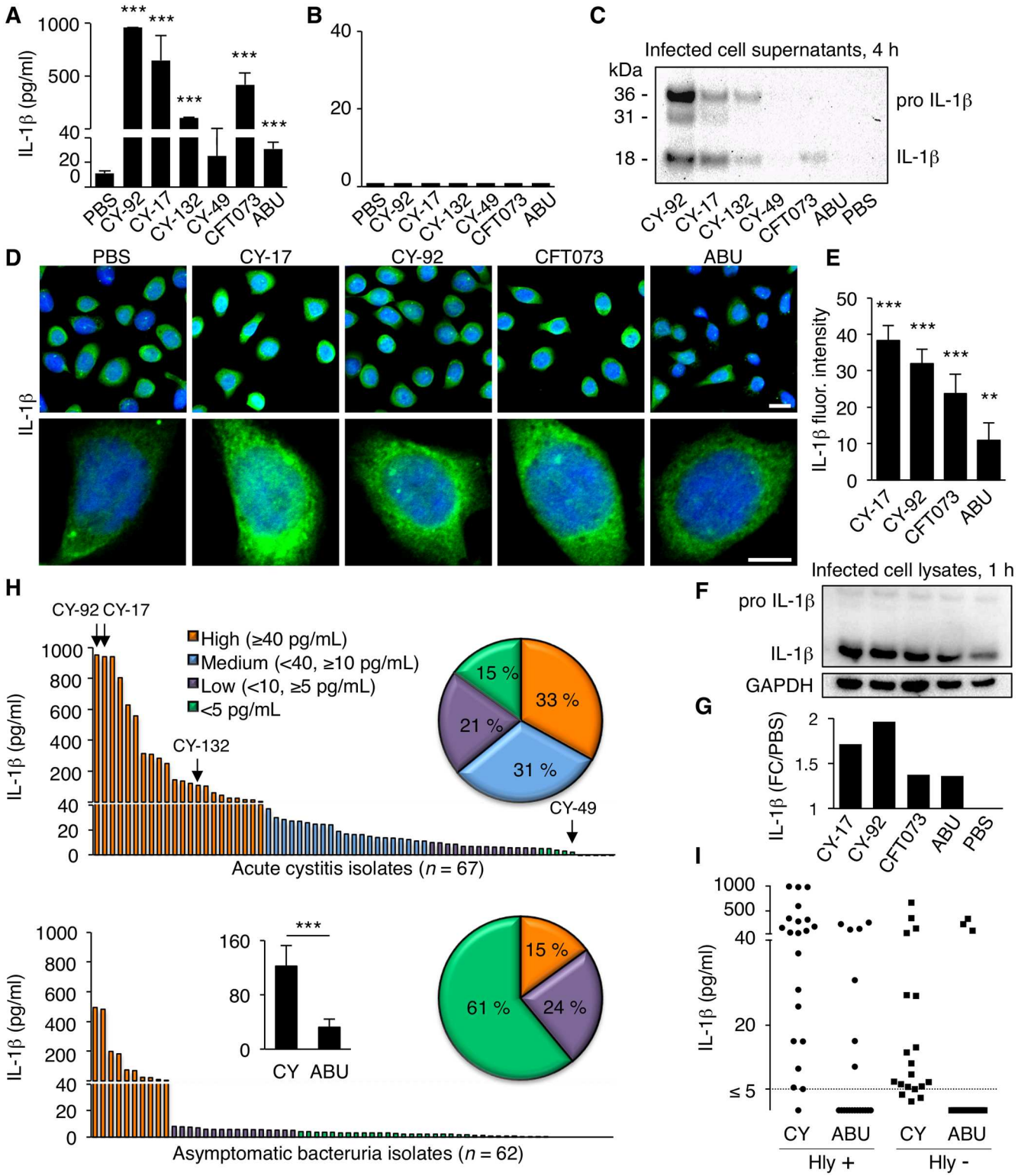

Fig 1. Acute cystitis strains activate an IL-1β response in human bladder epithelial cells. (**A**) IL-1β response in human bladder epithelial carcinoma cells (HTB-9) infected with acute cystitis strains CY-92, CY-17, CY-132 and CY-49 (4 hours). CFT073 and *E. coli* 83972 (ABU) were used as reference strains. CY-17, CY-92 and CY-132 triggered high IL-1β responses, as did CFT073. IL-1β was quantified, in cell supernatants, by ELISA (means ± SEMs of three independent experiments, *** $P < 0.001$ compared to PBS, two-tailed unpaired *t*-test). (**B**) Lack of IL-1β secretion by infected human kidney epithelial carcinoma cells (A498), infected as in **Fig 1A**. (**C**) Increased pro-IL-1β and mature IL-1β levels in

HTB-9 cells infected with CY-92, CY-17 and CY-132 (Western blot analysis of cell supernatants, 4 hours, one representative experiment of several repeats). (**D**) IL-1β staining of HTB-9 cells infected with CY-17, CY-92, CY-132, CFT073 or ABU compared to the background in uninfected cells (PBS). Scale bars = 20 μm (upper panel) and 10 μm (lower panel). One representative experiment is shown. (**E**) Quantification of the cellular IL-1β response to infection. Increase in total fluorescence intensity (open pin-hole) after subtraction of the background staining in uninfected cells (PBS) (means ± SEMs of 50 cells per sample, ** $P < 0.01$ and *** $P < 0.001$ compared to PBS, two-tailed unpaired *t*-test). One of three experiments is shown. (**F, G**) IL-1β response to infection (1 hour) quantified by Western blot of whole cell extracts. Quantification of integrated density relative to GAPDH normalized against the background of uninfected cells. One representative experiment of several repeats. (**H**) IL-1β response to an epidemiologically defined collection of pediatric acute cystitis strains ($n = 67$) compared to ABU strains ($n = 62$), obtained from children in the same geographic area. IL-1β was quantified in infected cell supernatants, by ELISA. Pie chart depicting the frequency of bacterial strains activating IL-1β responses: high (orange), intermediate (blue), low (purple) or negative (green). Histogram (inset) of the mean IL-1β response to CY versus ABU strains (means ± SEMs, *** $P < 0.001$, two-tailed Mann Whitney test). (**I**) IL-1β activation plotted against hemolytic activity in the collection of CY and ABU strains. No significant association was detected ($n = 18$–21, Hly+ versus Hly-, two-tailed Mann Whitney test).

doi:10.1371/journal.ppat.1005848.g001

cystitis strains, for example by assisting the release of IL-1β from cells infected with hemolysin-producing strains.

The results suggest that the majority of acute cystitis strains activate an IL-1β response in human bladder epithelial cells.

Genetic control of acute cystitis in the murine UTI model

As IL-1β is processed by the inflammasome, we subsequently examined if mice with intact or defective inflammasome function develop acute cystitis. We infected mice with genetic defects affecting the NLRP-3 inflammasome: NLRP-3 deficient mice (*Nlrp3*$^{-/-}$ [34]) or ASC deficient mice (*Asc*$^{-/-}$ [35]). In addition, *Il1b*$^{-/-}$ [36] and *Casp1*$^{-/-}$ [37] mice were used and C57BL/6 WT mice were included as controls (Fig 2). For sample sizes and number of experiments, please see each figure legend and an overview in S1 Table. The mice were infected by intravesical inoculation with *E. coli* strains that triggered high IL-1β responses in human bladder epithelial cells, *in vitro* (CFT073, CY-17 or CY-92). Infected bladders were evaluated macroscopically, at sacrifice after 7 days and assigned a gross pathology score, defined by size, edema and hyperemia. Tissue pathology was further evaluated by hematoxylin and eosin (H&E) staining and immunohistochemistry of frozen tissue sections, and a histo-pathology score was assigned to each mouse. Histology was scored, independently, by two experienced researchers. The analysis was not blinded. Infection kinetics was followed in urine samples obtained after 6 and 24 hours, 3 and 7 days.

Major, genotype-specific differences in bladder inflammation and pathology were detected after seven days (Fig 2). Two disease end points were distinguished. 1. Severe, progressive cystitis in mice lacking ASC or NLRP-3, resembling chronic human disease. 2. A moderate, self-limiting form of acute cystitis in C57BL/6WT mice with intact inflammasome function, resembling sporadic human cystitis.

Infected *Asc*$^{-/-}$ and *Nlrp3*$^{-/-}$ mice developed severe, acute cystitis with enlarged bladders, edema and hyperemia compared to uninfected bladders (Fig 2A and S2A Fig). By histology, most bladders from *Asc*$^{-/-}$ mice showed extensive loss of tissue structure, defined by a pronounced mucosal and submucosal edema, with disappearance of the tissue folds that characterizes the healthy mucosa. In addition, a massive inflammatory cell infiltrate was present, along the mucosal border and in the submucosa (10/14 mice, 71%). Similar tissue destruction was observed in bladders from *Nlrp3*$^{-/-}$ mice (7/11 mice, 64%), (Fig 2B). Mean gross bladder pathology score of infected *Asc*$^{-/-}$ and *Nlrp3*$^{-/-}$ mice were 7.9 and 7.2, respectively (Fig 2C).

Bladder pathology was accompanied by high bacterial counts in urine and bladder tissue (Fig 2D–2F). In *Asc*$^{-/-}$ mice, the neutrophil influx accelerated until day 7, indicating a loss of homeostatic control and progression to chronic inflammation. Infiltrating bacteria and neutrophil aggregates or micro-abscesses were detected in the mucosa of *Asc*$^{-/-}$ and *Nlrp3*$^{-/-}$ mice, with

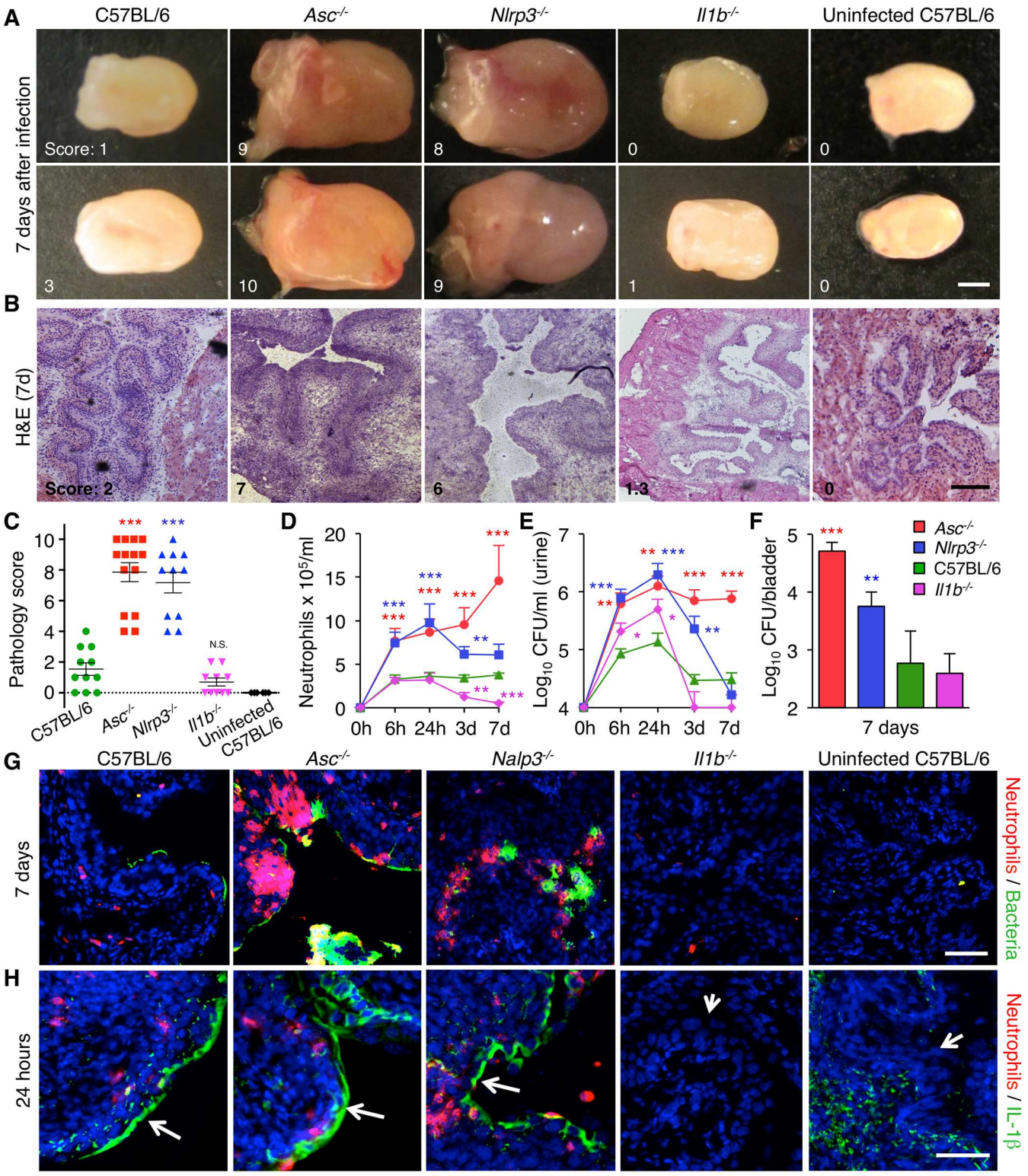

Fig 2. Genetic control of inflammation in acute cystitis. (**A**) Macroscopic evidence of acute cystitis in CFT073 infected mice, 7 days after infection. Slight increase in edema and hyperemia in C57BL/6 WT mice compared to uninfected controls, massively enlarged, hyper-inflamed bladders in *Asc*$^{-/-}$ and *Nlrp3*$^{-/-}$ mice and intact morphology in bladders from *Il1b*$^{-/-}$ mice. The macroscopic pathology score was based on edema, hyperemia and size on a scale of 0–10, where 10 the most edematous, hyperemic and largest bladder). Individual pathology scores are indicated. Scale bar = 1 mm. Two representative bladders are shown for each genotype. (For uninfected *Asc*$^{-/-}$, *Nlrp3*$^{-/-}$ and *Il1b*$^{-/-}$ mice see S2A Fig). (**B**)

Bladder tissue structure in H&E-stained tissue sections. Bladders from *Asc*$^{-/-}$ and *Nlrp3*$^{-/-}$ mice showed extensive edema, a loss of tissue structure and epithelial hypertrophy, compared to C57BL/6 WT and *Il1b*$^{-/-}$ mice or uninfected control mice. The histology score was assessed using H&E stained bladder sections based on neutrophil infiltration, tissue architecture and epithelial thickness on a scale of 0–10, where 10 is highest neutrophil infiltration, least preserved tissue architecture and maximum epithelial thickness). Individual histology scores are indicated. Scale bar = 200 μm. (**C**) Gross bladder pathology score in infected mice (7 days) and uninfected C57BL/6 WT controls (means ± SEMs of two experiments, *** $P < 0.001$, two-tailed unpaired *t*-test compared to WT mice). (**D**) Elevated neutrophil counts and (**E**) bacterial counts in urine and (**F**) bladder tissues from *Asc*$^{-/-}$ and *Nlrp3*$^{-/-}$ mice, compared to WT and *Il1b*$^{-/-}$ mice. Means ± SEMs of two experiments, *** $P < 0.001$, ** $P < 0.01$, * $P < 0.05$, two-tailed unpaired *t*-test compared to WT mice. (**G**) Detection of neutrophils and bacteria in the mucosa of infected and control mice, by immunohistochemistry. Increased staining for mucosal neutrophils (red) and bacteria (green) in *Asc*$^{-/-}$ and *Nlrp3*$^{-/-}$ mice, compared to C57BL/6 WT, *Il1b*$^{-/-}$ mice and uninfected controls. Tissues obtained 7 days after infection. Scale bar = 50 μm. (**H**) Mucosal IL-1β staining in bladder tissue sections, obtained 24 hours after infection. Infection increased epithelial IL-1β staining in C57BL/6 WT, *Asc*$^{-/-}$ and *Nlrp3*$^{-/-}$ mice. Scale bar = 50 μm. Experiments included 14 *Asc*$^{-/-}$, 11 *Nlrp3*$^{-/-}$, 11 C57BL/6 WT and 10 *Il1b*$^{-/-}$ mice.

doi:10.1371/journal.ppat.1005848.g002

extensive sloughing of epithelial cells into the lumen. Bacteria were mainly localized along the mucosal surface, with no evidence of bacterial invasion (Fig 2G). This hyper-inflammatory phenotype was also observed after infection of *Asc*$^{-/-}$ mice with the acute cystitis strains CY-92 and CY-17, which triggered high IL-1β responses *in vitro* (S3A–S3D Fig). In contrast, there was no disease phenotype in *Asc*$^{-/-}$ mice infected with the ABU strain *E. coli* 83972 or in C57BL/6 WT mice after 24 hours or 7 days (S3E Fig). There was no evidence of kidney involvement or pathology in mice infected with CY-92 and CY-17, despite positive bacterial cultures from renal tissues.

In contrast, C57BL/6 WT mice infected with CFT073 showed moderate macroscopic evidence of acute cystitis including a small increase in size, edema and hyperemia compared to uninfected controls (Fig 2A and 2C, mean pathology score 1.5). The low level of edema was confirmed by histology, with no evidence of tissue damage (Fig 2B). Infection was accompanied by an increase in urine neutrophil numbers (Fig 2D) and bacterial numbers reached a peak after 24 hours and then declined (Fig 2E and 2F). By immunohistochemistry, bacterial staining was weak and very few neutrophils were detected in the bladder mucosa (Fig 2G).

Il1b$^{-/-}$ mice showed an even more attenuated phenotype after infection with CFT073, consistent with a key role of IL-1β for bladder inflammation and pathology compared to uninfected bladders (Fig 2A and S2A Fig). There was no macroscopic evidence of acute cystitis (Fig 2A and 2C, mean pathology score 0.7) and bladder tissue morphology remained intact (Fig 2B, mean histo-pathology score 0.9, $P = 0.003$ compared to C57BL/6 WT mice). *Il1b*$^{-/-}$ mice had fewer infiltrating neutrophils and lower bacterial counts than the C57BL/6 WT mice on day seven ($P < 0.001$ and $P < 0.05$), (Fig 2D–2F). Furthermore, *Casp1*$^{-/-}$ mice, which have a functional IL-1β deficiency due to defective IL-1β processing and secretion [37], did not develop acute cystitis (S4A–S4D Fig). The bladders were enlarged and hyperemic, but there was no evidence of inflammatory changes or tissue damage. *Casp1*$^{-/-}$ mice showed reduced IL-1β secretion and tissue retention of IL-1β (S4E–S4G Fig). As a result, IL-1β dependent gene expression was low and *Casp1*$^{-/-}$ mice showed a lack of inflammation in bladder tissues. Neutrophils and bacteria were present in urine but did not accumulate in the tissues and the mucosal morphology was intact (S4 Fig).

Infection was accompanied by strong mucosal IL-1β staining in bladder tissue sections in C57BL/6 WT mice, *Asc*$^{-/-}$ and *Nlrp3*$^{-/-}$ mice after 24 hours (Fig 2H). Staining was mainly epithelial and was not seen in *Il1b*$^{-/-}$ mice or uninfected C57BL/6 WT mice. In parallel with the epithelial staining IL-1β was detected by ELISA in the urine of infected *Asc*$^{-/-}$ and *Nlrp3*$^{-/-}$ mice, with lower levels in C57BL/6 WT mice. By Western blot analysis, bands of approximately 36 and 18 kDa were detected (S2B Fig).

These studies identify genetic determinants of host susceptibility to acute cystitis. *Asc* and *Nlrp3* were defined as key resistance determinants and IL-1β activation as a crucial step in the pathogenesis of acute cystitis.

Asc and *Nlrp3* control gene expression in infected bladders

To define the mechanism of bladder pathology, we extracted total bladder RNA from infected *Asc*$^{-/-}$ and *Nlrp3*$^{-/-}$ mice with the highest pathology score after seven days and from C57BL/6 WT and *Il1b*$^{-/-}$ mice, with low pathology scores (Experiments 1 and 2 in S1 Table) and from uninfected bladders. The RNA was amplified, hybridized onto Mouse Genome array strips, washed, stained and scanned using the GeneAtlas system. Significantly altered genes were identified, by comparing infected- to uninfected mice of the same genetic background (*P*-values < 0.05 and absolute fold change > 1.41) and sorted by relative expression using 2-way ANOVA [38]. Heat-maps were constructed by Gitools 2.1.1 software and differentially expressed genes and regulated pathways were analyzed by Ingenuity Pathway Analysis software (see Materials and Methods).

We identified a set of strongly upregulated genes in *Asc*$^{-/-}$ and *Nlrp3*$^{-/-}$ mice with the highest bladder pathology score, but not in C57BL/6 WT mice or *Il1b*$^{-/-}$ mice (2,228 specifically regulated genes). The heat map in Fig 3A illustrates the similarities in gene expression between 5/7 *Asc*$^{-/-}$ and 2/5 *Nlrp3*$^{-/-}$ mice analyzed by this technology. Those mice also had high and comparable histology scores, defined by evaluation of the H&E-stained bladder tissue sections from the corresponding mice. To further understand the disease process, we identified the most strongly upregulated genes in these mice. Genes with a FC > 100 included metalloproteinase *Mmp7*, the neutrophil and monocyte chemoattractants *Cxcl6* and *Cxcl3*, the genes encoding calprotectin *S100a8* and *a9* and the stefin gene *Stfa1* (Fig 3B and S2 Table). By analysis of top-scoring canonical pathways, these genes were shown to control granulocyte and leucocyte diapedesis and signaling, acute phase responses including IL-6 and IL-1β signaling, IL-1R expression and NF-κB-signaling and dendritic cell maturation (S5A Fig). These genes and pathways were not significantly regulated in C57BL/6 WT or *Il1b*$^{-/-}$ mice, supporting a disease association.

The activation of inflammasome-genes and IL-1β-dependent gene network was analyzed, using Qiagen's list of 84 key inflammasome genes (Fig 3C). In the *Asc*$^{-/-}$ and *Nlrp3*$^{-/-}$ mice with a high histo-pathology score, *Il1b* expression was activated (FC 10–41), as were IL-1β-dependent and inflammasome-related genes including *Cxcl1*, *Cxcl3* and *Il33* (FC 5–200), (Fig 3C). These genes and pathways were not significantly regulated in C57BL/6 WT or *Il1b*$^{-/-}$ mice (Fig 3C). *Il1a* expression was activated in *Asc*$^{-/-}$ and *Nlrp3*$^{-/-}$ mice with bladder pathology, but not among the 40 top-regulated genes (FC 1.6–8.7). *Il18*, *Casp11* and inflammasome-related NLRP genes were not transcriptionally regulated (S2 Table).

The results identify IL-1β driven pro-inflammatory genes that are activated, exclusively in *Asc*$^{-/-}$ and *Nlrp3*$^{-/-}$ mice with severe bladder pathology. This response was not detected in the kidneys of infected C57BL/6 WT mice (S5B Fig).

Mechanism of atypical IL-1β processing in infected bladders

The *Mmp7* gene, which encodes the matrix metalloproteinase (MMP)-7 [39] was strongly upregulated in *Asc*$^{-/-}$ and *Nlrp3*$^{-/-}$ mice with a high histo-pathology score (Fig 3B). MMP-7 expression was therefore examined as a function of the histo-pathology score (Fig 4A). In *Asc*$^{-/-}$ and *Nlrp3*$^{-/-}$ mice, *Mmp7* expression showed a clear association to the overall bladder tissue pathology score and was not regulated in the *Il1b*$^{-/-}$ or C57BL/6 WT mice (Fig 4A). High MMP-7 protein expression was confirmed, by immunohistochemistry, in bladder tissue sections from *Asc*$^{-/-}$ and *Nlrp3*$^{-/-}$ mice (Fig 4B). Importantly, staining was exclusively epithelial, with shedding of MMP-7 positive cells into the bladder lumen. Epithelial MMP-7 activation was detected as early as 24 hours after infection and importantly, MMP-7 showed no detectable co-localization with neutrophils in the mucosa or sub-mucosa (S6 Fig) To further evaluate the involvement of MMP-7 in acute cystitis, we infected *Mmp7*$^{-/-}$ mice [40] with CFT073 and used *Asc*$^{-/-}$ mice as

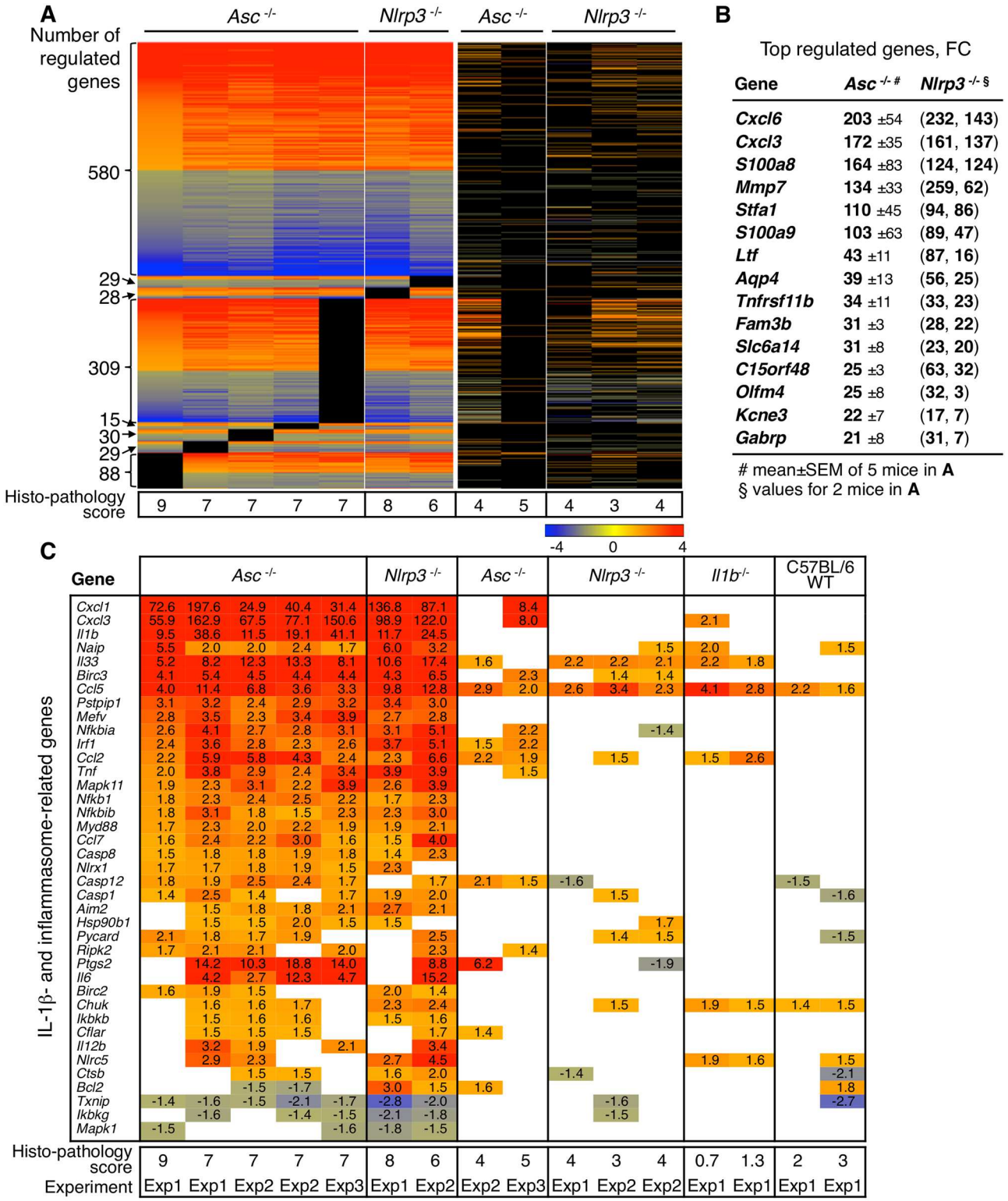

Fig 3. Hyper-activation of IL-1β dependent gene expression and bladder pathology in *Asc*$^{-/-}$ and *Nlrp3*$^{-/-}$ mice. Transcriptomic analysis of whole bladder RNA from infected mice (CFT073, 7 days), compared to uninfected controls of each genotype (cut off FC 1.41, $P < 0.05$). (**A**) Heatmap of regulated genes in *Asc*$^{-/-}$ and *Nlrp3*$^{-/-}$ mice with the highest bladder pathology score, defined by neutrophil infiltration, loss of tissue structure and epithelial thickness in H&E stained bladder tissue sections. Scale FC -4 to 4, red = upregulated, blue = downregulated. A distinct gene set distinguished the *Asc*$^{-/-}$ and *Nlrp3*$^{-/-}$ mice with a high histopathology score from C57BL/6 WT mice or *Il1b*$^{-/-}$ mice without pathology. (**B**) Top up-regulated genes in the pathology-associated gene set, compared to uninfected controls of each

genotype. Means ± SEMs of 5 mice for *Asc*$^{-/-}$ mice and 2 *Nlrp3*$^{-/-}$ mice. (**C**) Analysis of IL-1β, inflammasome activators and effectors in *Asc*$^{-/-}$ and *Nlrp3*$^{-/-}$ mice, detecting massive over-expression compared to *Il1b*$^{-/-}$ and WT mice. Red = upregulated, blue = suppressed. The data set included gene expression profiles from 7 *Asc*$^{-/-}$ and 5 *Nlrp3*$^{-/-}$ mice, and two each of the C57BL/6 WT and *Il1b*$^{-/-}$ controls. Uninfected control RNA of each genotype were used to define significantly regulated genes (≥ 2 mice per genotype). Histopathology scores and group numbers for individual mice (see also Experiments 1, 2 and 3 in S1 Table).

doi:10.1371/journal.ppat.1005848.g003

disease controls. Consistent with their intact inflammasome function, *Mmp7*$^{-/-}$ mice developed transient cystitis similar to C57BL/6 WT mice (Fig 4C). A moderate mucosal IL-1β response was observed by immunohistochemistry (Fig 4C). IL-1β levels in urine (Fig 4C) and IL-1β-dependent gene expression was comparable to that in WT mice, with expression of *Ccl5*, *Nlrc5*, *Irf1*, *Ctsb*, *Birc3*, and *MyD88*. Thus, *Mmp7* did not drive pathology in mice with intact ASC or NLRP-3 function.

To address if MMP-7 cleaves IL-1β, we exposed recombinant GST-tagged pro-IL-1β to recombinant active MMP-7 *in vitro* and detected proteolytic fragments by Western blot, using IL-1β specific antibodies (Fig 4D and S7A Fig). Kinetic analysis detected a time-dependent cleavage of IL-1β with a reduction in full-length protein from 10 to 60 minutes (Fig 4D). Using antibodies with higher affinity for the mature IL-1β, a band of 18 kDa was detected corresponding in size to the recombinant, active and mature IL-1β control. With increasing time, a band of 16 kDa was also observed (Fig 4D). Using the same experimental set up, we observed that ASC was degraded by MMP-7 over time (S7B Fig) while recombinant NLRP-3 was not cleaved by MMP-7 and therefore served as a negative control for unspecific effects of the enzyme (S7C Fig).

To address if the cleaved IL-1β fragments were biologically active, reaction mixtures containing pro-IL-1β and MMP-7 were collected after 30 minutes, when the mature product was detected by Western blot (Fig 4D). Human bladder epithelial cells were stimulated with the reaction mixture for one hour, and IL-1β activity was quantified, by measuring the prostaglandin E2 (PGE_2) response [41]. The 30 minutes reaction mixture activated a dose-dependent PGE_2 response but recombinant MMP-7 and pro-IL-1β (280 and 840 ng/ml) alone had no effect (Fig 4E).

The results identify a new, MMP-7-dependent mechanism of pro-IL-1β processing in *Asc*$^{-/-}$ and *Nlrp3*$^{-/-}$ mice.

NLRP-3 and ASC act as negative regulators of *MMP7* expression

To understand the mechanism of increased MMP-7 expression in infected *Asc*$^{-/-}$ and *Nlrp3*$^{-/-}$ mice, we examined if ASC and/or NLRP-3 may act as negative regulators of *MMP7* expression. After infection of human bladder epithelial cells, with CY-17 and CY-92, we detected a significant increase in MMP-7 staining (confocal microscopy, Fig 5A and 5B). In contrast, ASC staining was reduced after infection with the virulent strains ($P < 0.001$) and NLRP-3 showed a weaker staining ($P < 0.01$). The MMP-7 response to infection and the decrease in ASC and NLRP-3 levels were confirmed by Western blot analysis (Fig 5C).

ASC or NLRP-3 expression was subsequently inhibited by transfection of human bladder epithelial cells with *ASC*- or *NLRP3*- specific siRNAs and the effects on MMP-7 expression were examined by confocal imaging (Fig 5D and S8A Fig). MMP-7 expression increased drastically in transfected and infected cells, where the expression of *ASC* or *NLRP3* had been inhibited, but not in cells transfected with negative control siRNA (Fig 5D). Inhibition efficiency of ASC and NLRP-3 expression by specific siRNAs was confirmed by Western blot analysis. Infection of the cells with CY-17 caused a further decrease in ASC and NLRP-3 staining (Fig 5E, quantified in S8B Fig). Two protein bands where detected, one of 24 kDa, corresponding to the common ASC variant and one of 20 kDa (ASC-b), corresponding to an ASC variant that enhances IL-1β secretion in human promyelocytic leukemia cells (HL60) [42] (Fig 5E).

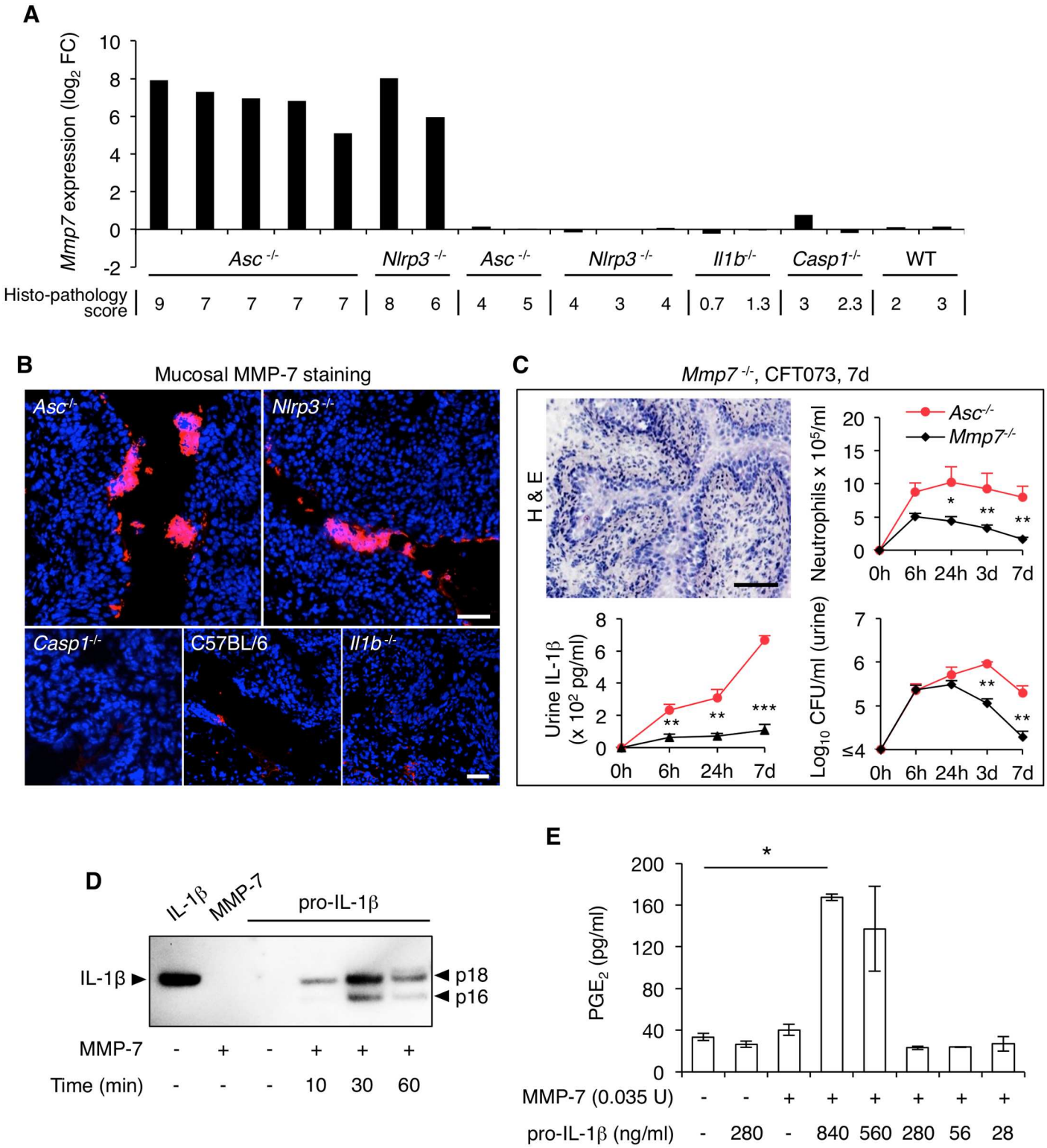

Fig 4. IL-1β processing by MMP-7. (**A**) Gene expression profiling identified *Mmp7* as one of the top up-regulated gene in *Asc*$^{-/-}$ and *Nlrp3*$^{-/-}$ mice with bladder pathology (CFT073 infected mice, 7 days). Log_2 fold change of *Mmp7* expression levels in individual mice are shown relative to the H&E pathology score. *Mmp7* was not regulated in C57BL/6 WT mice or in *Il1b*$^{-/-}$ or *Casp1*$^{-/-}$ mice. (**B**) Strong epithelial MMP-7 staining in *Asc*$^{-/-}$ and *Nlrp3*$^{-/-}$ mice with bladder pathology. MMP-7 staining was very low in C57BL/6 WT, *Il1b*$^{-/-}$ and *Casp1*$^{-/-}$ mice. Scale bars = 50 μm. (**C**) Phenotype of *Mmp7*$^{-/-}$ mice, 7 days after infection with CFT073. Intact mucosal tissue structure with inflammatory cell infiltration. Low bacterial and neutrophil counts in urine

compared to *Asc*$^{-/-}$ mice ($n = 5$ mice per group, means ± SEMs, ** $P < 0.01$, *** $P < 0.001$, two-tailed unpaired *t*-test). Scale bar = 1 mm. IL-1β levels were elevated in the urine of *Asc*$^{-/-}$ mice but not in *Mmp7*$^{-/-}$ mice, as detected by ELISA. (**D**) Proteolytic cleavage of pro-IL-1β by MMP-7 *in vitro*, using purified enzyme and GST-tagged pro-IL-1β. The IL-1β fragments generated by proteolysis were 18 and 16 kDa, defined by Western blot using an antibody specific for the mature form of IL-1β. Recombinant mature IL-1β and GST-tagged pro-IL-1β were used as controls, as well as recombinant MMP-7. One representative experiment out of three, see also S7A Fig. (**E**) Bioassay for IL-1β activity, measuring the PGE_2 response of human bladder epithelial cells to the IL-1β fragments generated by MMP-7 proteolysis of GST-tagged pro-IL-1β. The cleaved products activated PGE_2 but MMP-7 and pro-IL-1β had no effect (means ± SEMs of two experiments, ** $P < 0.01$, two-tailed Mann Whitney test).

doi:10.1371/journal.ppat.1005848.g004

To address if infection with cystitis strains modifies the interaction of ASC and NLRP-3 in cells, co-immunoprecipitation was performed. ASC was shown to pull down NLRP-3 in nuclear extracts of uninfected cells but after infection, a reduction in ASC/NLRP-3 interaction was detected suggesting that a loss of ASC/NLRP-3 interaction in the nuclear compartment accompanies *MMP7* activation (S8C Fig).

To determine if ASC and NLRP-3 interact with the *MMP7* promoter, DNA fragments spanning the entire promoter were used as probes in electrophoretic mobility shift assays (EMSA) (S9A Fig). A DNA fragment of 259 bp, adjacent to the transcription start site (P1, position -18/-276) was shown to interact with a nuclear protein extract from infected bladder cells, resulting in a significant band shift (Fig 5F and 5G). Specificity for ASC and NLRP-3 was confirmed by competition with specific antibodies (Fig 5G). In the absence of nuclear extract, the probe formed a single low molecular weight band, serving as a negative control. To confirm that ASC binds directly to the *MMP7* promoter, recombinant ASC protein was incubated with the 259 bp DNA sequence and examined by EMSA. Strong dose-dependent binding of ASC to *MMP7* promoter DNA was detected as a band shift, which was competitively inhibited by specific antibodies but not by the IgG isotype control (Fig 5H). Other *MMP7* promoter sequences did not interact with ASC or NLRP-3 in this assay (S9A and S9B Fig).

The results suggesting that NLRP-3 and ASC act as negative regulators of *MMP7* expression and identify an ASC binding site in *MMP7* promoter DNA, adjacent to the transcription start site.

Therapeutic attenuation of the IL-1β response

To address if IL-1β serves as target for immunomodulatory therapy, we selected the most susceptible genotype (*Asc*$^{-/-}$ mice) for treatment with the IL-1 receptor antagonist (IL-1RA) Anakinra. A dose of 1 mg per mouse in 100 μl of PBS was given intra-peritoneally, 30 minutes before infection and daily after infection with *E. coli* CFT073 (Fig 6A). This dose was selected based on previous studies in murine models [43].

A dramatic therapeutic effect was observed compared to infected *Asc*$^{-/-}$ control mice. By macroscopic evaluation, the extent of edema, hyperemia and enlargement was reduced, resulting in a significantly lower pathology score ($P < 0.001$), (Fig 6B and 6C). By histology, a reduced inflammatory response was seen in the bladders of treated mice and mucosal pathology was inhibited compared to untreated controls that developed extensive bladder pathology (Fig 6D). Mucosal neutrophil infiltration, which accompanies pathology, was prevented and urine neutrophil numbers were low (Fig 6E). As a control for unspecific effects of Anakinra on the bacteria, CFT073 was grown in Luria-Bertani with or without 500 ng/ml of IL-1RA for 10 hours. No difference in bacterial growth rate was detected (S10 Fig).

We subsequently treated susceptible *Asc*$^{-/-}$ mice with the matrix metalloproteinase inhibitor (MMPI) Batimastat. The MMPI was given 30 minutes before infection and on days 0–2 and 4–6 after infection (0.5 mg in 100 μl of PBS i.p., Fig 6A). The MMPI had a significant protective effect (Fig 6B–6D), detected by macroscopic evaluation, resulting in a reduced pathology score ($P = 0.002$). By histology neutrophil infiltration was reduced (Fig 6D). As in the IL-1RA-treated

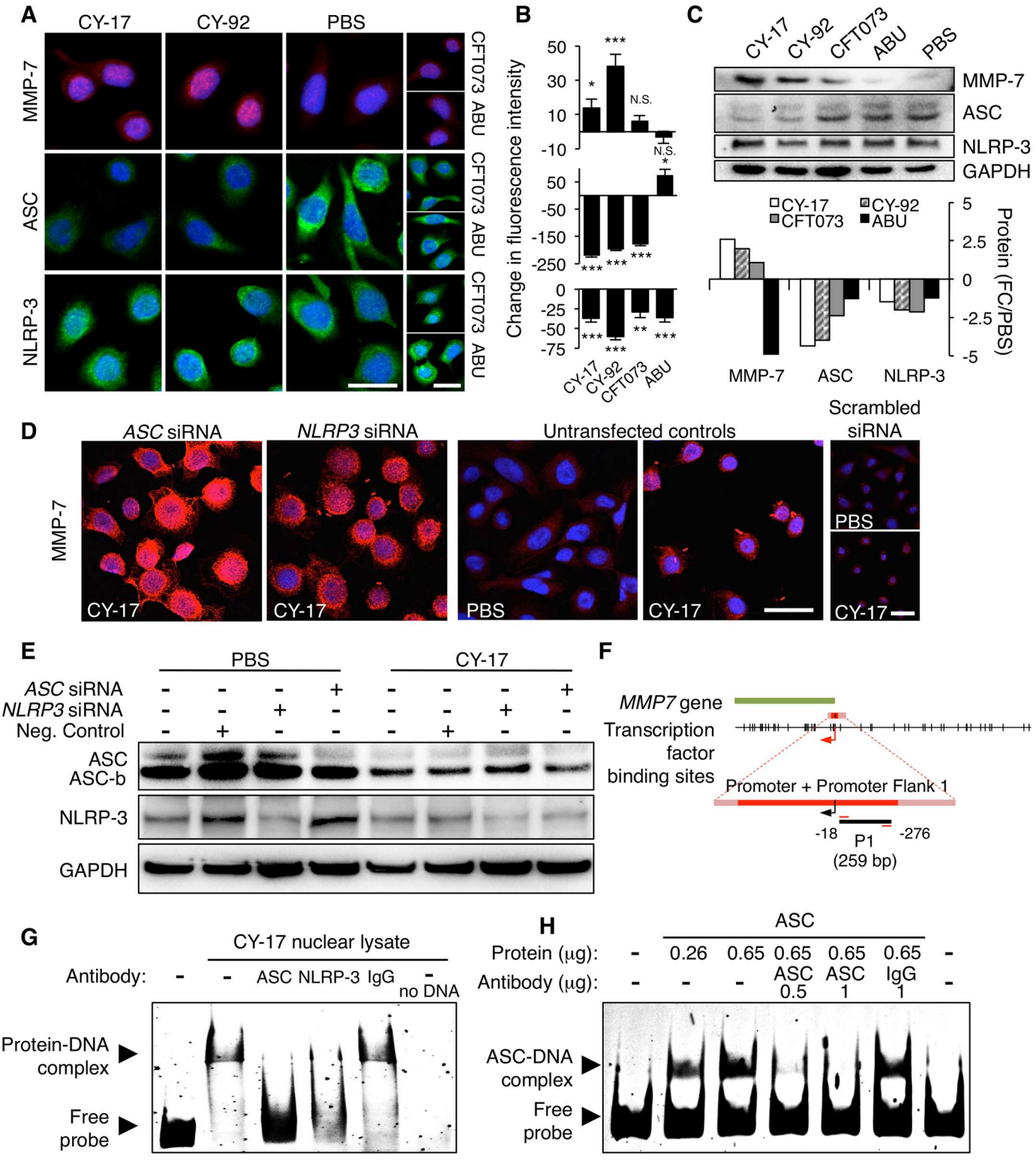

Fig 5. Regulation of *MMP7* expression by ASC and NLRP-3. (**A**) MMP-7, ASC and NLRP-3 responses to infection were visualized by confocal microscopy. An increase in MMP-7 and decrease in ASC staining were detected after infection of HTB-9 cells with CY-17 and CY-92 for 1 hour, compared to uninfected control cells. NLRP-3 staining was weakly affected. (**B**) Quantification of total fluorescence intensity (open pin-hole) after subtraction of the background staining in uninfected cells (PBS). Medians ± SEMs of 50 cells, * $P < 0.05$, ** $P < 0.01$, *** $P < 0.001$, compared to PBS control, two-tailed unpaired *t*-test (MMP-7 and NLRP-3) or two-tailed Mann Whitney test (ASC). One of three experiments is shown. (**C**) Western

blot confirming the change in cellular content of MMP-7, ASC and NLRP-3, 1 hour after infection with the indicated strains. Fold change compared to PBS of normalized values (against GAPDH). One experiment out of 2 is shown. (**D**) Increase in MMP-7 expression in HTB-9 cells transfected with siRNAs specific for *ASC* or *NLRP3* and infected with CY-17 (4 hours, scale bars = 20 μm). (**E**) Western blot confirming the knock-down of ASC or NLRP-3 with siRNAs. A further reduction in ASC expression was detected after CY-17 infection (4 hours, quantified in S8B Fig, one experiment out of 2 is shown.). (**F**) PCR amplification of a 259 bp fragment in the *MMP7* promoter (P1, -18/-276 relative to the transcription start site). (**G**) EMSA of the amplified fragment and nuclear extract from CY-17 infected HTB-9 cells (4 hours). Binding of ASC and NLRP-3 to P1 was identified as a band shift (arrow indicating protein-DNA complex). The band shift was inhibited by ASC- or NLRP-3-specific antibody. Free DNA formed a single low molecular weight band (arrow indicating free probe). The band shift was not affected by the IgG isotype control. One of three similar experiments is shown. (**H**) EMSA of the 259 bp *MMP7* promoter fragment P1 and recombinant ASC. Dose-dependent formation of an ASC-P1 complex is shown as a band shift (arrow indicating ASC-DNA complex), which was inhibited by 0.5 and 1.0 μg of anti-ASC antibodies. The band shift was not affected by negative control murine IgG control. One of three similar experiments is shown.

doi:10.1371/journal.ppat.1005848.g005

mice, bacterial numbers remained elevated (Fig 6E). Batimastat (250 ng/ml) did not affect bacterial growth *in vitro* for up to 10 hours. No difference in bacterial growth rate was detected (S10 Fig). As Batimastat is a broad metalloproteinase inhibitor, unspecific effects on other proteases might occur. Proteases inhibited by Batimastat other than MMP-7, were not transcriptionally regulated in any of the mice with acute cystitis or controls. MMP-15, which is not susceptible to Batimastat, was weakly activated in mice with bladder pathology (FC 2.0). These findings suggest that the therapeutic effect of Batimastat reflects inhibition of MMP-7.

The results confirm the importance of IL-1β and MMP-7 for the pathogenesis of acute cystitis and identify these molecules as functional targets for immunomodulatory therapy. Bacterial counts remained elevated in the IL-1RA and the MMPI treated mice in the absence of inflammation, suggesting that the treated $Asc^{-/-}$ mice might develop a condition more like asymptomatic bacteriuria than acute cystitis (Fig 6E).

IL-1β and MMP-7 responses in patients with acute cystitis

To examine the human relevance of the findings in the murine UTI model, we collected urine samples from patients with acute cystitis or ABU and quantified the IL-1β and MMP-7 levels, by ELISA (Fig 7). Samples from patients with sporadic episodes of acute cystitis were collected at the time of diagnosis, defined by a positive dipstick, dysuria, urgency and frequency of urination but no fever ($n = 9$). Samples were also obtained from patients with ABU ($n = 161$), who carried the prototype ABU strain *E. coli* 83972, following therapeutic inoculation [21]. The patients with ABU participated in a prospective study of *E. coli* 83972-inoculation with detailed monthly collection of symptom scores and urine samples. There were 20 patients with low symptom scores and 161 urine samples were obtained from this group.

We found elevated concentrations of IL-1β in patients with acute cystitis compared to the asymptomatic patient group (Fig 7A–7C) resulting in a means of 264.5 pg/ml and 1.5 pg/ml, respectively ($P < 0.001$).

In addition, all the patients with acute cystitis had positive MMP-7 levels, above the detection limit of 0.15 ng/ml (Fig 7D). In a subset of 28 ABU urine samples, the mean MMP-7 concentration was low, resulting in mean concentrations of 15.4 ng/ml and 4.3 ng/ml, respectively ($P < 0.001$).

The results show that patients with acute cystitis have more elevated concentrations of IL-1β and MMP-7 in urine, than patients with ABU, identifying IL-1β and MMP-7 as potential biomarkers of acute cystitis.

Discussion

Symptoms and disease are the price we pay for an efficient host defense against infection. As innate immune effectors are activated to clear tissues of bacteria, they may also cause inflammation, symptoms and tissue damage, especially if innate immune control is compromised.

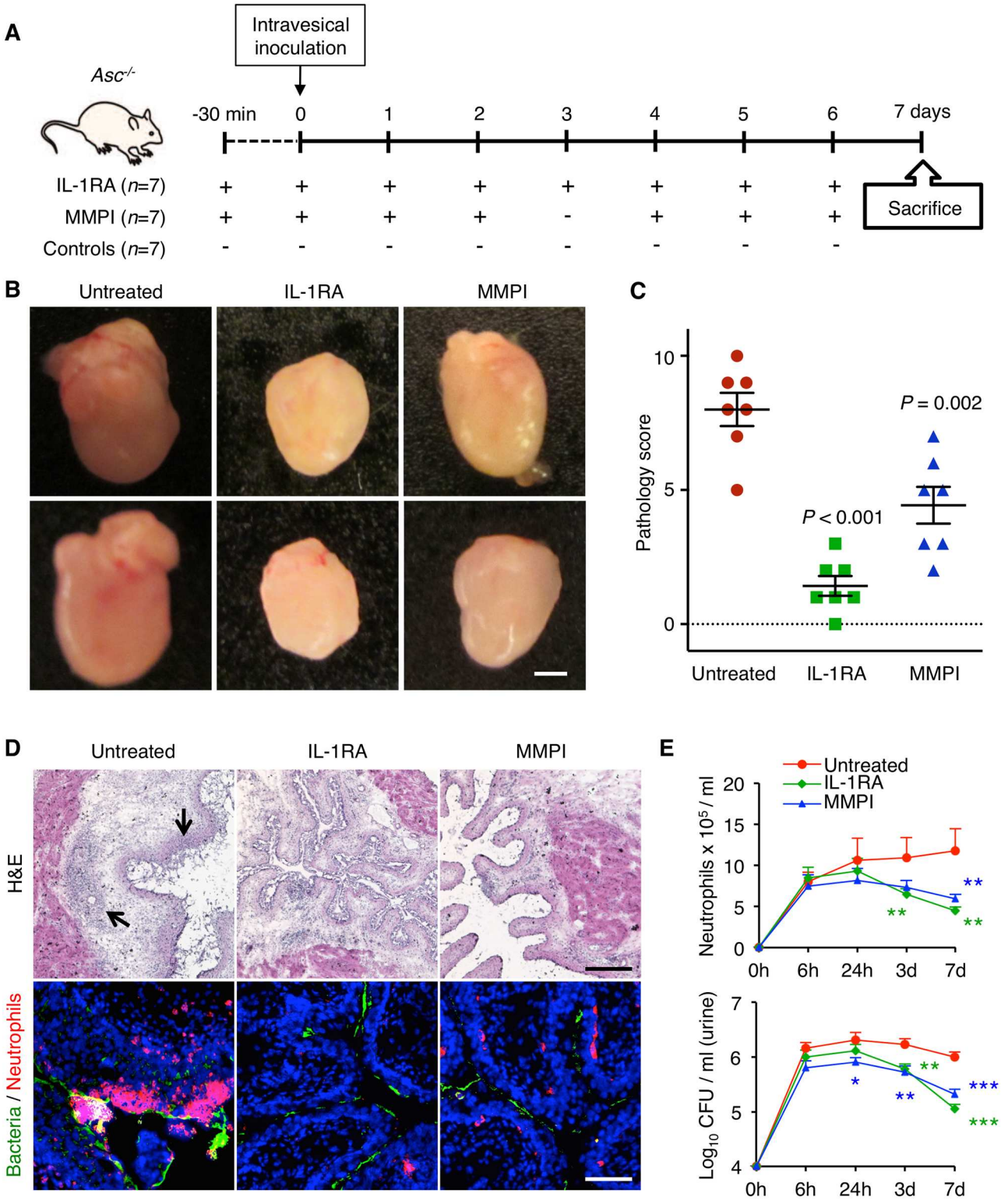

Fig 6. Acute cystitis immunotherapy, using an IL-1 receptor antagonist (IL-1RA) or an MMP inhibitor. (**A**) Overview of therapeutic regimen used to inhibit bladder pathology. *Asc*$^{-/-}$ mice were pre-treated with Anakinra (IL-1RA), 30 min before infection and daily after infection with *E. coli* CFT073 (1 mg in 100 μl of PBS i.p. per mouse) and sacrificed 7 days after infection. Alternatively, *Asc*$^{-/-}$ mice were pre-treated with the matrix metalloproteinase inhibitor (MMPI) Batimastat, 30 min before infection and daily after infection with *E. coli* CFT073 (0.5 mg in 100 μl of PBS i.p. per mouse, except day 3) ($n = 7$ per treatment group, total of two experiments). (**B**) Difference in gross bladder

pathology between untreated controls and IL-1RA or MMPI treated mice. Two representative mice per group are shown. The IL-1RA therapy reduced macroscopic bladder pathology in *Asc*$^{-/-}$ mice. Scale bar = 1 mm. The MMPI therapy showed a similar but less pronounced effect. (**C**) Edema, hyperemia and size of the bladders were used as scoring parameters for the pathology score. Pathology scores from individual mice are shown. The gross pathology score was reduced by the inhibitors ($P < 0.001$, for IL-1RA compared to untreated *Asc*$^{-/-}$ mice and $P = 0.002$, for MMPI, compared to untreated *Asc*$^{-/-}$ mice, means ± SEMs of two experiments, two-tailed Mann Whitney test). (**D**) Protection from bladder tissue pathology shown in H&E stained sections from treated versus control mice. Arrows indicate mucosal sloughing, edema and subepithelial abscesses in untreated mice. Inhibition of mucosal neutrophil aggregate formation in bladder sections from treated mice compared to untreated and infected mice. Scale bar = 200 μm (H&E) and 50 μm (immunofluorescence). (**E**) Kinetics of neutrophil recruitment and bacterial clearance in the urine of IL-1RA or MMPI treated *Asc*$^{-/-}$ mice, compared to untreated mice. ($n = 7$ mice per group, means ± SEMs, * $P < 0.05$, ** $P < 0.01$, *** $P < 0.001$, two-tailed unpaired *t*-test).

doi:10.1371/journal.ppat.1005848.g006

This is exemplified here by acute cystitis, which is a common, mostly self-limiting infection except in a subset of patients, who develop severe, recurrent infections, suggesting increased susceptibility. This study proposes a new, genetic basis of susceptibility, exemplified by the disease phenotype in *Asc*$^{-/-}$ or *Nlrp3*$^{-/-}$ mice or resistance in *Il1b*$^{-/-}$ mice that were protected from infection. The transition of the bladder mucosa from a homeostatic innate immune response to acute disease reflects the molecular control of IL-1β processing, through inflammasome-dependent or non-canonical mechanisms (Fig 8), [44–46]. The findings suggest that acute cystitis might resemble hyper-inflammatory disorders [28, 47, 48], where therapeutic efficacy of IL-1β inhibitors has been documented [49, 50]. The results provide a molecular context for acute cystitis and for the susceptibility to acute cystitis in patients with severe and chronic disease.

The severity of acute cystitis was clearly influenced by bacterial virulence as the acute cystitis strains activated IL-1β more efficiently than ABU strains. This comparison was especially valid, as the CY and ABU strains were isolated from the same pediatric population and geographic area, from children who either developed symptoms or were screened for asymptomatic carriage, by collection and culture of urine samples [31, 33]. The mechanism of IL-1β activation by the acute cystitis strains remains unclear, however. Schaale *et al*. have studied the IL-1β response of macrophages infected with UPEC strains CFT073 or UTI89 and reported that IL-1β activation and secretion is hemolysin-dependent in murine macrophages but not in human [20]. Consistent with their studies, we saw high IL-1β responses to virulent and hemolysin positive CY strains, but we did not detect a direct association with hemolysin production, suggesting that additional features control the induction and secretion of IL-1β. Schaale *at al*. also pointed to the diversity among different UPEC strains, showing that some are able to boost the inflammasome while others may escape detection by not activating IL-1β. Nagamatsu *et al*. examined hemolysin and the IL-1β response to UTI89, by inactivating a two-component signal transduction system. The mutant induced significantly higher IL-1β responses than the WT strain, in a hemolysin-dependent manner [19]. In addition, pyroptosis was linked to the presence of hemolysin, through activation of Caspase-1 and Caspase-4. In the present study, bacterial determinants of pathology were not identified but the CY isolates are being subjected to whole-genome sequence analysis for this purpose.

Paradoxically, *Il1b*$^{-/-}$ mice were resistant to infection, unlike the invasive enteropathogens *Salmonella* and *Shigella*, which are lethal for *Il1b*$^{-/-}$ mice [51, 52]. Internalization of uro-pathogens by cells in the bladder mucosa has been extensively studied and intracellular communities have been highlighted as a niche for bacterial persistence [53–55]. Specific signaling pathways involved in bacterial uptake by bladder epithelial cells include the ubiquitin-proteasome machinery [56], and especially type 1 fimbriae have been identified as essential ligands [57]. As *Il1b*$^{-/-}$ mice did not develop infection or mucosal inflammation, and proinflammatory genes were not expressed, the IL-1β response may help render the bladder mucosa susceptible to infection, possibly by enhancing bacterial growth [58] or tissue invasion. The ability to activate

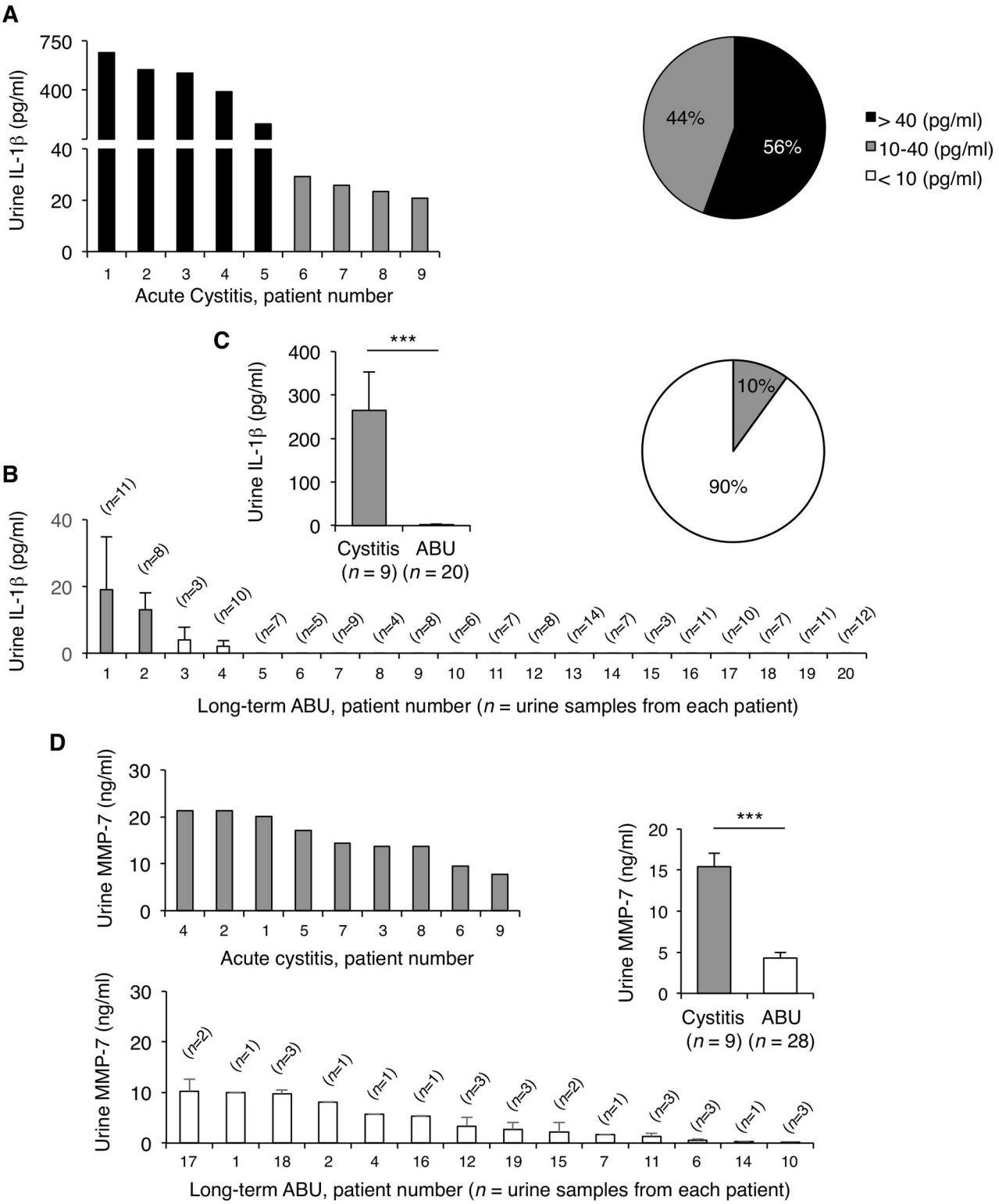

Fig 7. Elevated concentrations of IL-1β and MMP-7 in the urine of patients with acute cystitis. (**A**) IL-1β concentrations in urine samples from patients with acute cystitis ($n = 9$). (**B**) IL-1β concentrations in consecutive urine samples from patients with ABU, who were long-term asymptomatic carriers of *E. coli* 83972 [21] (means ± SEMs, 20 patients, 161 urine samples). Elevated levels of IL-1β in the cystitis patients compared to the ABU group. Pie chart (inset) depicts the distribution of IL-1β concentrations in each patient group. (**C**) Histogram compares IL-1β concentrations between the two patient groups (means ± SEMs, *** $P < 0.001$, two-tailed Mann Whitney test).

(**D**) MMP-7 concentrations were higher in urine samples from the patients with acute cystitis than in patients with long-term ABU (means ± SEMs, *** $P < 0.001$, two-tailed unpaired *t*-test). Urine samples were obtained from patients with sporadic acute cystitis at the time of diagnosis. The patients with ABU participated in a prospective study of therapeutic inoculation with *E. coli* 83972 and were subjected to long-term follow up [21]. Multiple samples were obtained during asymptomatic carriage (3–14 samples per patient).

doi:10.1371/journal.ppat.1005848.g007

IL-1β production in host cells may therefore be a key to bacterial virulence, as suggested by the epidemiologic survey of strains used in the present study. The findings add MMP-7 to the list of metalloproteinases (MMP-2, MMP-3 and MMP-9) that cleave pro-IL-1β or degrade IL-1β in other cell types [59]. MMP-7 has also been shown to process and modulate the activity of anti-bacterial peptides produced by the Paneth cells in the mouse small intestine [60], where cryptdins played a protective role during *Salmonella typhimurium*- [61] or *Chlamydia trachomatis* infections [62]. In that model, pro-inflammatory effects of MMP-7 were also detected in the intestinal mucosa [63].

ASC and NLRP-3 have recently been identified as transcriptional regulators of innate immune responses. ASC forms a complex with NF-κB and modifies NF-κB-dependent gene expression [64]. NLRP-3 is involved in the T_H2 cell differentiation program and facilitates the binding of IRF-4 to DNA [65]. Here, we identify ASC and NLRP-3 as negative regulators of *MMP7* transcription, based on 1) inverse regulation of MMP-7 with ASC and NLRP-3 in cells infected with CY-17; 2) strongly upregulated *MMP7* expression after transfection of human cells with specific siRNAs against *ASC* and *NLRP3*; 3) identification of a specific *MMP7* promoter DNA sequence, to which nuclear proteins from infected cells bind; 4) inhibition by antibodies to ASC or NLRP-3 of the interaction between nuclear proteins and the *MMP7* promoter; 5) binding of recombinant ASC to the *MMP7* promoter. As HDAC6 was recently found to interact with NLRP-3 and to modulate its inflammasome function [66], we speculate that NLRP-3 may act as a co-repressor by binding to ASC and recruiting histone deacetylase (HDAC) to the *MMP7* promoter, thereby generating a tight chromatin structure refractory to transcription. This was supported by evidence of a direct interaction between ASC and NLRP-3 in the nuclei of CY-17 infected cells. Future studies are required to address in greater detail the regulation of *MMP7* expression by ASC and NLRP-3.

Acute cystitis is a handicap, socially and emotionally but despite its prevalence and importance for patients and society, acute cystitis is a poorly understood disease [6, 67]. Social and behavioral factors have been emphasized as a cause of recurrent infections and until recently, therapeutic options have included a variety of shorter or longer antibiotic regimens, many of which have been discontinued, due to resistance development. It comes as no surprise, that this highly painful condition has been the focus of various interventions in addition to antibiotic therapy. Deliberate establishment of competitive microflora has shown promising clinical effects [21, 22] but novel, therapeutic approaches are needed in this large patient group. In this study, we show that acute cystitis is amenable to IL-1 receptor inhibition and/or MMP blockade. As IL-1RA is in clinical use, short-term immunotherapy might be a realistic option as an adjunct to antibiotics in acute cystitis patients. The identified molecular disease determinants may also be helpful to address the unmet need for diagnostic tools in this patient group. The frequency of genetic variants, such as *ASC* mutations, and their relevance to disease would be an interesting focus of prospective clinical studies.

Materials and Methods

Bacterial strains and cell infection procedure

Cystitis (CY) and asymptomatic bacteriuria (ABU) strains were prospectively isolated during a study of childhood UTI in Göteborg, Sweden, using standard microbiological techniques [32,

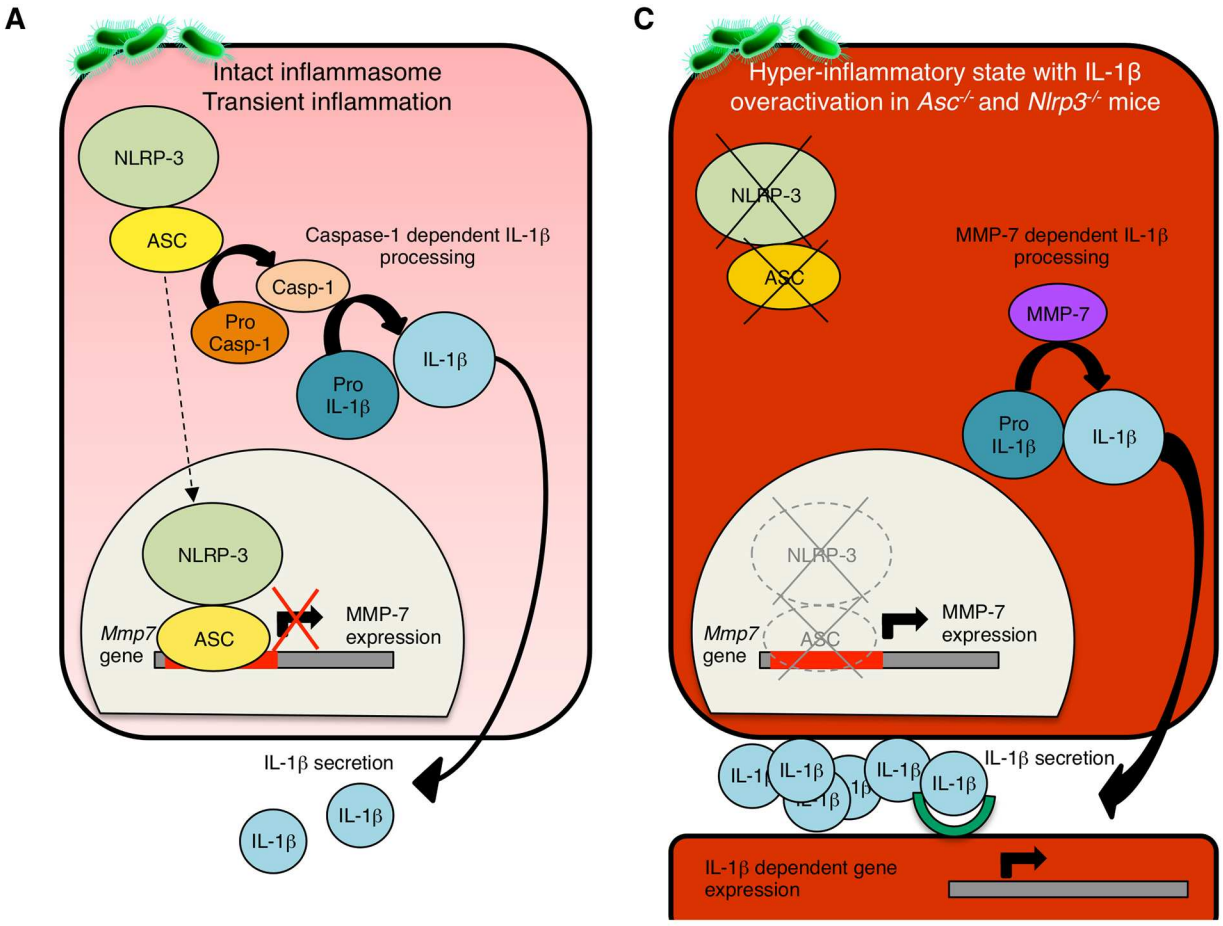

B

Genotype	Pathology score	Phenotype
C57BL/6 WT	2	transient response, no disease
Il1b$^{-/-}$	1	low bacterial and neutrophil counts, protection from disease
Casp1$^{-/-}$	6	high urine bacterial and neutrophil counts, mild disease

D

Genotype	Pathology score	Phenotype
Nlrp3$^{-/-}$	9	tissue destruction, high bacterial and neutrophil counts, severe disease
Asc$^{-/-}$	9	tissue destruction, high bacterial and neutrophil counts, severe disease

E

IL-1RA treated *Asc*$^{-/-}$	2	low bacterial and neutrophil counts, significant therapeutic effect
MMPI treated *Asc*$^{-/-}$	4	low bacterial and neutrophil counts, moderate therapeutic effect

Fig 8. Models of IL-1β processing—cellular determinants and biological effects. (**A**) Caspase-1 dependent pro-IL-1β processing by the NLRP-3 inflammasome in mice with intact inflammasome function. The NLRP-3/ASC complex activates Caspase-1, which in turn cleaves pro-IL-1β and supports the secretion of mature IL-1β by infected cells. The production of MMP-7 is normally low, due to transcriptional repression by ASC and NLRP-3, bound to the MMP-7 promoter. (**B**) C57BL/6 WT mice develop a mild form of acute cystitis with transient inflammation. *Il1b*$^{-/-}$ mice were protected against infection and inflammation and *Casp1*$^{-/-}$

mice, showed an atypical phenotype without tissue damaging inflammation or neutrophil recruitment into the urine. (**C**) A new mechanism of IL-1β processing by MMP-7 in infected *Asc*$^{-/-}$ and *Nlrp3*$^{-/-}$ mice. MMP-7 over-activation in *Asc*$^{-/-}$ mice and *Nlrp3*$^{-/-}$ mice is triggered by infection and de-repression of *Mmp7* transcription. (**D**) In the absence of functional *Asc* or *Nlrp3* genes, infected mice therefore produce excessive amounts of IL-1β, causing massive bladder inflammation, with elevated neutrophil counts, edema and hypertrophy of the bladder epithelium. (**E**) Immunotherapy by suppression of the IL-1-dependent inflammatory response in susceptible *Asc*$^{-/-}$ mice. Mice were treated with the IL-1RA (Anakinra) or the protease inhibitor MMPI (Batimastat), which showed therapeutic effects.

doi:10.1371/journal.ppat.1005848.g008

33]. The strain collection has been extensively studied and characterized with fimbrial genotype and phenotype, virulence factor expression, OKH antigen profiles and multilocus enzyme typing [31, 68]. The hemolytic activity was assessed with blood agar plates, where the hemolytic zone surrounding the central stab of bacteria is recorded. The phenotype has been compared to the *hly* genotype and found to be a very close fit. The UPEC strain, *E. coli* CFT073 (O6:K2:H1) [69] and the ABU strain *E. coli* 83972 (OR:K5:H-) [25] have been extensively characterized, including whole genome sequencing and were used as positive or negative controls. Bacteria were cultured on tryptic soy agar (TSA, 16 h, 37°C), harvested in phosphate-buffered saline (PBS, pH 7.2) and diluted as appropriate in RPMI without FCS. In the screen of IL-1β responses to acute cystitis or ABU strains, cells were exposed to 10^8 CFU/ml of bacteria with Gentamicin for 4 hours. In remaining experiments, cells were exposed to 10^5 CFU/ml for 1 hour or 4 hours without antibiotics. Overnight static cultures of *E. coli* CFT073, CY-17 or CY-92 or 83972 in Luria-Bertani (LB) broth were used for experimental infection.

Cell culture

Human bladder grade II carcinoma cells (5637, ATCC# HTB-9) were cultured, to 70–80% confluency on 8-well chamber Permanox slides ($6x10^4$ cells/well), in 6-well plates ($6x10^5$ cells/well) or 96-well plates ($5x10^4$ cells/well), (all from Thermo Scientific) in RPMI-1640 supplemented with 1 mM sodium pyruvate, 1 mM non-essential amino acids and 10% heat-inactivated FBS (PAA) at 37°C with 5% CO_2. Gentamicin (50 μg/ml) was from GE Healthcare.

Cell viability assay

HTB-9 cells in 96-well plates were infected for 1h or 4h. PrestoBlue (Invitrogen, A13262) was added to each well to a final concentration of 10%. After 20 min of incubation at 37°C, total well fluorescence was measured using a microplate reader Infinite F200 (Tecan), with 585 nm excitation and 620 nm emission filters.

Cytokine measurements

IL-1β concentrations in filtered supernatants (Syringe Filter w/0.2 μm PES, VWR) from cells infected with 10^8 CFU/ml (with Gentamicin, 4 hours) were determined by Immulite 1000 (Siemens) and IL-1β concentrations in cell supernatants or urine by Human or Mouse IL-1β/IL-1F2 DuoSet ELISA kits (all from R&D Systems). Urine MMP-7 levels were quantified with Human total MMP-7 Immunoassay Quantikine ELISA (R&D Systems).

Confocal microscopy

Cells were infected, fixed (3.7% formaldehyde, 10 min), permeabilized (0.25% Triton X-100, 5% FBS, 15 min), blocked (5% FBS, 1h at RT), incubated with primary antibodies in 5% FBS overnight at 4°C (anti-IL-1 beta, 1:100, ab9722; anti-MMP7, 1:25, ab4044, all Abcam; anti-ASC, 1:50, sc-22514-R, Santa Cruz; anti-NLRP3/Cryo-2, 1:100, AG-20B-0014-C100, Adipogen) and appropriate secondary antibody (Alexa Fluor 488 goat anti-rabbit IgG, A-11034, or

goat anti-mouse IgG, A-11001; Life Technologies), (1h at RT). After nuclear staining (DRAQ5, Abcam), slides were mounted (Fluoromount, Sigma-Aldrich), imaged by laser-scanning confocal microscopy (LSM510 META confocal microscope, Carl Zeiss) and quantified by ImageJ software 1.46r (NIH).

Western blotting

Cells were lysed with RIPA lysis buffer, supplemented with protease and phosphatase inhibitors (both from Roche Diagnostics) and fractionated using the NE-PER Nuclear and Cytoplasmic extraction reagents (Thermo Scientific). Supernatants were filtered and concentrated by trichloroacetic acid precipitation, followed by aceton desiccation. Proteins were run on SDS-PAGE (4–12% Bis-Tris gels, Invitrogen), blotted onto PVDF membranes (GE Healthcare) blocked with 5% bovine serum albumin (BSA) or non-fat dry milk (NFDM), incubated with primary antibody: rabbit anti-IL-1 beta (1:2,500 in 5% NFDM, ab9722, Abcam), rabbit anti-ASC (1:200 in 5% BSA, sc-22514-R, Santa Cruz), mouse anti-NLRP3/NALP3 (1:1,000 in 5% milk, Cryo-2, Adipogen) or rabbit anti-MMP7 (1:200 in 5% BSA, ab4044, Abcam), washed with PBS tween 0.1% and incubated with secondary antibodies in 5% NFDM (goat anti rabbit-HRP or goat anti-mouse-HRP, Cell Signaling). Bands were imaged using ECL Plus detection reagent (GE Health Care) and quantified using ImageJ. GAPDH (1:1,000, sc-25778, Santa Cruz) was used as loading control.

Co-immunoprecipitation

Nuclear fractions, extracted as described in **Western blotting**, were incubated with rabbit anti-ASC antibody (sc-22514-R, Santa Cruz, 1 μg/ml) overnight and complexes were collected with magnetic Dynabeads Protein G (Life technologies), analyzed by SDS-PAGE with rabbit anti-ASC and mouse anti-NLRP3 (Cryo-2, Adipogen) primary antibodies (1:200–1:1,000, 5% BSA), followed by secondary anti-rabbit (Cell Signaling) or anti-mouse (DAKO) antibodies (1:4,000, 5% NFDM).

Global gene expression

Total RNA was extracted from murine bladders or kidneys in RLT buffer with 1% β-Mercaptoethanol after disruption in a tissue homogenizer (TissueLyser LT, Qiagen) using Precellys Lysing kits (Bertin Technologies), with the RNeasy Mini Kit (Qiagen), 100 ng of RNA was amplified using GeneChip 3´IVT Express Kit, 6 μg of fragmented and labeled aRNA was hybridized onto Mouse Genome 430 PM array strips for 16 hours at 45°C, washed, stained and scanned using the Geneatlas system (all Affymetrix). All samples passed the internal quality controls included in the array strips (signal intensity by signal to noise ratio; hybridization and labeling controls; sample quality by GAPDH signal and 3'-5' ratio < 3).

Transcriptomic data was normalized using Robust Multi Average implemented in the Partek Express Software (Partek) [70, 71]. Fold change was calculated by comparing infected (7 days) to uninfected mice of the same genetic background. Significantly altered genes were sorted by relative expression (2-way ANOVA model using Method of Moments, *P*-values < 0.05 and absolute fold change > 1.41) [38]. Heat-maps were constructed by Gitools 2.1.1 software. Differentially expressed genes and regulated pathways were analyzed by Ingenuity Pathway Analysis software (IPA, Ingenuity Systems, Qiagen). Qiagen's list of 84 key inflammasome genes was selected for analysis.

The microarray data are available in the NCBI's Gene Expression Omnibus repository (accession number GSE86096).

In vitro proteolysis

Recombinant human IL-1β, NLRP-3 or PYCARD (ASC) (280 ng, H00003553-P02, H00114548-P01 or H00029108-P01, Abnova) were incubated with recombinant active human MMP-7 (0.035U, #444270 Merck Millipore) in MMP reaction buffer (20 mM Tris, pH 7.6, 5 mM $CaCl_2$, 0.1 M NaCl) at 37°C until stopped with 100 mM DDT. Fragments were detected by Western blot, using rabbit anti-IL-1 beta (1:2 000, ab9722, Abcam), rabbit anti-ASC (1:1 000, p9522-75, US Biological) and rabbit anti-NLRP3 (1:500, sc-66846, Santa Cruz).

IL-1β activity assay

HTB-9 cells were treated with the products of the *in vitro* proteolysis of pro-IL-1β by MMP-7 at different concentrations or with pro-IL-1β or MMP-7 alone, serving as negative controls. Prostaglandin E2 (PGE_2) concentrations were measured in filtered supernatants (Syringe Filter w/0.2 μm PES, VWR) by ELISA (R&D systems).

siRNA transfection

HTB-9 cells were transfected with *PYCARD*/*ASC* and *NLRP3* specific siRNAs (0.09 μM, Flexi-Tube GeneSolution, #GS29108 and #GS114548, Qiagen) or with AllStars Negative Control siRNA (#SI03650318, Qiagen) using the HiPerFect Transfection Reagent (#301705, Qiagen) for 17 hours, then infected. Transfection efficiency was assessed by Western blotting.

PCR analysis

MMP7 promoter and promoter flanks were amplified in 10 different fragments by PCR using 15 ng of total human genomic DNA. For forward and reverse primers (http://primer3.ut.ee/), see S3 Table. Thermal cycling conditions were as follows: 95°C for 2 min, 35 cycles (95°C for 30 s, 60°C for 30 s and 72°C for 40 s) and 72°C for 5 min.

Electrophoretic mobility shift assay (EMSA)

Amplified DNA sequences from the *MMP7* promoter were used as probes and labeled with GelGreen (Biotium). Each reaction contained 3–5 μg of DNA probe with, 5 μg of nuclear extract from infected HTB-9 cells, or 0.2–0.65 μg recombinant ASC (Abnova, H00029108-P01) or NLRP-3 (Abnova, H00114548-P01) in binding buffer (100 mM Tris, 500 mM NaCl and 10 mM DTT, pH 7). For the band shift competition assay, 0.5–1 μg of rabbit anti-ASC (Santa Cruz, sc-22514-R,) or 0.5 μg of rabbit anti-NLRP3 (Cryo-2, Adipogen) antibodies were used. Binding reactions were incubated at 15°C for 30 min, loaded onto a 6% non-denaturing, non-reducing polyacrylamide gel and ran in a 50 mM Tris (pH 7), 0.38 M glycine, and 2 mM EDTA buffer at 100 V for 2–3 hours. Mouse IgG2A isotype control (R&D Systems, MAB003) was used as negative control antibody. Gels were imaged using the Bio-RAD ChemiDoc system.

Experimental urinary tract infection

Mice were bred and housed in the specific pathogen-free MIG animal facilities (Lund, Sweden) with free access to food and water. Female C57BL/6 mice or *Il1b*$^{-/-}$ [36], *Nlrp3*$^{-/-}$ [34] *Asc*$^{-/-}$ [35], *Casp1*$^{-/-}$ [37], *Mmp7*$^{-/-}$ [40] mice were used at 9–15 weeks of age. The *Il1b*$^{-/-}$ mice have recently been shown to be functionally defective for IL-1α [72]. The *Casp1*$^{-/-}$ mice were also deficient for Caspase-11 [73]. *Nlrp3*$^{-/-}$ and *Asc*$^{-/-}$ mice were from Jürg Tschopp's laboratory, Department of Biochemistry, University of Lausanne and Institute for Arthritis Research (aIAR). *Mmp7*$^{-/-}$ and *Casp1*$^{-/-}$ mice were purchased from The Jackson Laboratories, USA.

Mice were intravesically infected under Isofluorane anesthesia (10^8 CFU in 0.1 ml), through a soft polyethylene catheter (outer diameter 0.61 mm; Clay Adams). Animals were sacrificed under anesthesia; bladders and kidneys were aseptically removed and macroscopic pathology was documented by photography. Tissues were fixed with 4% paraformaldehyde or frozen for sectioning and RNA extraction. Viable counts in homogenized tissues (Stomacher 80, Seward Medical) were determined on TSA (37°C, overnight). Urine samples were collected prior to and at regular times after infection and quantitatively cultured. Neutrophils in uncentrifuged urine were counted, using a hemocytometer.

Gross pathology was scored based on the macroscopic appearance of the bladders at sacrifice. The score was based on edema, hyperemia and size, on a scale of 0–10, where 0 is unchanged compared to the uninfected controls and 10 is most edematous, most hyperemic and largest size.

Histology and immunohistochemistry

Tissues were embedded in O.C.T. compound (VWR) and 5-μm-thick fresh cryosections on positively charged microscope slides (Superfrost/Plus; Thermo Scientific) were fixed with 4% paraformaldehyde or acetone-methanol (1:1 v/v). For H&E or immunohistochemistry, sections were blocked and permeabilized (0.2% Triton X-100, 5% goat normal serum (DAKO) or 1% BSA (Sigma), stained (anti-neutrophil antibody [NIMP-R14] (ab2557, Abcam), polyclonal *E. coli* antibody (1:100, NB200-579, Novus Biologicals), anti-IL-1 beta (1:50, ab9722, Abcam) or anti-MMP-7 (1:100, ab4044, Abcam), all rabbit antibodies). Alexa 488 anti-rat IgG or anti-rabbit IgG and Alexa 568 anti-rabbit IgG (A-21210, A-11001 and A-11011, Life Technologies) were secondary antibodies and nuclei were counterstained with DAPI (0.05 mM, Sigma-Aldrich). Imaging was by fluorescence microscopy (AX60, Olympus Optical). Richard-Allan Scientific Signature Series Hematoxylin 7211 and Eosin-Y 7111 (Thermo Scientific) were used to counterstain the tissue sections.

Histology was scored using H&E stained bladder sections. The score was based on neutrophil infiltration, tissue architecture and epithelial thickness on a scale of 0–10, where 0 is unchanged compared to uninfected controls and 10 the highest neutrophil infiltration, most destroyed tissue architecture and maximum epithelial thickness.

IL-1β and MMP-7 therapy

The IL-1 receptor antagonist, Anakinra (Kineret, SOBI) or the broad-spectrum MMP inhibitor, Batimastat (ab142087, Abcam) were injected intraperitoneally (i.p.) as described in Fig 6A.

Patients

Urine samples from patients with sporadic acute cystitis were obtained at two primary care clinics in Lund, Sweden. A diagnosis of acute cystitis was based on a urine dipstick analysis positive for bacteria and symptoms from the lower urinary tract, including frequency, dysuria and suprapubic pain. Midstream urine specimens were obtained at the time of diagnosis.

Patients with ABU were included in a placebo-controlled study of asymptomatic bacteriuria, following intravesical inoculation with *E. coli* 83972 [21]. Briefly, *E. coli* 83972 bacteriuria was established by intravesical inoculation (10^5 CFU/ml in saline), daily for three days and the outcome was measured as the total number of UTIs during an optimal period of 12 months followed by a cross over to a similar period without *E. coli* 83972 bacteriuria. Urine samples were obtained for cytokine analysis during *E. coli* 83972 bacteriuria, with negative symptom scores [21].

Statistics

ELISA results, fluorescence intensity, Pathology, bacterial numbers and neutrophil responses were analyzed by unpaired two-tailed *t*-test or Mann-Whitney test after assessment of normality with the d'Agostino & Pearson omnibus normality test. Significance was accepted at $P < 0.05$ (*), $P < 0.01$ (**) or $P < 0.001$ (***). For animal numbers, see S1 Table. Data was examined using Prism (v. 6.02, GraphPad).

Ethics statement

Experimental infections were approved by the Malmö/Lund Animal Experimental Ethics Committee at the Lund District Court in Sweden (approval number M44-13). All animal care and protocols were governed by the European Parlement and Council Directive 2010/63/EU, the Swedish Animal Welfare Act (Djurskyddslag 1988:534), the Swedish Animal Welfare Ordinance (Djurskyddsförordning 1988:539) and Institutional Animal Care and Use Committee (IACUC) guidelines. Experiments were reported according to the ARRIVE guidelines. The clinical studies were approved by the Human Ethics Committee at Lund University (approval numbers LU106-02, LU236-99 and Clinical Trial Registration RTP-A2003, International Committee of Medical Journal Editors, www.clinicaltrials.gov). Patients gave their informed written consent.

Supporting Information

S1 Fig. Cell viability assay. Human bladder carcinoma (HTB-9) cells were infected with CY-17, CY-92, CY-132 and CY-49, CFT073 or ABU for 1 hour or 4 hours. Cell viability was measured by PrestoBlue assay. Cell viability was > 95% after 1 hour and > 90% after 4 hours.
(TIF)

S2 Fig. Uninfected bladders and IL-1β secretion. (**A**) Bladder morphology of uninfected mice from *Asc*$^{-/-}$, *Nlrp3*$^{-/-}$ and *Il1b*$^{-/-}$ genotypes. Scale bars = 1 mm. (**B**) Urine IL-1β concentrations, followed from 6 hours to 7 days after infection with CFT073, quantified by ELISA (left panel), $n = 6–7$ mice per group, means ± SEMs, * $P < 0.05$, ** $P < 0.01$, *** $P < 0.001$, unpaired Mann Whitney test, compared to C57BL/6 WT mice. Western blot of IL-1β in urine samples obtained after 7 days (right panel).
(TIF)

S3 Fig. Bladder pathology in *Asc*$^{-/-}$ mice infected with acute cystitis strains CY-17 or CY-92. No pathology in *Asc*$^{-/-}$ mice infected the ABU strain *E. coli* 83972. (**A**) Dramatic increase in size, compared to uninfected controls, with general hyperemia and protruding edematous areas. (**B**) Inflammation and tissue destruction (H&E stained sections). Scale bar = 100 μm. (**C**) Strong bacterial- and neutrophil staining detected by immunohistochemistry. Scale bar = 50 μm. (**D**) Elevated bacterial and neutrophil counts in urine ($n = 4$ mice per group, means ± SEMs). (**E**) No evidence of disease in *Asc*$^{-/-}$ mice infected with the ABU strain *E. coli* 83972 or in C57BL/6 WT mice, shown by gross bladder pathology and neutrophil counts in urine after 24 hours and 7 days ($n = 5$ mice per group). See also S1 Table.
(TIF)

S4 Fig. *Casp1*$^{-/-}$ mice are protected from tissue damage but show a macroscopic response to infection. *Casp1*$^{-/-}$ mice were infected with CFT073 and sacrificed after 7 days. *Asc*$^{-/-}$ mice were used as positive controls for bladder pathology. In contrast to *Asc*$^{-/-}$ mice, *Casp1*$^{-/-}$ mice did not develop bladder tissue pathology. (**A**) Intact tissue structure by H&E staining and no evidence of inflammatory cell infiltration. Few neutrophils and bacteria were detected in the

tissues, by immunohistochemistry. Scale bars = 50 μm. (**B**) Bladder edema and hyperemia in *Casp1*$^{-/-}$ mice infected with CFT073. Less pronounced response than in *Asc*$^{-/-}$ mice (see Fig 2A). Scale bar = 1 mm. (**C**) Elevated bacterial- and neutrophil counts in urine of *Casp1*$^{-/-}$ mice and *Asc*$^{-/-}$ mice (Exp 3 in S1 Table, 5 mice per group). Neutrophils were elevated in urine of both mouse strains. (**D**) Elevated bacterial counts in tissue samples. The elevated bacterial numbers in *Casp1*$^{-/-}$ and *Asc*$^{-/-}$ mice suggested that a functional inflammasome is essential for bacterial clearance from infected bladders. (**E**) Detection of IL-1b by immunohistochemistry of bladder tissue sections. Massive retention of IL-1b in the bladder mucosa of *Casp1*$^{-/-}$ mice but not in *Asc*$^{-/-}$ mice. Scale bar = 50 μm. (**F**) Secretion of IL-1b into the urine in *Asc*$^{-/-}$ and *Casp1*$^{-/-}$ mice, detected by ELISA. Urine IL-1b levels were low in *Casp1*$^{-/-}$ mice ($n = 5$, means ± SEMs, ** $P < 0.01$, *** $P < 0.001$ compared to *Asc*$^{-/-}$ mice, unpaired t-test). (**G**) Lack of inflammasome gene activation in infected *Casp1*$^{-/-}$ mice compared to *Asc*$^{-/-}$ mouse (7d).
(TIF)

S5 Fig. Transcriptomic regulation during infection. (**A**) Top regulated pathways in mice with bladder pathology. Gene expression analysis comparing whole bladder RNA from *Asc*$^{-/-}$ and *Nlrp3*$^{-/-}$ mice with severe acute cystitis to protected *Il1b*$^{-/-}$ mice and C57BL/6 WT mice with mild bladder inflammation (Ingenuity Pathway Analysis). Bars show the -log(*P*-value) of the submitted gene list. (**B**) Lack of IL-1β dependent gene expression in the kidneys of infected C57BL/6 WT mice.
(TIF)

S6 Fig. MMP-7 staining in mice bladder tissue. (**A**) Lack of MMP-7 staining in uninfected control mice. (**B**) Separate MMP-7 and neutrophil staining in infected bladder tissue (24 h). Immunohistochemistry of bladder sections obtained 24 hours after infection of *Asc*$^{-/-}$ mice with CFT073. MMP-7 (red) was detected in the epithelium and recruited neutrophils (green) were present throughout with increased density towards the lumen. In most areas with recruited neutrophils, MMP-7 co-localization was not detected. Scale bar = 50 μm.
(TIF)

S7 Fig. Processing by MMP-7 of IL-1β, ASC and NLRP-3. (**A**) Western blot analysis of the time-dependent cleavage of GST-tagged pro-IL-1β by MMP-7, using an antibody to mature IL-1β. Arrows indicate mature IL-1b (18 kDa) and a 16 kDa band. Weak staining of the GST-tagged pro-IL-1β. (**B**) Time-dependent degradation of ASC by MMP-7. (**C**) NLRP-3 was not cleaved by MMP-7 and was used as a negative control.
(TIF)

S8 Fig. Controls for Fig 5. (**A**) MMP-7 immunofluorescence staining of uninfected HTB-9 cells transfected with *NLRP3* and *ASC* siRNA. In the absence of infection, *NLRP3* siRNA or *ASC* siRNA did not increase MMP-7 expression. (**B**) Quantification of the Western blot in Fig 5E. Each band was normalized against its corresponding GAPDH band. (**C**) Co-immunoprecipitation of nuclear extracts with anti-ASC antibodies. Pull-down of NLRP-3 is detected in control cells but attenuated in CY-17 infected cells.
(TIF)

S9 Fig. Mapping of the amplified P1 fragment in the *MMP7* gene promoter. (**A**) The human *MMP7* gene is located on chromosome 11 q22.3. Ensemble GRCh37 (release 81, July 2015) sequence of chromosome 11 region 102,391,471–102,421,479 including the *MMP7* gene and promoter. Transcription factor binding sites were identified using the Champion ChiP Transcription Factor Search Portal. Various primers were designed to map the promoter and the two promoter flanking regions. DNA sequences were amplified by PCR and used for

EMSA (Fig 5F–5H). (**B**) EMSA using different DNA fragments from the *MMP7* promoter and ASC or NLRP-3 recombinant proteins. Binding was only seen with the P1 fragment and ASC protein, arrow (see Fig 5H).
(TIF)

S10 Fig. IL-1RA or MMPI did not influence bacterial growth. Bacterial growth in Luria-Bertani (LB) broth in the presence of Anakinra (500 ng/ml) or Batimastat (250 ng/ml) for 10 hours. No significant effect was observed.
(TIF)

S1 Table. Number of mice used for experimental infection, specified for each group of experiments. The total number of mice was 147.
(PDF)

S2 Table. Genes regulated in mice with pathology compared to mice without pathology.
(PDF)

S3 Table. Primers used to amplify the *MMP7* promoter and promoter flanks.
(PDF)

Acknowledgments

We thank the Capio City Clinic Lund and the Primary health center Getinge for collecting urine samples from patients with acute cystitis. The authors thank Pierre Morin for his input during the redaction of the discussion.

Author Contributions

Conceived and designed the experiments: IA MP KN CC AN GR CS.

Performed the experiments: IA MP KN CC AN GR NAF DSCB.

Analyzed the data: IA MP KN CC AN GR NAF CS.

Contributed reagents/materials/analysis tools: BW CS.

Wrote the paper: IA MP KN CC GR DSCB TM CS.

Performed bioinformatics: IA.

Performed and analyzed animal experiments: MP DSCB.

Performed the patient study: BW.

References

1. Antimicrobial resistance. World Health Organization: Fact sheet N˚194 [updated April 2015]. Available: http://www.who.int/mediacentre/factsheets/fs194/en/.
2. Auer S, Wojna A, Hell M. Oral treatment options for ambulatory patients with urinary tract infections caused by extended-spectrum-beta-lactamase-producing Escherichia coli. Antimicrob Agents Chemother. 2010; 54(9): 4006–4008. doi: 10.1128/AAC.01760-09 PMID: 20585127
3. Sanchez GV, Master RN, Karlowsky JA, Bordon JM. In vitro antimicrobial resistance of urinary Escherichia coli isolates among U.S. outpatients from 2000 to 2010. Antimicrob Agents Chemother. 2012; 56 (4): 2181–2183. doi: 10.1128/AAC.06060-11 PMID: 22252813
4. Wagenlehner FM, Bartoletti R, Cek M, Grabe M, Kahlmeter G, Pickard R, et al. Antibiotic stewardship: a call for action by the urologic community. Eur Urol. 2013; 64(3): 358–360. doi: 10.1016/j.eururo.2013.05.044 PMID: 23746854

5. Kunin CM. Urinary tract infections: detection, prevention, and management. 5th ed. Baltimore: Williams & Wilkins; 1997. ix, 419 p. p.
6. Stamm WE. Urinary tract infections. Infect Dis Clin North Am. 2003; 17(2): xiii–xiv. doi: 10.1097/00001432-198904000-00006 PMID: 12848467
7. Foxman B, Barlow R, D'Arcy H, Gillespie B, Sobel JD. Urinary tract infection: self-reported incidence and associated costs. Ann Epidemiol. 2000; 10(8): 509–515. doi: 10.1016/S1047-2797(00)00072-7 PMID: 11118930
8. Ikaheimo R, Siitonen A, Heiskanen T, Karkkainen U, Kuosmanen P, Lipponen P, et al. Recurrence of urinary tract infection in a primary care setting: analysis of a 1-year follow-up of 179 women. Clin Infect Dis. 1996; 22(1): 91–99. doi: 10.1093/clinids/22.1.91 PMID: 8824972
9. Kumar S, Dave A, Wolf B, Lerma EV. Urinary tract infections. Dis Mon. 2015; 61(2): 45–59. doi: 10.1016/j.disamonth.2014.12.002 PMID: 25732782
10. de Man P, van Kooten C, Aarden L, Engberg I, Linder H, Svanborg Eden C. Interleukin-6 induced at mucosal surfaces by gram-negative bacterial infection. Infect Immun. 1989; 57(11): 3383–3388. PMID: 2680971
11. Candela JV, Park E, Gerspach JM, Davidoff R, Stout L, Levy SM, et al. Evaluation of urinary IL-1alpha and IL-1beta in gravid females and patients with bacterial cystitis and microscopic hematuria. Urol Res. 1998; 26(3): 175–180. doi: 10.1007/s002400050043 PMID: 9694599
12. Otto G, Burdick M, Strieter R, Godaly G. Chemokine response to febrile urinary tract infection. Kidney Int. 2005; 68(1): 62–70. doi: 10.1111/j.1523-1755.2005.00381.x PMID: 15954896
13. Agace W, Hedges S, Ceska M, Svanborg C. IL-8 and the neutrophil response to mucosal Gram negative infection. J Clin Invest. 1993; 92: 780–785. doi: 10.1172/JCI116650 PMID: 8349817
14. Frendeus B, Wachtler C, Hedlund M, Fischer H, Samuelsson P, Svensson M, et al. Escherichia coli P fimbriae utilize the Toll-like receptor 4 pathway for cell activation. Mol Microbiol. 2001; 40(1): 37–51. doi: 10.1046/j.1365-2958.2001.02361.x PMID: 11298274
15. Ragnarsdottir B, Fischer H, Godaly G, Gronberg-Hernandez J, Gustafsson M, Karpman D, et al. TLR- and CXCR1-dependent innate immunity: insights into the genetics of urinary tract infections. Eur J Clin Invest. 2008; 38 Suppl 2: 12–20. doi: 10.1111/j.1365-2362.2008.02004.x PMID: 18826477
16. de Man P, Jodal U, Vankooten C, Svanborg C. Bacterial Adherence as a Virulence Factor in Urinary-Tract Infection. APMIS. 1990; 98(12): 1053–1060. doi: 10.1111/j.1699-0463.1990.tb05034.x PMID: 2282201
17. Abraham SN, St John AL. Mast cell-orchestrated immunity to pathogens. Nat Rev Immunol. 2010; 10 (6): 440–452. doi: 10.1038/nri2782 PMID: 20498670
18. Ingersoll MA, Albert ML. From infection to immunotherapy: host immune responses to bacteria at the bladder mucosa. Mucosal Immunol. 2013; 6(6): 1041–1053. doi: 10.1038/mi.2013.72 PMID: 24064671
19. Nagamatsu K, Hannan TJ, Guest RL, Kostakioti M, Hadjifrangiskou M, Binkley J, et al. Dysregulation of Escherichia coli alpha-hemolysin expression alters the course of acute and persistent urinary tract infection. Proc Natl Acad Sci U S A. 2015; 112(8): E871–880. doi: 10.1073/pnas.1500374112 PMID: 25675528
20. Schaale K, Peters KM, Murthy AM, Fritzsche AK, Phan MD, Totsika M, et al. Strain- and host species-specific inflammasome activation, IL-1beta release, and cell death in macrophages infected with uropathogenic Escherichia coli. Mucosal Immunol. 2016; 9(1): 124–136. doi: 10.1038/mi.2015.44 PMID: 25993444
21. Sunden F, Hakansson L, Ljunggren E, Wullt B. Escherichia coli 83972 bacteriuria protects against recurrent lower urinary tract infections in patients with incomplete bladder emptying. J Urol. 2010; 184 (1): 179–185. doi: 10.1016/j.juro.2010.03.024 PMID: 20483149
22. Lutay N, Ambite I, Gronberg Hernandez J, Rydstrom G, Ragnarsdottir B, Puthia M, et al. Bacterial control of host gene expression through RNA polymerase II. J Clin Invest. 2013; 123(6): 2366–2379. doi: 10.1172/JCI66451 PMID: 23728172
23. Nicolle LE. Asymptomatic bacteriuria. Curr Opin Infect Dis. 2014; 27(1): 90–96. doi: 10.1097/QCO.0000000000000019 PMID: 24275697
24. Gronberg-Hernandez J, Sunden F, Connolly J, Svanborg C, Wullt B. Genetic control of the variable innate immune response to asymptomatic bacteriuria. PLoS One. 2011; 6(11): e28289. doi: 10.1371/journal.pone.0028289 PMID: 22140570
25. Zdziarski J, Brzuszkiewicz E, Wullt B, Liesegang H, Biran D, Voigt B, et al. Host Imprints on Bacterial Genomes-Rapid, Divergent Evolution in Individual Patients. PLoS Pathog. 2010; 6(8). doi: 10.1371/journal.ppat.1001078 PMID: 20865122

26. Rydstrom G, The molecular basis of acute cystitis; IL-1beta and inflammasome dysregulation. At Molecular UTI Conference (Urinary Tract Infection; molecular advances and novel therapies); 2014; Malmö, Sweden.
27. Ambite I, The molecular basis of acute cystitis; IL-1b and inflammasome dysregulation. At the 17th International Congress of Mucosal Immunology (ICMI 2015) 2015; Berlin, Germany.
28. Dinarello CA. Interleukin-1beta and the autoinflammatory diseases. N Engl J Med. 2009; 360(23): 2467–2470. doi: 10.1056/NEJMe0811014 PMID: 19494224
29. Dinarello CA. Immunological and inflammatory functions of the interleukin-1 family. Annu Rev Immunol. 2009; 27: 519–550. doi: 10.1146/annurev.immunol.021908.132612 PMID: 19302047
30. Qu Y, Franchi L, Nunez G, Dubyak GR. Nonclassical IL-1 beta secretion stimulated by P2X7 receptors is dependent on inflammasome activation and correlated with exosome release in murine macrophages. J Immunol. 2007; 179(3): 1913–1925. doi: 10.4049/jimmunol.179.3.1913 PMID: 17641058
31. Leffler H, Svanborg-Eden C. Glycolipid receptors for uropathogenic Escherichia coli on human erythrocytes and uroepithelial cells. Infect Immun. 1981; 34(3): 920–929. PMID: 7037645
32. Caugant DA, Levin BR, Orskov I, Orskov F, Svanborg Eden C, Selander RK. Genetic diversity in relation to serotype in Escherichia coli. Infect Immun. 1985; 49(2): 407–413. PMID: 2410366
33. Lindberg U, Claesson I, Hanson LA, Jodal U. Asymptomatic bacteriuria in schoolgirls. VIII. Clinical course during a 3-year follow-up. J Pediatr. 1978; 92(2): 194–199. PMID: 340626
34. Mariathasan S, Weiss DS, Newton K, McBride J, O'Rourke K, Roose-Girma M, et al. Cryopyrin activates the inflammasome in response to toxins and ATP. Nature. 2006; 440(7081): 228–232. doi: 10.1038/nature04515 PMID: 16407890
35. Mariathasan S, Newton K, Monack DM, Vucic D, French DM, Lee WP, et al. Differential activation of the inflammasome by caspase-1 adaptors ASC and Ipaf. Nature. 2004; 430(6996): 213–218. doi: 10.1038/nature02664 PMID: 15190255
36. Horai R, Asano M, Sudo K, Kanuka H, Suzuki M, Nishihara M, et al. Production of mice deficient in genes for interleukin (IL)-1alpha, IL-1beta, IL-1alpha/beta, and IL-1 receptor antagonist shows that IL-1beta is crucial in turpentine-induced fever development and glucocorticoid secretion. J Exp Med. 1998; 187(9): 1463–1475. doi: 10.1084/jem.187.9.1463 PMID: 9565638
37. Kuida K, Lippke JA, Ku G, Harding MW, Livingston DJ, Su MS, et al. Altered cytokine export and apoptosis in mice deficient in interleukin-1 beta converting enzyme. Science. 1995; 267(5206): 2000–2003. doi: 10.1126/science.7535475 PMID: 7535475
38. Eisenhart C. The assumptions underlying the analysis of variance. Biometrics. 1947; 3(1): 1–21. doi: 10.2307/3001534 PMID: 20240414
39. Ra HJ, Harju-Baker S, Zhang F, Linhardt RJ, Wilson CL, Parks WC. Control of promatrilysin (MMP7) activation and substrate-specific activity by sulfated glycosaminoglycans. J Biol Chem. 2009; 284(41): 27924–27932. doi: 10.1074/jbc.M109.035147 PMID: 19654318
40. Wilson CL, Heppner KJ, Labosky PA, Hogan BL, Matrisian LM. Intestinal tumorigenesis is suppressed in mice lacking the metalloproteinase matrilysin. Proc Natl Acad Sci U S A. 1997; 94(4): 1402–1407. doi: 10.1073/pnas.94.4.1402 PMID: 9037065
41. Ito A, Mukaiyama A, Itoh Y, Nagase H, Thogersen IB, Enghild JJ, et al. Degradation of interleukin 1beta by matrix metalloproteinases. J Biol Chem. 1996; 271(25): 14657–14660. doi: 10.1074/jbc.271.25.14657 PMID: 8663297
42. Matsushita K, Takeoka M, Sagara J, Itano N, Kurose Y, Nakamura A, et al. A splice variant of ASC regulates IL-1beta release and aggregates differently from intact ASC. Mediators Inflamm. 2009; 2009: 287387. doi: 10.1155/2009/287387 PMID: 19759850
43. Petrasek J, Bala S, Csak T, Lippai D, Kodys K, Menashy V, et al. IL-1 receptor antagonist ameliorates inflammasome-dependent alcoholic steatohepatitis in mice. J Clin Invest. 2012; 122(10): 3476–3489. doi: 10.1172/JCI60777 PMID: 22945633
44. Symington JW, Wang C, Twentyman J, Owusu-Boaitey N, Schwendener R, Nunez G, et al. ATG16L1 deficiency in macrophages drives clearance of uropathogenic E. coli in an IL-1beta-dependent manner. Mucosal Immunol. 2015; 8(6): 1388–1399. doi: 10.1038/mi.2015.7 PMID: 25669147
45. Netea MG, van de Veerdonk FL, van der Meer JW, Dinarello CA, Joosten LA. Inflammasome-independent regulation of IL-1-family cytokines. Annu Rev Immunol. 2015; 33: 49–77. doi: 10.1146/annurev-immunol-032414-112306 PMID: 25493334
46. Lee MS, Kwon H, Lee EY, Kim DJ, Park JH, Tesh VL, et al. Shiga Toxins Activate the NLRP3 Inflammasome Pathway To Promote Both Production of the Proinflammatory Cytokine Interleukin-1beta and Apoptotic Cell Death. Infect Immun. 2015; 84(1): 172–186. doi: 10.1128/IAI.01095-15 PMID: 26502906

47. Zhao R, Zhou H, Su SB. A critical role for interleukin-1beta in the progression of autoimmune diseases. Int Immunopharmacol. 2013; 17(3): 658–669. doi: 10.1016/j.intimp.2013.08.012 PMID: 24012439

48. Dujmovic I, Mangano K, Pekmezovic T, Quattrocchi C, Mesaros S, Stojsavljevic N, et al. The analysis of IL-1 beta and its naturally occurring inhibitors in multiple sclerosis: The elevation of IL-1 receptor antagonist and IL-1 receptor type II after steroid therapy. J Neuroimmunol. 2009; 207(1–2): 101–106. doi: 10.1016/j.jneuroim.2008.11.004 PMID: 19162335

49. Jesus AA, Goldbach-Mansky R. IL-1 blockade in autoinflammatory syndromes. Annu Rev Med. 2014; 65: 223–244. doi: 10.1146/annurev-med-061512-150641 PMID: 24422572

50. Leite CA, Alencar VT, Melo DL, Mota JM, Melo PH, Mourao LT, et al. Target Inhibition of IL-1 Receptor Prevents Ifosfamide Induced Hemorrhagic Cystitis in Mice. J Urol. 2015; 194(6): 1777–1786. doi: 10.1016/j.juro.2015.07.088 PMID: 26220217

51. Sansonetti PJ, Phalipon A, Arondel J, Thirumalai K, Banerjee S, Akira S, et al. Caspase-1 activation of IL-1beta and IL-18 are essential for Shigella flexneri-induced inflammation. Immunity. 2000; 12(5): 581–590. doi: 10.1016/S1074-7613(00)80209-5 PMID: 10843390

52. Raupach B, Peuschel SK, Monack DM, Zychlinsky A. Caspase-1-mediated activation of interleukin-1beta (IL-1beta) and IL-18 contributes to innate immune defenses against Salmonella enterica serovar Typhimurium infection. Infect Immun. 2006; 74(8): 4922–4926. doi: 10.1128/IAI.00417-06 PMID: 16861683

53. Mulvey MA, Schilling JD, Hultgren SJ. Establishment of a persistent Escherichia coli reservoir during the acute phase of a bladder infection. Infect Immun. 2001; 69(7): 4572–4579. doi: 10.1128/IAI.69.7.4572-4579.2001 PMID: 11402001

54. Hunstad DA, Justice SS. Intracellular lifestyles and immune evasion strategies of uropathogenic Escherichia coli. Annu Rev Microbiol. 2010; 64: 203–221. doi: 10.1146/annurev.micro.112408.134258 PMID: 20825346

55. Schwartz DJ, Chen SL, Hultgren SJ, Seed PC. Population dynamics and niche distribution of uropathogenic Escherichia coli during acute and chronic urinary tract infection. Infect Immun. 2011; 79 (10): 4250–4259. doi: 10.1128/IAI.05339-11 PMID: 21807904

56. Doye A, Mettouchi A, Bossis G, Clement R, Buisson-Touati C, Flatau G, et al. CNF1 exploits the ubiquitin-proteasome machinery to restrict Rho GTPase activation for bacterial host cell invasion. Cell. 2002; 111(4): 553–564. doi: 10.1016/S0092-8674(02)01132-7 PMID: 12437928

57. Mulvey MA, Lopez-Boado YS, Wilson CL, Roth R, Parks WC, Heuser J, et al. Induction and evasion of host defenses by type 1-piliated uropathogenic Escherichia coli. Science. 1998; 282(5393): 1494–1497. doi: 10.1126/science.282.5393.1494 PMID: 9822381

58. Porat R, Clark BD, Wolff SM, Dinarello CA. Enhancement of growth of virulent strains of Escherichia coli by interleukin-1. Science. 1991; 254(5030): 430–432. doi: 10.1126/science.1833820 PMID: 1833820

59. Schonbeck U, Mach F, Libby P. Generation of biologically active IL-1 beta by matrix metalloproteinases: a novel caspase-1-independent pathway of IL-1 beta processing. J Immunol. 1998; 161(7): 3340–3346. PMID: 9759850

60. Wilson CL, Ouellette AJ, Satchell DP, Ayabe T, Lopez-Boado YS, Stratman JL, et al. Regulation of intestinal alpha-defensin activation by the metalloproteinase matrilysin in innate host defense. Science. 1999; 286(5437): 113–117. doi: 10.1126/science.286.5437.113 PMID: 10506557

61. Eisenhauer PB, Harwig SS, Lehrer RI. Cryptdins: antimicrobial defensins of the murine small intestine. Infect Immun. 1992; 60(9): 3556–3565. PMID: 1500163

62. Pal S, Schmidt AP, Peterson EM, Wilson CL, de la Maza LM. Role of matrix metalloproteinase-7 in the modulation of a Chlamydia trachomatis infection. Immunology. 2006; 117(2): 213–219. doi: 10.1111/j.1365-2567.2005.02281.x PMID: 16423057

63. Vandenbroucke RE, Vanlaere I, Van Hauwermeiren F, Van Wonterghem E, Wilson C, Libert C. Pro-inflammatory effects of matrix metalloproteinase 7 in acute inflammation. Mucosal Immunol. 2014; 7 (3): 579–588. doi: 10.1038/mi.2013.76 PMID: 24129163

64. Stehlik C, Fiorentino L, Dorfleutner A, Bruey JM, Ariza EM, Sagara J, et al. The PAAD/PYRIN-family protein ASC is a dual regulator of a conserved step in nuclear factor kappaB activation pathways. J Exp Med. 2002; 196(12): 1605–1615. doi: 10.1084/jem.20021552 PMID: 12486103

65. Bruchard M, Rebe C, Derangere V, Togbe D, Ryffel B, Boidot R, et al. The receptor NLRP3 is a transcriptional regulator of TH2 differentiation. Nat Immunol. 2015; 16(8): 859–870. doi: 10.1038/ni.3202 PMID: 26098997

66. Hwang I, Lee E, Jeon SA, Yu JW. Histone deacetylase 6 negatively regulates NLRP3 inflammasome activation. Biochem Biophys Res Commun. 2015. doi: 10.1016/j.bbrc.2015.10.033 PMID: 26471297

67. Norinder BS, Koves B, Yadav M, Brauner A, Svanborg C. Do Escherichia coli strains causing acute cystitis have a distinct virulence repertoire? Microb Pathog. 2012; 52(1): 10–16. doi: 10.1016/j.micpath.2011.08.005 PMID: 22023989

68. Hagberg L, Jodal U, Korhonen TK, Lidin-Janson G, Lindberg U, Svanborg Eden C. Adhesion, hemagglutination, and virulence of Escherichia coli causing urinary tract infections. Infect Immun. 1981; 31 (2): 564–570. PMID: 7012012

69. Welch RA, Burland V, Plunkett G 3rd, Redford P, Roesch P, Rasko D, et al. Extensive mosaic structure revealed by the complete genome sequence of uropathogenic Escherichia coli. Proc Natl Acad Sci U S A. 2002; 99(26): 17020–17024. doi: 10.1073/pnas.252529799 PMID: 12471157

70. Irizarry RA, Bolstad BM, Collin F, Cope LM, Hobbs B, Speed TP. Summaries of Affymetrix GeneChip probe level data. Nucleic Acids Res. 2003; 31(4): e15. doi: 10.1093/nar/gng015 PMID: 12582260

71. Bolstad BM, Irizarry RA, Astrand M, Speed TP. A comparison of normalization methods for high density oligonucleotide array data based on variance and bias. Bioinformatics. 2003; 19(2): 185–193. doi: 10.1093/bioinformatics/19.2.185 PMID: 12538238

72. Freigang S, Ampenberger F, Weiss A, Kanneganti TD, Iwakura Y, Hersberger M, et al. Fatty acid-induced mitochondrial uncoupling elicits inflammasome-independent IL-1alpha and sterile vascular inflammation in atherosclerosis. Nat Immunol. 2013; 14(10): 1045–1053. doi: 10.1038/ni.2704 PMID: 23995233

73. Kayagaki N, Warming S, Lamkanfi M, Vande Walle L, Louie S, Dong J, et al. Non-canonical inflammasome activation targets caspase-11. Nature. 2011; 479(7371): 117–121. doi: 10.1038/nature10558 PMID: 22002608

II.

SCIENTIFIC REPORTS

OPEN

Neuroepithelial control of mucosal inflammation in acute cystitis

Daniel S. C. Butler[1], Ines Ambite[1], Karoly Nagy[1,2], Caterina Cafaro[1], Abdulla Ahmed[1], Aftab Nadeem[1], Nina Filenko[1], Thi Hien Tran[1], Karl-Erik Andersson[3,4], Björn Wullt[1], Manoj Puthia[1] & Catharina Svanborg[1]

Received: 1 December 2017
Accepted: 3 May 2018
Published online: 20 July 2018

The nervous system is engaged by infection, indirectly through inflammatory cascades or directly, by bacterial attack on nerve cells. Here we identify a neuro-epithelial activation loop that participates in the control of mucosal inflammation and pain in acute cystitis. We show that infection activates Neurokinin-1 receptor (NK1R) and Substance P (SP) expression in nerve cells and bladder epithelial cells *in vitro* and *in vivo* in the urinary bladder mucosa. Specific innate immune response genes regulated this mucosal response, and single gene deletions resulted either in protection (*Tlr4*$^{-/-}$ and *Il1b*$^{-/-}$ mice) or in accentuated bladder pathology (*Asc*$^{-/-}$ and *Nlrp3*$^{-/-}$ mice), compared to controls. NK1R/SP expression was lower in *Tlr4*$^{-/-}$ and *Il1b*$^{-/-}$ mice than in C56BL/6WT controls but in *Asc*$^{-/-}$ and *Nlrp3*$^{-/-}$ mice, NK1R over-activation accompanied the exaggerated disease phenotype, due, in part to transcriptional de-repression of *Tacr1*. Pharmacologic NK1R inhibitors attenuated acute cystitis in susceptible mice, supporting a role in disease pathogenesis. Clinical relevance was suggested by elevated urine SP levels in patients with acute cystitis, compared to patients with asymptomatic bacteriuria identifying NK1R/SP as potential therapeutic targets. We propose that NK1R and SP influence the severity of acute cystitis through a neuro-epithelial activation loop that controls pain and mucosal inflammation.

Infections are accompanied by characteristic symptoms from the site of infection and by general malaise, in case of systemic involvement. Pain serves as a key indicator of disease severity and as a warning signal for the host. Pain is also one of the classical hallmarks of inflammation, together with hyperemia, edema and increased temperature in inflamed tissue foci. Neuropeptides and receptors that mediate nociception and pain signalling include Substance P (SP) and its receptor Neurokinin-1 receptor (NK1R)[1,2]. SP is secreted by nerves and inflammatory cells and affects nociceptive signalling in the dorsal horn and the dorsal root ganglia. SP mediates interactions between neurons and immune cells and nerve-derived SP modulates immune cell proliferation rates and cytokine production[3,4]. Interestingly, the nervous system senses the presence of microbes and participates actively in the antimicrobial defense. As virulence factors engage specific receptors on nerve cells, bacteria activate ion fluxes, leading to nerve cell activation[5]. Examples of such interactions include recognition of Lipopolysaccharide (LPS) by Toll like receptor-4 (TLR-4) and of Shiga toxin by glycolipid receptors[6,7]. Specific nerve cell activation products also modulate inflammation, suggesting broad relevance for a number of infection-induced disease states[8,9].

Pain from the site of infection characterizes acute cystitis; an extremely common bacterial infection affecting about 50% of all women at least once[10]. In addition to painful urination (dysuria), characteristic clinical symptoms include urgency and frequency of urination, caused by activation of the micturition reflex and contractions of the bladder detrusor muscle[11]. This symptom profile indicates that the nervous system is engaged in the pathogenesis of acute cystitis[12] but molecular determinants of this process have not been defined. NK1R and SP are activated in patients with interstitial cystitis and in pelvic pain models where pseudorabies virus and LPS O-antigen have been proposed as pain agonists[13–17]. The extent of nerve cell activation by pathogenic bacteria is not well understood, yet some studies on bacterial toxin and sensory nerve cell activation suggest an important TLR4-independent link between LPS and transient receptor potential channel A1, as well as *E. coli* derived formyl peptides and formyl peptide receptor 1[5,18]. However, the nerve cell determinants of acute cystitis have not been defined.

[1]Department of Microbiology, Immunology and Glycobiology, Institute of Laboratory Medicine, Lund University, 223 62, Lund, Sweden. [2]Jahn Ferenc (South Pest) Teaching Hospital, 1204, Budapest, Hungary. [3]Institute for Regenerative Medicine, Wake Forest University School of Medicine, Winston Salem, NC, USA. [4]Institute of Clinical Medicine, Department of Obstetrics and Gynecology, Aarhus University, 8200, Aarhus, Denmark. Correspondence and requests for materials should be addressed to C.S. (email: Catharina.Svanborg@med.lu.se)

Recent immuno-genetic studies have identified a molecular basis for acute cystitis, involving Interleukin-1β (IL-1β) as a key regulator of the innate immune response to bladder infection. Uropathogenic *E. coli* activate IL-1β through a TLR4-dependent signaling pathway and as a result the acute cystitis phenotype is attenuated in *Tlr4*$^{-/-}$ and *Il1b*$^{-/-}$ mice[19,20]. *Asc*$^{-/-}$ and *Nlrp3*$^{-/-}$ mice, in contrast, develop severe acute cystitis, due to an IL-1β hyper-activation disorder[20]. In this study, we address if acute cystitis strains activate a neuropeptide- and neuropeptide receptor response in the urinary bladder mucosa and if the genes that regulate acute cystitis severity also control nerve cell activation. The study was prompted by the characteristic symptoms of acute cystitis and by preliminary evidence of neuropeptide receptor activation in patients with bacteriuria.

Results

Neuro-epithelial response to *E. coli* infection. To address if infection activates neurokinin-1 receptor (NK1R) and its ligand Substance P (SP) in the urinary tract, we first infected nerve cells (SH-SY5Y) and bladder epithelial cells (HTB9) with relevant *E. coli* strains *in vitro* (Fig. 1). Prior to infection, the SH-SY5Y nerve cells were differentiated by treatment with Retinoic Acid (1%) and serum starvation for 7 days and differentiation was confirmed by staining for the neuronal markers βIII-tubulin and NeuN (Fig. 1a). The acute cystitis strain CY-17 was selected for these studies, based on its ability to stimulate IL-1β production and to induce bladder pathology *in vivo*, in the murine acute cystitis model[20].

CY-17 infection stimulated dose-dependent cellular NK1R and SP responses, quantified by confocal imaging and western blot analysis (Fig. 1, Supplementary Fig. S1). Nerve cells and bladder epithelial cells showed similar dose response profiles, peaking at 10^4 CFU/ml (MOI of 0.05). In addition, CY-17 stimulated the secretion of SP into cell supernatants ($P < 0.05$), (Fig. 1b–i). The NK1R and SP response to CY-17 infection was further investigated in two additional cell lines (MOI = 0.05, 4 hours). The DLD1 colonic epithelial cell line showed the same response kinetics as the SH-SY5Y and HTB9 cells. In infected kidney cells, in contrast, NK1R expression decreased compared to uninfected cells and SP expression was not affected (Supplementary Fig. S1).

We subsequently compared CY-17 to the acute pyelonephritis (APN) strain *E. coli* CFT073 and the asymptomatic bacteriuria (ABU) strain *E. coli* 83972 (MOI = 0.05, 4 hours, Fig. 1). The APN strain actively induced SP expression in nerve cells and NK1R and SP expression in bladder epithelial cells ($P < 0.05$ compared to uninfected cells). The ABU strain, in contrast, did not induce a SP or NK1R response. To further address if acute cystitis strains are efficient NK1R/SP inducers, we compared additional pediatric acute cystitis strains ($n = 7$) to pediatric ABU strains ($n = 7$)[21]. The acute cystitis strains activated NK1R and SP expression more efficiently than the ABU strains ($P < 0.05$, Supplementary Fig. S2).

Neuro-epithelial response to bladder infection, *in vivo*. To address the *in vivo* relevance of these findings, we established acute cystitis in C57BL/6WT mice (Fig. 2)[20]. The severity of acute cystitis was quantified as the gross pathology score (edema, hyperemia and bladder enlargement). Neuropeptide expression was quantified by immunohistochemistry after staining with specific antibodies and by qRT-PCR of whole bladder RNA extracts, using primers specific for *Tacr1 and Ppt-A*.

In mice infected with CY-17, bladder pathology was detected after 24 hours and at seven days, compared to uninfected mice ($P < 0.05$, both time points Fig. 2a,b). Urine neutrophil counts increased after 6 hours and remained elevated until sacrifice on day 7 at $4–6 \times 10^5$ cells per ml. Bacterial counts in urine showed similar kinetics and plateaued at 10^5 CFU/ml ($P < 0.001$, Fig. 2c,d).

Infection stimulated an increase in mucosal NK1R and SP staining ($P = 0.004$ and $P = 0.02$ compared to uninfected controls, Fig. 2e,f). NK1R was clearly visible in infected bladders, with a distinct staining pattern of the mucosal nerve plexus in the lamina propria. Using βIII tubulin as a neuronal marker, co-localization of nerve cells with NK1R was confirmed. SP, in contrast, was mainly observed in the epithelial layer of infected bladders. Co-localization with βIII tubulin was more restricted than for NK1R and only detected along the epithelial-nerve cell interface (Supplementary Fig. S3).

The increase in NK1R and SP expression was confirmed by qRT-PCR of total bladder RNA (Fig. 2g). *Tacr1* and *Ppt-A* mRNA levels were increased, compared to uninfected mice ($P = 0.02$ and $P = 0.008$ for *Tacr1* and *Ppt-A* respectively). Urine SP levels were elevated after 24 hours and 7 days in infected C57BL/6WT mice compared to uninfected controls (128 pg/ml and 217 pg/ml respectively, compared to 43 pg/ml, $P < 0.05$, Fig. 2H).

Symptoms were documented by video recording of the mice before and at defined times post infection (24 hours and 7 days). A significant change in behavior was detected and quantified as a decrease in rearing and locomotion and an increase in grooming behavior ($P < 0.05$ for each of the three variables compared to uninfected controls, Fig. 2h). The results suggest that acute cystitis in C57BL/6WT mice is accompanied by a mucosal neuropeptide response and symptoms from the site of infection.

NK1R and SP response *in Tlr4*$^{-/-}$ and *IL1b*$^{-/-}$ mice. *Tlr4* is an essential, upstream regulator of the host response to gram-negative bacterial infection[22]. Downstream signaling varies with the virulence repertoire of the infecting strain and in acute cystitis, IL-1β is critically involved in the generation of tissue pathology[20]. To examine if TLR-4 and IL-1β also regulate the neuropeptide response, we infected *Tlr4*$^{-/-}$ and *Il1b*$^{-/-}$ mice with the CY-17 strain and compared NK1R and SP staining to C57BL/6WT mice with intact TLR-4 and IL-1β function.

NK1R or SP levels were low in bladder tissue from infected *Tlr4*$^{-/-}$ and *Il1b*$^{-/-}$ mice, with little change after 7 days (Fig. 2i,j, Supplementary Fig. S4). Significant bladder pathology was not detected in these mice. The results identify *Tlr4* and *Il1b* as important upstream regulators of mucosal NK1R and SP responses.

NK1R and SP hyper-activation in *Nlrp3*$^{-/-}$ and *Asc*$^{-/-}$ mice. The inflammasome proteins NLRP3 and ASC control the processing of pro-IL-1β together with caspase-1. In previous studies, we have identified a new, non-canonical mechanism of IL-1β processing, involving the metalloproteinase MMP7. This pathway is hyperactive in *Nlrp3*$^{-/-}$ and *Asc*$^{-/-}$ mice, which develop IL-1β driven hyper-inflammation and severe acute cystitis[20].

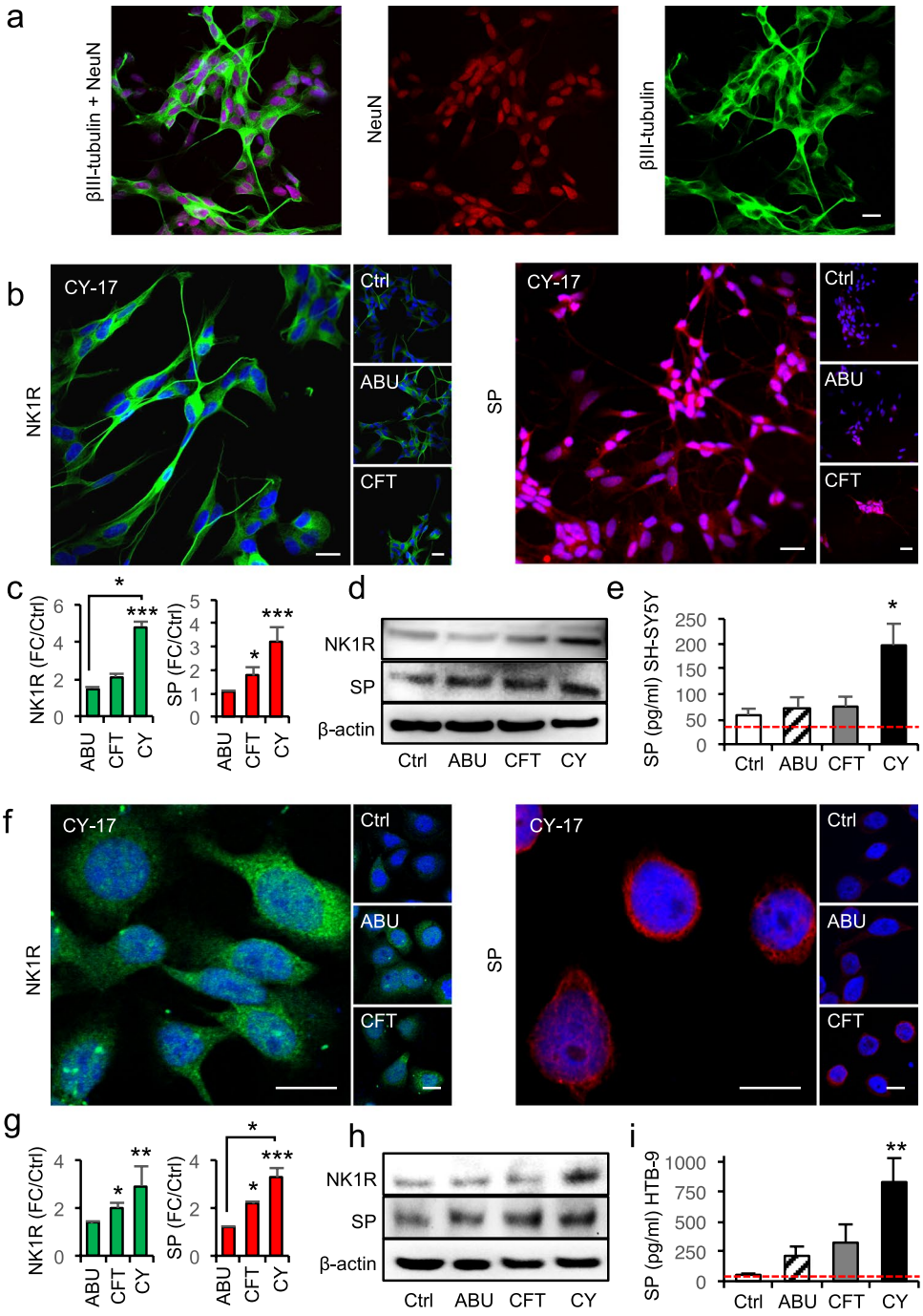

Figure 1. Bacterial SP/NK1R activation in differentiated nerve cells and bladder epithelial cells. (**a**) SH-SY5Y cells, differentiated using retinoic acid and serum starvation, showed characteristic morphology and staining for neuron-specific markers βIII-tubulin (green) and NeuN (red). (**b**) Increase in NK1R (green) and SP (red) staining after infection of differentiated nerve cells with the cystitis isolate CY-17, the APN strain CFT073 or the ABU strain *E. coli* 83972 (10^4 CFU/ml, four hours). (**c**) Quantification of fluorescence intensities in (**b**). FC compared to uninfected cells ($n = 50$ cells per condition, four repeats) (**d**) Western blot confirming the increase in NK1R and SP protein levels in infected nerve cells (4 repeats). (**e**) Quantification of SP in supernatants from infected nerve cells compared to uninfected cells by ELISA, red line represents the detection limit of the ELISA ($n = 7$ samples, 2 repeats). (**f**) Increase in NK1R (green) and SP (red) staining in bladder epithelial cells infected with CY, CFT or ABU. (**g**) Quantification of fluorescence intensities in (**f**), FC compared to uninfected cells, ($n = 50$ cells per condition, four repeats). (**h**) Western blots confirming the increase in NK1R and SP protein levels in infected bladder epithelial cells (4 repeats). (**i**) SP levels in supernatants from bladder epithelial cells infected with ABU, APN or CY compared to uninfected cells, red line represents the detection limit of the ELISA ($n = 6$ samples, 2 repeats). The data is presented as means + SEMs and analysed using Kruskal Wallis test, Dunn's correction. Scale bars = 20 µm. $^*P < 0.05$, $^{**}P < 0.01$, $^{***}P < 0.001$.

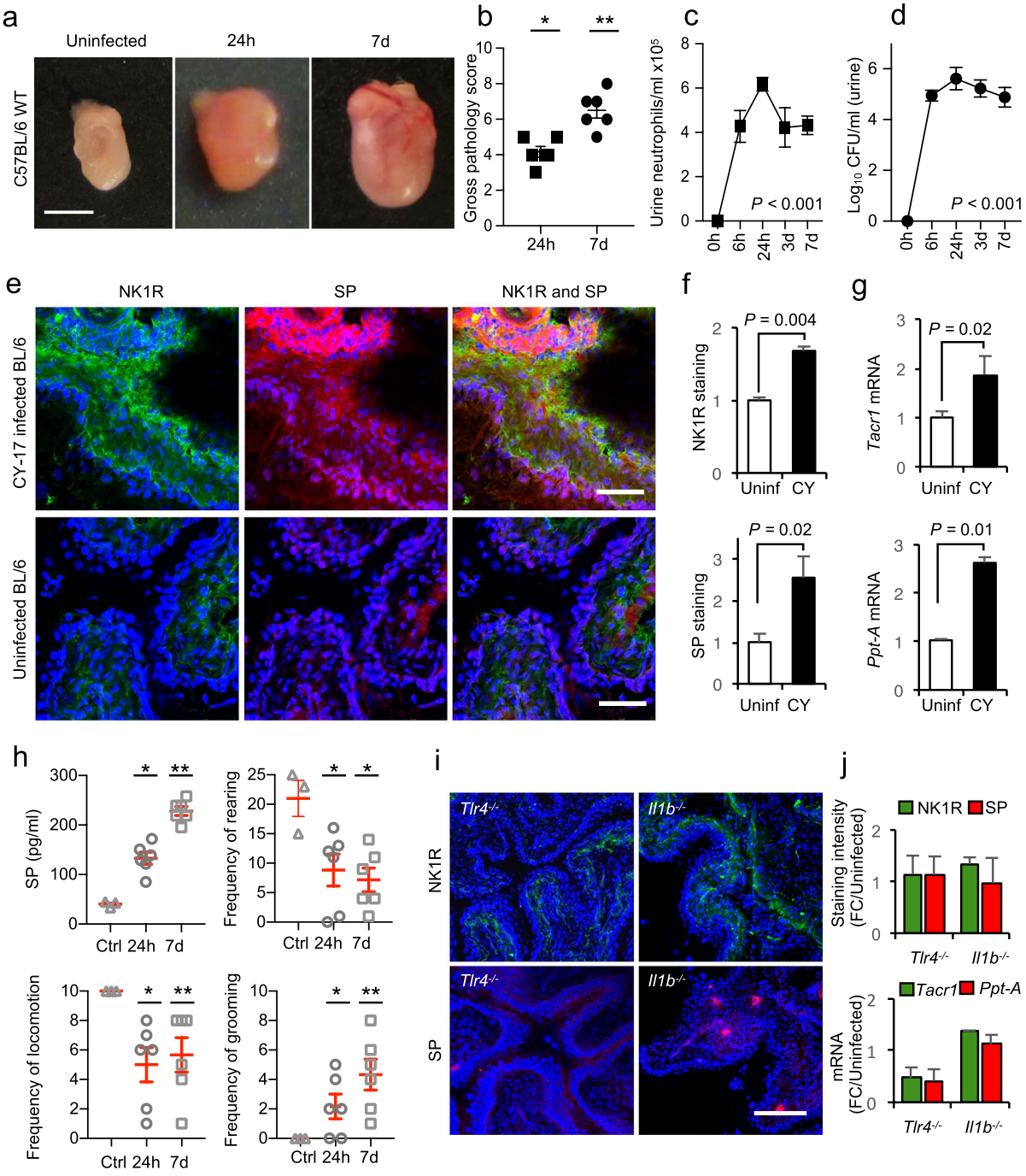

Figure 2. Mucosal neuropeptide response to acute cystitis. (**a**) Evidence of acute cystitis in C57BL/6WT mice infected with CY-17, defined by macroscopic inspection (Scale bar = 1 mm). (**b**) Gross pathology score of bladders from infected C57BL/6WT mice compared to uninfected controls. (**c**) Kinetics of the neutrophil response and (**d**) bacterial persistence, quantified in urine samples obtained 6 hours and 24 hours, 3 days and 7 days post infection. (**e**) NK1R and SP staining, quantified by immunohistochemistry of bladder sections. Mice were infected with CY-17 for 7 days. SP staining (red) was increased in the epithelium and NK1R (green) in the subepithelial compartment, compared to uninfected controls. (**f**) Quantification of NK1R and SP staining in (**e**). (**g**) Increased expression of *Tacr1* and *Ppt-A* in bladders infected with CY-17 for 7 days, quantified by qRT-PCR. (**h**) Urine concentration of SP detected by ELISA and pain assessed in C57BL/6WT mice after 24 hours and 7 days of CY-17 infection. Mice behavior was recorded and scored according to locomotion, frequency of rearing and frequency of grooming compared to uninfected controls. (**i**) Genes controlling the NK1R and SP response were identified by CY-17 infection of mice carrying single gene deletions known to affect the susceptibility to acute cystitis (*Tlr4*$^{-/-}$, *Il1b*$^{-/-}$ mice). NK1R (green) and SP (red) staining in infected *Tlr4*$^{-/-}$ and *Il1b*$^{-/-}$ mice. (**J**) Quantification of SP and NK1R staining in *Il1b*$^{-/-}$ and *Tlr4*$^{-/-}$ mice compared to their respective uninfected controls. Data is represented as means ± SEMs from $n = 4$–6 mice per group, (two repeats) and analysed by Mann-Whitney U-test. $^{*}P < 0.05$ $^{**}P < 0.01$, $^{***}P < 0.001$.

To examine if the NK1R/SP response is controlled by a similar mechanism, *Asc*$^{-/-}$ and *Nlrp3*$^{-/-}$ mice were infected with CY-17 and sacrificed 7 days post infection. The gross pathology score was higher in *Asc*$^{-/-}$ and *Nlrp3*$^{-/-}$ mice than in C57BL/6WT mice, as determined by enlarged bladders, edema and hyperemia ($P = 0.008$ and $P = 0.034$ respectively, Fig. 3a,b). The disease response was further accompanied by general tissue destruction, as shown by a massive neutrophil influx and epithelial hyperplasia, compared to uninfected controls (Fig. 3c,d).

Bladder pathology was accompanied by an increase in NK1R and SP staining in infected *Asc*$^{-/-}$ and *Nlrp3*$^{-/-}$ mice ($P < 0.01$ compared to uninfected controls, Fig. 3e,f). SP was detected throughout the epithelial layer but NK1R staining mainly in the lamina propria with co-localization basolaterally, along the interphase between the nerve plexus and the epithelium. NK1R-positive fibers between the epithelial cells were observed in inflamed regions with epithelial hyperplasia. Further, *Tacr1* and *Ppt-A* expression was higher in *Asc*$^{-/-}$ and *Nlrp3*$^{-/-}$ mice than in C57BL/6WT mice ($P < 0.05$, Fig. 3g) and urine SP levels were elevated compared to uninfected controls (248 pg/ml and 170 pg/ml respectively, $P < 0.05$, Fig. 3h). The results suggest that *Asc* and *Nlrp3* regulate important aspects of NK1R and SP expression in acute cystitis.

Contributions of neutrophils and macrophages. To address if recruited neutrophils or resident macrophages express NK1R and SP, tissue sections from infected C57BL/6WT- or *Nlrp3*$^{-/-}$ mice were stained for NK1R- and SP and counter-stained with neutrophil- or macrophage-specific antibodies. While a massive neutrophil influx was detected, there was little evidence of co-localization with NK1R or SP in most infiltrating neutrophils. Scattered sub-epithelial macrophages were visible in infected mice, but showed no staining for NK1R or SP (Supplementary Fig. S3). The results suggest that resident nerve and epithelial cells are important sources of NK1R and SP, also in the hyper-inflamed mucosa.

Effects of NK1R inhibition on mucosal inflammation. To inhibit the neuropeptide response *in vivo*, we used the irreversible non-peptide NK1R antagonist SR140333, which prevents SP from binding NK1R and is suitable for *in vivo* use[23]. *Nlrp3*$^{-/-}$ mice were given SR140333 or vehicle intra-peritoneally, one hour before infection or 30 minutes after infection with CY-17 (Fig. 4a). The severity of acute cystitis was quantified as the gross pathology score and tissue pathology score after 24 hours (Figs 4b,c and S5). SR140333 reduced the gross pathology ($P < 0.05$ for pre-and post-infection treatment), tissue pathology ($P = 0.005$ and $P = 0.03$ for pre-and post-infection treatment) as well as urine neutrophil recruitment ($P = 0.02$ and $P = 0.002$ for pre-and post-infection treatment). The post-treatment also affected bacterial clearance, as shown by a reduction in urine CFUs ($P = 0.02$, Fig. 4c). SR140333 treatment inhibited NK1R staining in infected bladders and the reduction in NK1R expression was confirmed by qRT-PCR (Fig. 4d,e).

The effect of SR140333 treatment was subsequently confirmed in C57BL/6WT mice, using the post-infection treatment protocol (Supplementary Fig. S5). SR140333 treated mice showed a significant reduction in gross pathology ($P = 0.02$) and the tissue pathology score and urine neutrophil counts were reduced ($P < 0.001$ after 24 hours and $P < 0.05$ after 7 days, Supplementary Fig. S5).

The effects of SR140333 inhibition were validated, *in vitro*, using two additional NK1R antagonists (CP99994 and L703.606). Pre-treatment of bladder epithelial cells (30 min) reduced the NK1R and SP response to CY-17 infection, to the same extent as SR140333 (Supplementary Fig. S6, MOI = 0.05, 4 hours). In addition, a dose-dependent effect on cellular ATP levels was detected, consistent with the known mechanism of action of SR140333 (Supplementary Fig. S6). The results identify NK1R as a potential therapeutic target in acute cystitis.

Inhibition of IL-1β-dependent mucosal inflammation by SR140333. To further understand the protective effect of NK1R inhibition, we analyzed the profile of genes expressed in SR140333-treated *Nlrp3*$^{-/-}$ mice (Fig. 4f). About 50% of regulated genes were suppressed by SR140333, including genes involved in sensory perception of pain (Supplementary Fig. S7). Furthermore, SR140333 reduced the expression of inflammasome- and IL-1-superfamily genes by about 70%, including *Il18, Il33, Il6* and *Il1b* (Fig. 4g,h and Supplementary Table S1). *Cxcl2*, which encodes the neutrophil chemoattractant MIP-2/Groβ was the most strongly inhibited gene, consistent with the reduced number of neutrophils in treated mice, compared to untreated controls.

Inhibition of NK1R/SP responses by Anakinra. The attenuation of the NK1R/SP response in *Il1b*$^{-/-}$ mice and the effects of the NK1R inhibitor on the expression of IL-1-superfamily genes identified IL-1β as a potential regulator of the neuropeptide response. To address this question, we used the IL-1 receptor (IL-1R) antagonist Anakinra®, which has shown therapeutic activity against acute cystitis in *Asc*$^{-/-}$ mice[20]. Anakinra® pre-treatment reduced SP/NK1R expression in C57BL/6 mice compared to sham treated controls, suggesting that IL-1β regulates neuropeptide levels in the infected bladder mucosa ($P = 0.04$, Fig. 5a–d). Furthermore, we observed a reduction in acute bladder pathology in treated mice, as well as bacterial and neutrophil counts in urine (24 hours $P < 0.05$, Fig. 5b).

This mutually inhibitory effect suggests that an activation loop involving NK1R, SP and IL-1β controls the inflammatory response in infected bladders.

Transcriptional regulation of NK1R and SP expression. ASC and NLRP-3 were recently identified as transcriptional repressors of *MMP7*; a protease responsible for non-canonical processing of pro-IL-1β in hosts lacking a functional inflammasome[20]. The over-activation of SP/NK1R in *Nlrp3*$^{-/-}$ mice suggested that a similar mechanism might regulate SP/NK1R expression. To address this question, we transfected bladder epithelial cells *in vitro* with *ASC*- or *NLRP3*-specific siRNAs (17 hours) and confirmed the inhibition of ASC and NLRP3 expression by confocal imaging and western blot analysis ($P < 0.001$ for *NLRP3*- and *ASC*-siRNA transfected cells, Fig. 6a and Supplementary Fig. S8). The transfected cells were then infected with CY-17 (MOI = 0.05, 4 hours) and changes in SP/NK1R expression were analyzed (Fig. 6b–d).

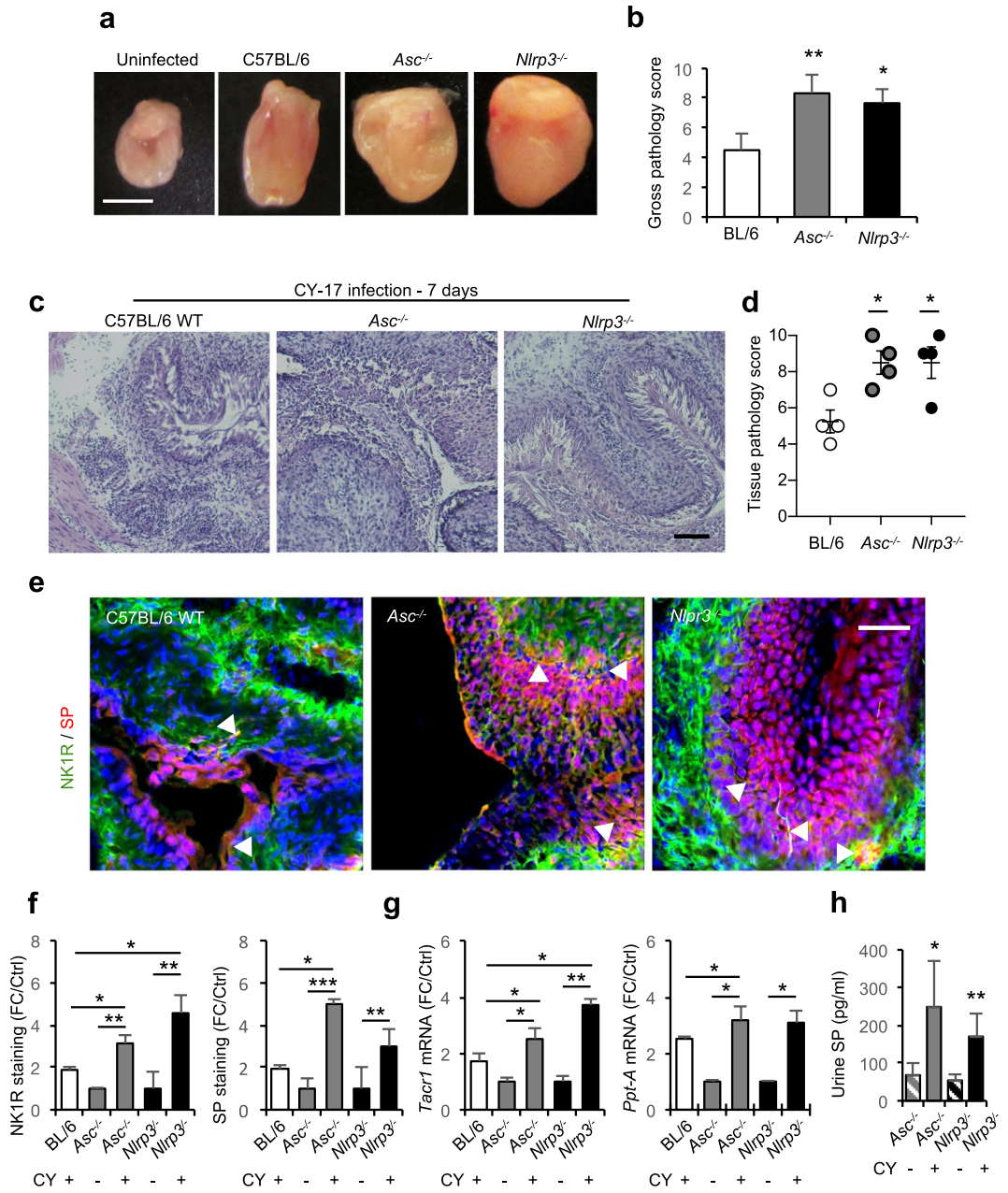

Figure 3. Severe acute cystitis is accompanied by a strong mucosal neuropeptide response in *Asc*$^{-/-}$ *and Nlrp3*$^{-/-}$ mice. (**a**) Severe acute cystitis in *Asc*$^{-/-}$ *and Nlrp3*$^{-/-}$ mice infected with CY-17 compared to uninfected mice, defined by macroscopic inspection (7 days post infection). (**b**) Gross pathology score of infected bladders. (**c**) Tissue pathology, defined by H&E staining of frozen bladder sections. Increase in inflammatory cell infiltration, edema and loss of tissue structure definition. (**d**) Increased tissue pathology score in infected *Asc*$^{-/-}$ *and Nlrp3*$^{-/-}$ mice, defined by histology. (**e**) Augmented NK1R (green) and SP (red) staining in infected *Asc*$^{-/-}$ *and Nlrp3*$^{-/-}$ mice bladder tissue. White arrowheads indicate points of co-localization. (**f**) Quantification of NK1R and SP staining in (**e**). (**g**) Elevated *Tacr1* and *Ppt-A* mRNA levels in *Asc*$^{-/-}$ and *Nlrp3*$^{-/-}$ mice, normalized against uninfected controls. (**h**) Elevated urine SP levels in *Asc*$^{-/-}$ and *Nlrp3*$^{-/-}$ mice infected with CY-17. Data is presented as means ± SEMs from $n = 3$–5 mice and analysed using Kruskal Wallis test with Dunn's correction. The response kinetics was analysed by AUC *Welsch's t*-test. $^{*}P < 0.05$, $^{**}P < 0.01$, $^{***}P < 0.001$.

NK1R and SP staining increased by about 70% in cells transfected with *ASC*- or *NLRP3*-specific siRNA (Fig. 6b–d and Supplementary Fig. S8). The effect was further enhanced by infection, compared to the scrambled siRNA control or non-transfected cells ($P < 0.01$ for *NLRP3*- or *ASC*-siRNA transfected cells, respectively), (Fig. 6b–d). To exclude that this effect was secondary to ASC and NLRP-3 dependent IL-1β activation, the transfected cells were treated with the IL-1R antagonist Anakinra. An IL-1β independent increase in NK1R was detected (Supplementary Fig. S8).

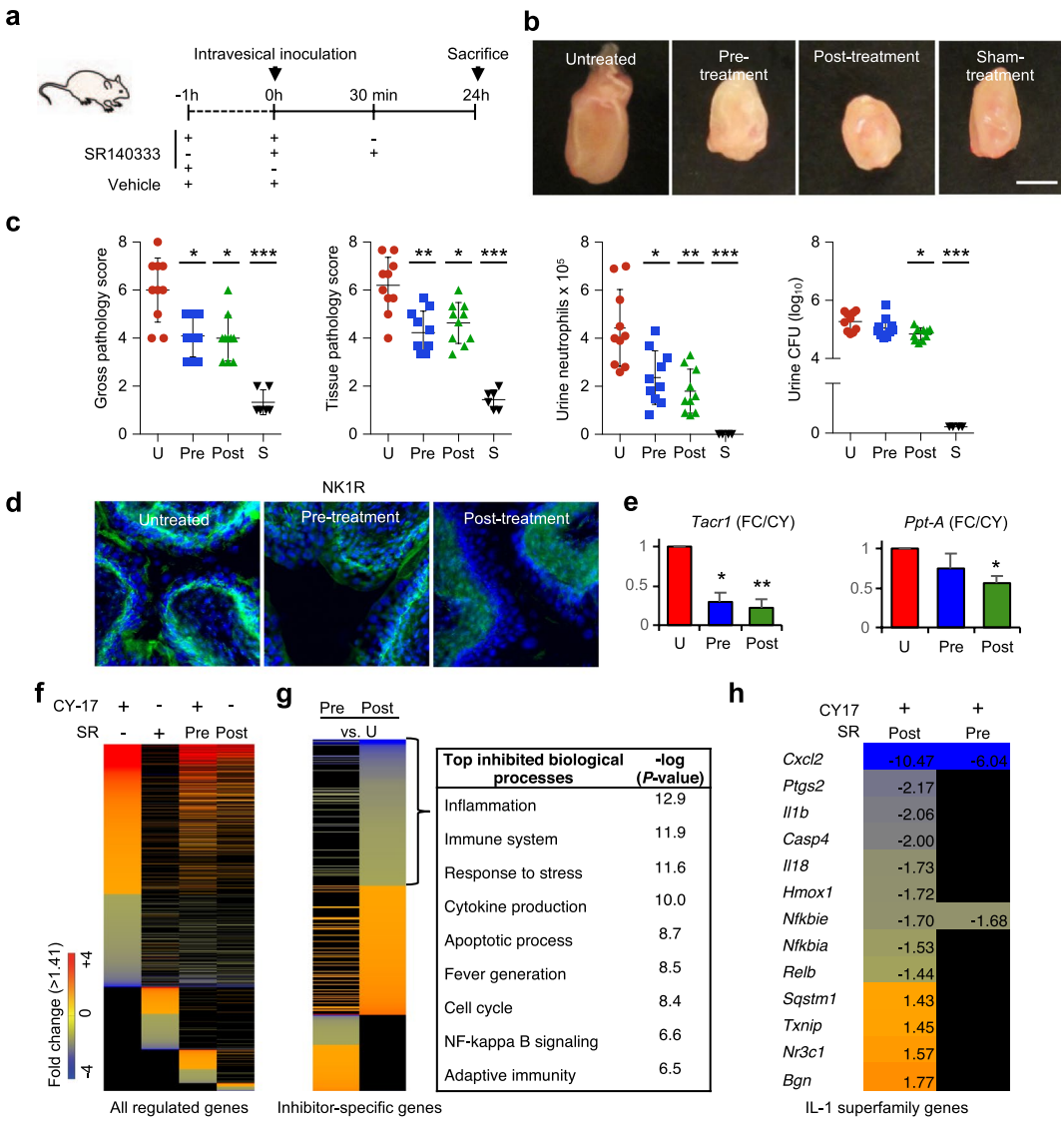

Figure 4. Therapeutic effect of NK1R inhibition in *Nlrp3*$^{-/-}$. (**a**) Treatment protocol. The irreversible, non-peptide NK1R antagonist SR140333 was used to inhibit the NK1R-dependent host response to CY-17 infection. Susceptible *Nlrp3*$^{-/-}$ mice were either pre-treated with SR140333 or treated post-infection (1 mg/kg i.p. 30 minutes prior to, or 1 hour after infection) before being sacrificed after 24 hours. Infected, un-treated mice were used as controls. (**b**) Protective effect of SR140333 treatment, shown by macroscopic inspection of infected bladders. Scale bar = 1 mm. (**c**) Decrease by SR140333 treatment of gross bladder pathology score, tissue pathology score (defined by H&E staining) and urine neutrophil counts. No change significant in bacterial counts in urine. (**d**) Inhibition of NK1R (green) staining in SR140333 treated *Nlrp3*$^{-/-}$ mice compared to infected, untreated controls. Scale bar = 100 µm. (**e**) Reduced bladder *Tacr1* and *Ppt-A* expression in SR140333 treated *Nlrp3*$^{-/-}$ mice by qRT-PCR ($n = 5$ mice. (**f**) Reduced gene expression in SR140333 treated mice compared to infected untreated controls defined by gene expression analysis of whole bladder mRNA ($n = 2$ mice per group, red = up-regulated, blue = down-regulated, $P < 0.05$, FC > 1.41, compared to uninfected controls). (**g**) Heat-map showing genes affected by SR treatment ($P < 0.05$, FC > 1.41 compared to infected untreated controls). Inhibited biological processes included inflammation and innate immune signaling. (**h**) Inhibition of inflammasome- and IL-1β related genes by SR140333 treatment, compared to untreated infected controls. Data is presented as means ± SEMs $n = 10$ mice per group (two repeats). Data was analyzed by Kruskal Wallis with Dunn's correction, *$P < 0.05$, **$P < 0.01$, ***$P < 0.001$.

The results suggested that NLRP-3 and ASC may bind to *TACR1* promoter DNA and act as repressors of *NK1R* expression (see model in Fig. 6f). This question was addressed, using a 214 base pair *TACR1* promoter fragment as a template in an Electro Mobility Shift Assay (EMSA, Fig. 6g). Lysates from uninfected HTB-9 cells created a triple band shift (a, b and c in Fig. 5h) and ASC and NLRP3 were identified as potential binding partners. Specific NLRP-3 antibodies inhibited the formation of band a and attenuated band b. Anti-ASC antibodies reduced band

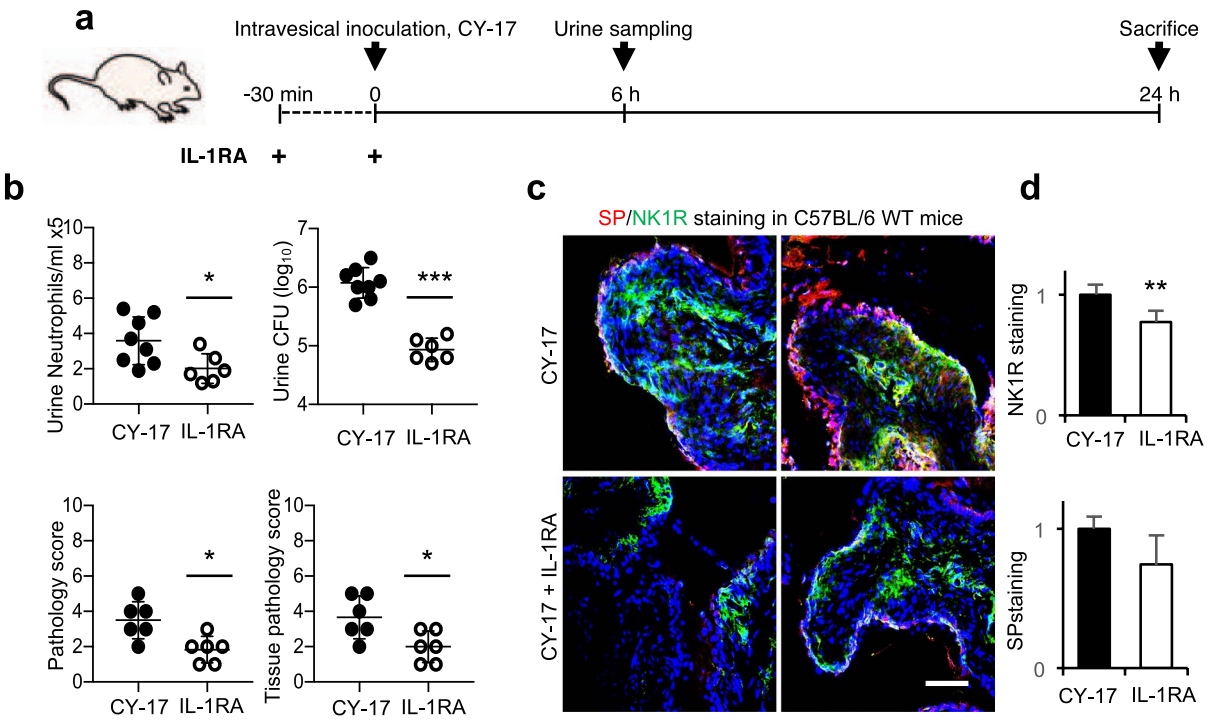

Figure 5. The IL-1 receptor antagonist Anakinra reduces mucosal neurokinin response. (**a**) Treatment protocol. C57BL/6WT mice were treated with the IL-1R antagonist Anakinra (IL-1RA), 30 minutes prior to infection and at the time of infection (1 mg/kg) with CY-17 and were sacrificed after 24 hours ($n = 6$ from two experiments). (**b**) IL-1RA treatment decreased the gross bladder pathology score, tissue pathology score (defined by H&E staining) and urine neutrophil counts as well as bacterial counts in urine compared to untreated, infected controls. (**c**) Reduction in NK1R (green) and SP (red) staining in IL-1RA treated mice compared to untreated, infected controls. Data from two representative mice are shown. (**d**) Quantification of NK1R and SP staining in (**c**). Data is represented as means ± SEMs and was analyzed by Mann-Whitney U-test, *$P < 0.05$, **$P < 0.01$, ***$P < 0.001$.

a and the two antibodies in combination inhibited bands a and b, consistent with the formation of an ASC and NLRP-3 complex on promoter DNA.

SP response in acute cystitis patients. Relevance of these findings to acute cystitis was supported by quantification of SP levels in patient urine. Patients with acute cystitis had significantly higher urine SP levels at the time of diagnosis ($n = 15$ samples from 13 patients), than patients with asymptomatic bacteriuria (ABU, $n = 42$ samples from 20 patients, $P < 0.001$, Fig. 7a,b)[24]. Low SP levels were detected in urine samples from healthy controls (Fig. 7c).

In a second analysis, we compared paired urine samples obtained from patients with asymptomatic carriage of *E. coli* 83972 who experienced symptomatic flares from the lower urinary tract induced by super-infection with a different strain. All but one of the patients had higher urine SP levels at the time of symptoms than during ABU ($n = 24$ samples from 12 patients, 191 pg/ml vs. 109 pg/ml by ELISA, $P = 0.004$, Fig. 7d). The results suggest that acute cystitis is accompanied by a SP response in the bladder mucosa.

Discussion

Infections threaten the integrity of mucosal surfaces, which retaliate, with the help of an intricate and a tightly controlled anti-microbial defense. Epithelial cells are essential for the mucosal barrier function and, when activated, they recruit a range of resident and circulating cells, to execute the defense. Mucosal surfaces are also richly innervated[25,26] and it has been proposed that the mucosal immune system is closely controlled by the nervous system[27,28]. Here we show that the mucosal immune response is regulated by direct bacterial effects on nerve cells and epithelial cells, through the activation of neuropeptides and neuropeptide receptors. The example is acute cystitis, a bacterial infection of the urinary bladder characterized by pain at voiding, urgency and frequency of urination. We show that the pathogenesis of acute cystitis involves infected nerve cells and that epithelial cells resemble nerve cells, in that they express neuropeptide receptors and secrete neuropeptides in response to infection. The results suggest that a concerted action of these two cell types may contribute significantly to pain at the site of infection and increased afferent and efferent CNS activity, which accompany mucosal infections. We also propose that these receptors may be targeted therapeutically, to alleviate symptoms associated with acute infection.

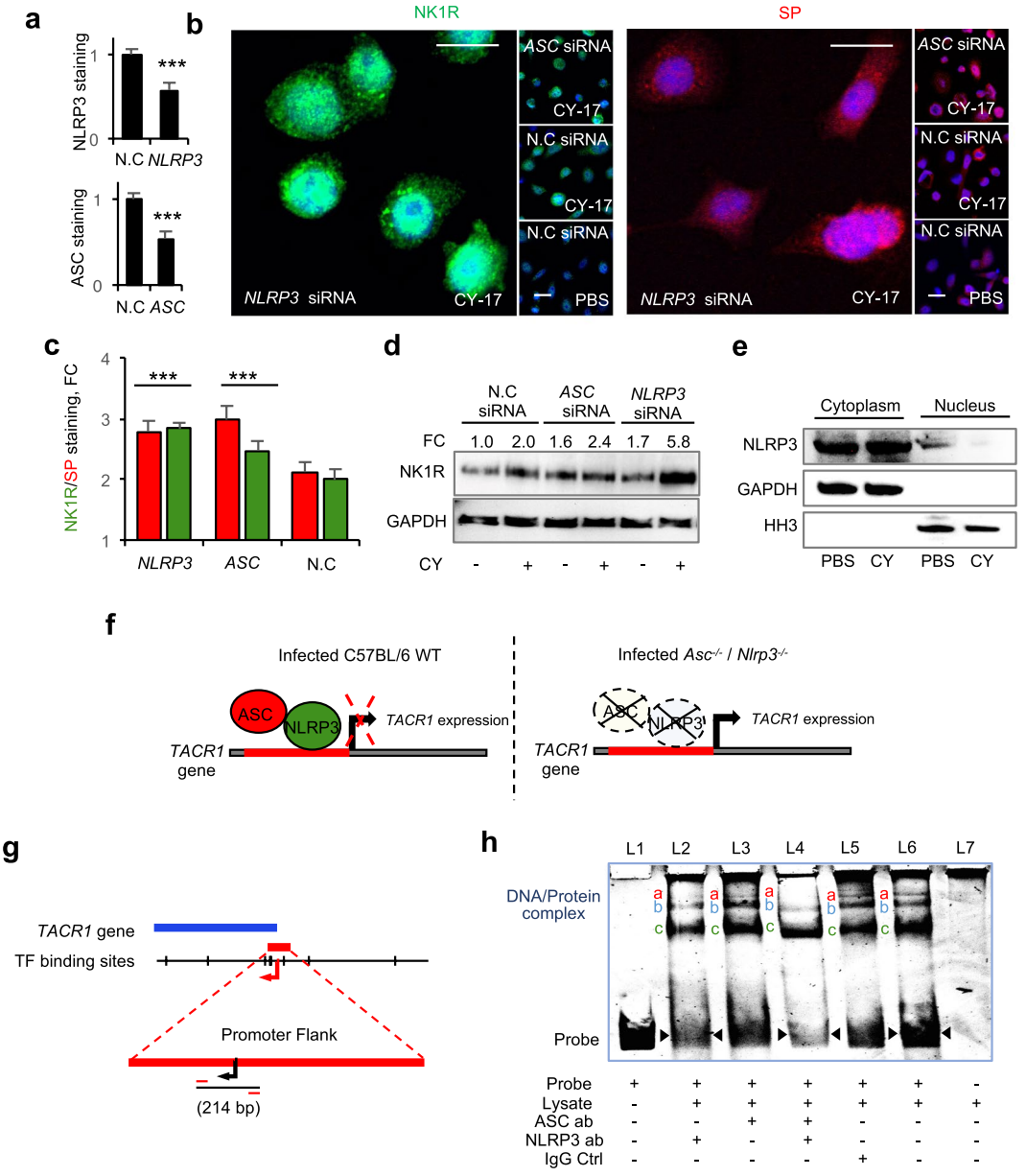

Figure 6. Transcriptional regulation of NK1R by ASC and NLRP3. To understand if NLRP-3 and ASC regulate the mucosal neurokinin response, bladder epithelial cells were transfected with specific siRNA prior to CY-17 infection and NK1R expression was quantified by confocal imaging and western blot analysis of whole cell lysates. (**a**) Evaluation of the efficacy of the siRNA treatments to inhibit ASC and NLRP3 expression in cells transfected with *ASC* or *NLRP3* siRNA (quantification of immunocytochemistry staining, FC to N.C.). (**b**) Confocal imaging of the siRNA effects on NK1R (green) and SP (red) response to infection in siRNA transfected bladder epithelial cells compared to scrambled, negative control siRNA (N.C). (**c**) Quantification of staining intensity of CY-17 infected cells in (**b**), (FC to uninfected negative control siRNA, means + SEMs ($n = 3$ experiments, 50 cells per condition). (**d**) Western blot analysis of whole cell lysates confirming the increase in NK1R seen in (**b**) (FC to uninfected negative control siRNA, $n = 3$ blots). (**e**) NLRP-3 levels in cytoplasmic and nuclear fractions of bladder cells with or without infection with CY-17 as shown by Western blot analysis ($n = 2$ blots). (**f**) Tentative model depicting transcriptional control of *TACR1* expression by ASC and NLRP3. The model predicts that the ASC/NLRP3 complex represses *TACR1* expression by binding to the *TACR1* promoter. *TACR1* expression is therefore de-repressed in cells lacking *ASC* or *NLRP3*, leading to increased cellular NK1R levels. (**g**) Representation of the *TACR1* gene with promoter flank showing the 214 bp DNA fragment used for of electrophoretic mobility shift assay (EMSA). (**h**) DNA band shifts were detected in the presence of whole cell extracts (bands a, b and c in lane 6). Specificity for NLRP-3, shown by competition with NLRP-3-specific antibodies (lane 2). Band (**a**) was removed and band (**b**) was attenuated. The ASC-specific antibody had no independent effect (lane 3), but the NLRP-3-and ASC-specific antibodies in combination removed the upper band (**a**) and further reduced band (**b**), compared to the NLRP-3 antibody alone (lane 4). The IgG antibody control did not affect the shifted bands (lane 5) (1 of 3 representative EMSAs). Data is presented as means ± SEMs and analyzed by two-tailed *t*-test. $^{**}P < 0.01$, $^{***}P < 0.001$.

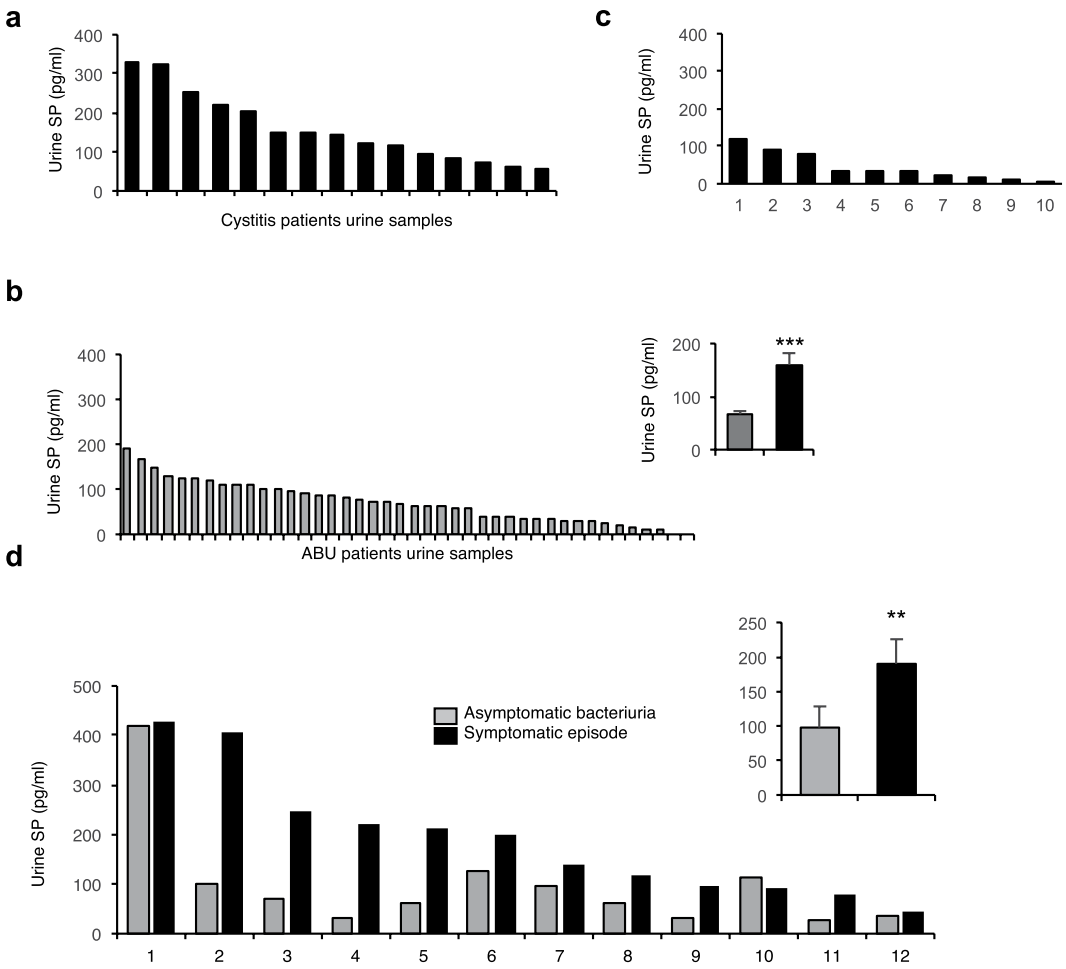

Figure 7. Urine SP levels in patients with acute cystitis compared to asymptomatic bacteriuria. Urine SP concentrations were quantified by ELISA in patients diagnosed with acute cystitis compared to healthy controls and patients with long-term ABU. (**a**) Patients with acute cystitis ($n = 15$). (**b**) Patients with long-term ABU ($n = 40$). Histogram (inset) shows elevated mean SP concentrations in patients with acute cystitis compared to ABU (Mann-Whitney U-test). (**c**) Healthy controls (n = 10). (**d**) Quantification of SP levels in paired urine samples obtained during asymptomatic carriage of *E. coli* 83972 or symptomatic episodes from the lower urinary tract caused by other bacterial strains[24] ($n = 12$ patients, 24 samples, Wilcoxon signed rank test). The red lines indicate the detection limit of the ELISA. The data is presented as means + SEMs. $^{**}P < 0.01$.

The bladder epithelium has been proposed to share key features with sensory neurons[29], including the ability to express neuropeptides and neuropeptide receptors[30,31]. As a result, the epithelium may participate in the regulation of pain and influence the micturition reflex, either by a direct myogenic detrusor effect[32] or by causing increased afferent activity[33]. This hypothesis is supported by the results of the present study. In addition, ligand release by each infected cell type was shown to trigger an amplification loop for co-activation of both cell types. We speculate that the symptoms of acute cystitis might be caused by the combined activation of the epithelial barrier and mucosal nerve cells (see model, Fig. 8). Triggered directly by infection, this response may increase afferent activity via C fibers, extending to the spinal cord and central nervous system, resulting in nociception as well as increased efferent activity, activating the lamina muscularis[34,35]. Additional cells in the lamina propria might play a role in this loop as well, including eosinophils and mast cells, which play an important role in acute cystitis and are known to produce and release SP in mice models and patients with interstitial cystitis/bladder pain syndrome[36–39].

SP/NK1R signaling has also been linked to pro-inflammatory signaling in mast cells and macrophages, and in astrocytes, IL-1β induces NK1R expression[8,40,41], suggesting that neurocrine and innate immune responses may converge. The genetic control of the NK1R/SP response was investigated here using mice carrying single gene deletions of *Tlr4*, *Il1b*, *Asc* and *Nlrp3*. Two patterns were observed. $Tlr4^{-/-}$ and $Il1b^{-/-}$ mice showed an attenuated phenotype, with markedly reduced background NK1R/SP expression and little or no response to infection. Consistent with the roles of *Tlr4*, *Il1b* as regulators of innate immunity, the mice were also unresponsive to inflammation and tissue damage and thus protected from disease. In $Asc^{-/-}$ and $Nlrp3^{-/-}$ mice, in contrast, NK1R and SP responses were markedly increased, as was tissue pathology. Interestingly, this disease phenotype was controlled by a new regulatory node, involving ASC and NLRP-3 as transcriptional repressors of *Tacr1*. The same mechanism has recently been shown to control pro-IL-1β processing, suggesting a common mechanism of

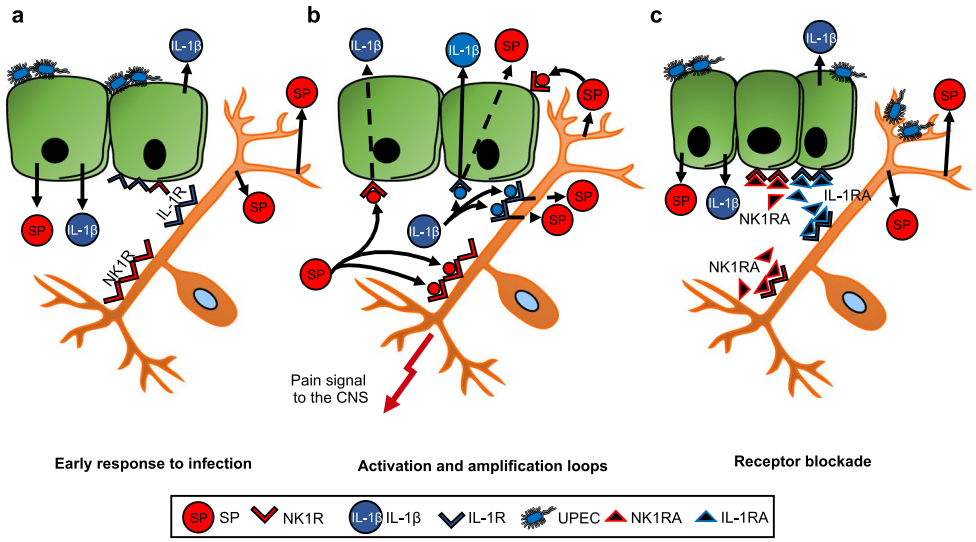

Figure 8. Model of the neuroepithelial response to *E. coli* infection – "the IL-1 - neurokinin loop". (**a**) *Early response*: Bacteria activate SP/NK1R expression in bladder epithelial cells, which are in parallel activated to produce IL-1R and to secrete IL-1β, creating an inflammatory response. (**b**) *Activation and amplification loops:* SP stimulates NK1R activation in nerve cells and activates IL-1β secretion in bladder epithelial cells, as shown by adding SP to uninfected cells. IL-1β then activates SP/NK1R expression in both nerve- and epithelial cells, which express IL-1R. (**c**) *Receptor blockade:* By treating the cells with IL-1RA or NK1R antagonists (NK1RA) both the pain signal and the inflammatory signal are inhibited (Supplementary Fig. S9). Drawings were modified from biodraw pictures (© motifolio.com).

transcriptional regulation affecting NK1R expression and IL-1β processing. NF-κB family genes were also regulated during bladder infection in *Nlrp3*$^{-/-}$ mice and *Nfkb* expression was suppressed by SR140333 treatment of infected mice, supporting previous studies indicating that NF-κB might be involved as an upstream regulator of SP/NK1R and pro-inflammatory signaling[8,42].

The predicted outcome of SP binding to NK1R is pain, as shown in numerous studies[43] and a link between the neuropeptide response and lower urinary tract symptoms has previously been documented in models of pelvic pain, interstitial cystitis and UTI where an increase in SP-reactive varicose nerve fibers has been observed within the lamina propria, additionally, Duell *et al*. detected an increase in *Tac1* gene expression after bladder infection in mice[44,45]. In addition, elevated urine SP concentrations were detected in patients with interstitial cystitis and in UTI patients with pyuria[46–49]. Consistent with these studies, we found elevated SP levels in patients with acute cystitis compared to patients with ABU and healthy controls. Furthermore, in a longitudinal study of ABU, a pair-wise, intra-individual comparison of SP levels revealed a difference between asymptomatic and symptomatic episodes in individual patients, suggesting that neuropeptides may serve as biomarkers of mucosal involvement in this patient group. Consistent with pain from the urinary bladder area, we detected elevated urine SP levels and a loss of locomotion, lack of rearing and grooming behavior in infected C57BL/6 mice with bladder pathology.

Anti-inflammatory agents are emerging as a novel therapeutic approach in acute cystitis, suppressing the symptoms while the host clears the infection. We have previously shown that inhibition of IL-1β by Anakinra treatment is efficient in the murine acute cystitis model[20]. In this study, we further suggest that NK1R inhibition might constitute an interesting alternative approach to prevent inflammation and pathology. Several studies have documented the therapeutic efficacy of different NK1R antagonists in rodent models of nociception[17,50], and in patients with irritable bowel syndrome, pain and anxiety was reduced by chronic NK1R antagonist treatment[51]. In addition, NK1R antagonist treatment has proved effective in clinical studies of overactive bladder syndrome, characterized by urgency and frequency, symptoms shared with acute cystitis[52–54]. In clinical trials investigating analgesic effects, these drugs have often failed, however[55]. Our findings suggest that the use of NK1R antagonist therapy should be explored in patients with acute cystitis or recurrent UTIs, where antibiotic resistance is creating an urgent need for novel therapeutic alternatives.

Methods

Cellular assays. *Bacterial strains.* The cystitis isolates including CY-17 and ABU isolates were isolated during a prospective study of childhood UTI in Gothenburg, Sweden[56,57] *E. coli* CFT073 (O6:K2:H1)[58] and *E. coli* 83972 (OR:K5:H-)[59] were used as controls. Bacteria were cultured on tryptic soy agar plates (TSA, 16 h, 37 °C), harvested in phosphate buffered saline (PBS, pH 7.2) and diluted to appropriate concentration for infection.

Cell culture. Grade II human bladder epithelial cells HTB-9 (ATCC, 5637), kidney epithelial cells A-498 (ATCC, HTB-44), and DLD-1 colon epithelial cells (ATCC, CCL-221) were cultured in RPMI-1640 and human neuroblastoma cells (ATCC, SH-SY5Y) were cultured in DMEM/F12 supplemented with sodium pyruvate, non-essential amino acids and 10% heat inactivated FBS and incubated at 37 °C with 5% CO_2.

In vitro infection. HTB9, A498 and DLD1 cells were grown on 8-well glass chamber slides (6×10^4 cells/well) or in 6 well plates (6×10^5 cells/well) overnight in media supplemented with 10% FBS. SH-SY5Y cells were differentiated in 8-well chamber slides (2×10^4 cells/well) or 6 well plates (1.5×10^5 cells/well) using 1% Retinoic acid and serum starvation for 7 days[60]. Cells were washed with PBS and serum free media were added prior to infection with appropriately diluted bacteria in PBS (MOI = 0.05) and incubated for 4 hours at 37 °C with 5% CO_2.

NK1R and IL-1β inhibition assays. Cultured cells were pre-treated with NK1R antagonists (5–500 ng/ml) (SR140333, CP-99994 or L-703 606) or IL-1RA (500 ng/ml) (Kineret, Sobi) 30 minutes before infection.

NLRP3 and ASC siRNA transfection. HTB-9 cells were transfected with PYCARD/ASC or NLRP3 specific siRNAs (0.09 μM, Flexi-Tube GeneSolution, #GS29108 and #GS114548, Qiagen) or with AllStars Negative Control siRNA (#SI03650318, Qiagen) using the HiPerFect Transfection Reagent (#301705, Qiagen) for 17 hours, then infected.

Immunostaining of nerve cells and epithelial cells, in vitro. Cells were stained using anti-NK1R. anti-substance P, anti-NLRP3, anti-ASC anti-IL-1β as well as antibodies to nerve cell markers anti-βIII tubulin and anti-NeuN (5% FBC overnight at 4 °C) followed by appropriatly Alexa fluor conjugated secondary antibodies (Molecular Probes) (5% FBS and 0.025% Triton X-100, 1 hour at room temperature), then counterstained with DRAQ5 (Abcam) and examined by laser scanning confocal microscope (Carl Zeiss) and quantified by ImageJ. Antibody controls included primary antibody absorption with specific antigens to NK1R or SP before staining (5:1 ratio, 16 hours at 4 °C), and secondary antibody controls (Supplementary Fig. S10).

Western blotting. Cells were lysed with NP-40 lysis buffer or by NE-PER Nuclear and Cytoplasmic Extraction Reagents (Thermo Fisher Scientific) supplemented with protease and phosphatase inhibitors (Roche Diagnostics). 7 μg of proteins were run on SDS-PAGE (4–12% Bis-Tris gels, Invitrogen) and blotted onto PVDF membranes (GE Healthcare), blocked (5% NFDM) and stained using anti-NK1R, anti-Substance-P, anti NLRP-3 or anti-ASC primary antibodies. β-actin or GAPDH served as the loading control. Bands were imaged using ECL plus detection reagent (GE Health Care) and were quantified by ImageJ.

ELISA. SP and IL-1β in filtered supernatants from uninfected and infected cells were measured by Substance P parameter kit (R&D systems) or IL-1β DuoSet (R&D systems).

Electromobility shift assay (EMSA). A 214 DNA fragment from the *TACR1* promoter was used as probe and stained with GelGreen (Biotium). Each reaction contained 3–5 μg of DNA probe and 5 μg of cell extracts from uninfected HTB-9 cells in binding buffer (100 mMTris, 500 mM NaCl and 10 mM DTT, pH 7). For the band shift competition assay, 1 μg of anti-ASC or anti-NLRP3 antibodies were used separately and together. Binding reactions were incubated at 15 °C for 30 min, loaded onto a 6% non-denaturing, non-reducing polyacrylamide gel and ran in a 50 mM Tris (pH 7), 0.38 M glycine, and 2 mM EDTA buffer at 125 V for 2 hours. Mouse IgG2A isotype control was used as negative control antibody. Gels were imaged using the Bio-RAD ChemiDoc system.

PMN and PBMC isolation and flow cytometry. PMNs and PBMCs were isolated from healthy controls according to the protocol from Olsson *et al.*[61]. Isolated PBMCs and PMNs were stimulated with filtered supernatants from infected or uninfected HTB-9 cells (1 h at 37 °C) before staining using anti-NK1R primary antibodies (PBS, 45 min RT) and alexa-488 conjugated secondary antibodies (PBS, 30 min RT). The stained cells were analyzed using Accuri C6 (BD biosciences).

Mice. Female C57BL/6 mice or *Tlr4*$^{-/-}$, *Il1b*$^{-/-}$ [62,63], *Nlrp3*$^{-/-}$, *Asc*$^{-/-}$ [64] mice were used for experiments at 9–15 weeks of age. *Nlrp3*$^{-/-}$ and *Asc*$^{-/-}$ mice were from Jürg Tschopp's laboratory, Department of Biochemistry, University of Lausanne and Institute for Arthritis Research (aIAR). *Il1b*$^{-/-}$ mice were generated by the Iwakura lab, Laboratory Animal Research Center, Institute of Medical Science, University of Tokyo. *Tlr4*$^{-/-}$ mice were generated in the BIKEN animal facilities, Osaka, Japan. Mice were bred and housed in the specific pathogen-free MIG animal facilities (Lund, Sweden) with free access to food and water. For number of mice used, see respective figure legend.

Experimental acute cystitis. Mice were intravesically infected with CY-17 under Isofluorane anesthesia (10^8 CFU in 0.1 ml), through a soft polyethylene catheter. Pain behavior (lack of rearing, lack of locomotion and grooming behavior) was recorded for each mouse for 3 minutes in a clear cage at 24 hours and 7 days, modified from Ruddick *et al.*[65]. Bladders were aseptically removed at sacrifice and documented by photography for gross pathology analysis, before being embedded in O.C.T compound for H&E and IHC analysis as previously described[20], scoring was non-blinded and performed by two independent researchers. Urine samples were obtained before infection and at regular times after infection. Bacterial burden was quantitatively cultured and urine neutrophils were quantified in a hemocytometer. Urine SP was quantified by Substance P parameter kit (R&D systems).

NK1R and IL-1RA therapy. SR140333 was injected intraperitonally (i.p.) in *Nlrp3*$^{-/-}$ (1 mg/kg), either 1 hour prior to infection or 30 minutes after infection with CY-17 for 24 hours. C57BL/6WT mice were treated with the post-infection regime (1 mg/kg) 24 hours or 7 days. IL-1RA was injected (1 mg/kg, i.p.) in C57BL/6WT mice 1 hour prior to CY-17 infection for 24 hours.

Immunohistochemistry. 7-µm-thick cryosections were mounted on positively charged microscope slides and stained as previously described using anti-NK1R, anti-substance P, anti-βIII tubulin antibodies, anti-neutrophil and anti-macrophage antibodies[20]. Sections were imaged by laser scanning confocal microscopy or by fluorescence microscopy. Staining controls included antibody absorption and secondary antibody controls (Supplementary Fig. S10).

mRNA isolation. Total RNA was extracted from murine bladders in RLT buffer with added β-Mercaptoethanol (1%) after disruption in a tissue homogenizer (TissueLyser LT, Qiagen) using Precellys® Lysing kits (Bertin Technologies), with the RNeasy® Mini Kit (Qiagen).

Global gene expression in infected bladders. Total bladder RNA was amplified using GeneChip 3´IVT Express Kit, hybridized onto Mouse Genome 430 PM array strips (16 hours at 45 °C), washed, stained and scanned using the Geneatlas system (Affymetrix). Data was normalized using Robust Multi Average implemented in the Partek Express Software (Partek). Significantly altered genes were sorted by relative expression (2-way ANOVA model using Method of Moments, P-values < 0.05 and absolute fold change >1.41) and analysed using Ingenuity Pathway Analysis software (Ingenuity Systems, Qiagen) and ToppGene[66]. Heat-maps were constructed using Gitools 2.1.1 software.

Quantitative RT-PCR. Quantitative RT-PCR was performed as previously described using primers pairs against *Mus Musculus Tacr1*, *Ppt-A, Cxcl2 and Il1b* per the MIQE guidelines on a Rotor Gene Q (Qiagen) (Supplementary Table S3)[20,67]. qRT-PCR reactions were run in technical duplicates and gene expression was analyzed based on **ΔΔ**CT comparison to *Mus Musculus Gapdh*.

Clinical urine samples. Urine samples from adult patients with community acquired acute cystitis were collected at two primary health care units in Lund, Sweden[20]. A diagnosis of acute cystitis was based on a urine dipstick analysis positive for bacteria and lower urinary tract symptoms (dysuria, suprapubic pain and no fever). Urine samples from patients with asymptomatic bacteriuria were obtained from a previous study[24] from patients who carried *E. coli* 83972 asymptomatically or from the control arm of the study (Placebo control or after spontaneous clearance of *E. coli* 83972). Urine SP levels were quantified by ELISA using the Human Substance-P ELISA kit (ab133029, Abcam).

Ethical statement. Experiments were approved by the Malmö/Lund Animal Experimental Ethics Committee at the Lund District Court, Sweden (numbers M104-10 and M44-13). All animal care and protocols were governed by the European Parlement and Council Directive (2016/63, EU) The Swedish Animal Welfare Act (Djurskyddslagen 1988:534), the Swedish Welfare Ordinance (Djurskyddsförordningen 1988:539) and Institutional Animal Care and Use Committee (IACUC) Guidelines. All the experiments were reported per the ARRIVE guidelines. The studies of human UTI were approved by the Ethics Committee of the medical faculty, Lund University, Sweden (LU106-02, LU236-99, Dnr 298/2006; 463/2010 and Clinical Trial Registration RTP-A2003, International Committee of Medical Journal Editors, www.clinicaltrials.gov), Patients gave their informed written consent and all experiments were performed in accordance with the relevant guidelines and regulations.

Statistics. Unpaired t-tests and one-way ANOVA (Bonferroni for Post-Hoc analysis) were used for data determined to follow a normal distribution defined by D'agostino & Pearson normality test. Mann-Whitney U-tests, Wilcoxon signed ranked tests and Kruskal Wallis tests (Dunn's test for Post-Hoc analysis) were used for non-parametric analyses. Welsh's t-test were used to determine statistics for kinetic responses. $^{*}P < 0.05$, $^{**}P < 0.01$ and $^{***}P < 0.001$. The data was examined by using Prism (v. 6.0 GraphPad).

References

1. Gautam, M. *et al.* Role of neurokinin type 1 receptor in nociception at the periphery and the spinal level in the rat. *Spinal Cord* **54**, 172–182, https://doi.org/10.1038/sc.2015.206 (2016).
2. Luccarini, P., Henry, M., Alvarez, P., Gaydier, A. M. & Dallel, R. Contribution of neurokinin 1 receptors in the cutaneous orofacial inflammatory pain. *Naunyn Schmiedebergs Arch Pharmacol* **368**, 320–323, https://doi.org/10.1007/s00210-003-0799-z (2003).
3. O'Connor, T. M. *et al.* The role of substance P in inflammatory disease. *J Cell Physiol* **201**, 167–180, https://doi.org/10.1002/jcp.20061 (2004).
4. Weinstock, J. V. & Substance, P. and the regulation of inflammation in infections and inflammatory bowel disease. *Acta Physiol (Oxf)* **213**, 453–461, https://doi.org/10.1111/apha.12428 (2015).
5. Chiu, I. M. *et al.* Bacteria activate sensory neurons that modulate pain and inflammation. *Nature* **501**, 52–57, https://doi.org/10.1038/nature12479 (2013).
6. Obata, F., Hippler, L. M., Saha, P., Jandhyala, D. M. & Latinovic, O. S. Shiga toxin type-2 (Stx2) induces glutamate release via phosphoinositide 3-kinase (PI3K) pathway in murine neurons. *Frontiers in molecular neuroscience* **8**, 30, https://doi.org/10.3389/fnmol.2015.00030 (2015).
7. Acosta, C. & Davies, A. Bacterial lipopolysaccharide regulates nociceptin expression in sensory neurons. *J Neurosci Res* **86**, 1077–1086, https://doi.org/10.1002/jnr.21565 (2008).
8. Azzolina, A., Bongiovanni, A. & Lampiasi, N. Substance P induces TNF-alpha and IL-6 production through NF kappa B in peritoneal mast cells. *Biochim Biophys Acta* **1643**, 75–83 (2003).
9. Callsen-Cencic, P. & Mense, S. Expression of neuropeptides and nitric oxide synthase in neurones innervating the inflamed rat urinary bladder. *Journal of the autonomic nervous system* **65**, 33–44 (1997).
10. Stamm, W. E. & Norrby, S. R. Urinary tract infections: Disease panorama and challenges. *Journal of Infectious Diseases* **183**, S1–S4, https://doi.org/10.1086/318850 (2001).
11. Frazier, E. P., Peters, S. L., Braverman, A. S., Ruggieri, M. R. Sr. & Michel, M. C. Signal transduction underlying the control of urinary bladder smooth muscle tone by muscarinic receptors and beta-adrenoceptors. *Naunyn Schmiedebergs Arch Pharmacol* **377**, 449–462, https://doi.org/10.1007/s00210-007-0208-0 (2008).

12. Norinder, B. S., Koves, B., Yadav, M., Brauner, A. & Svanborg, C. Do *Escherichia coli* strains causing acute cystitis have a distinct virulence repertoire? *Microbial pathogenesis* **52**, 10–16, https://doi.org/10.1016/j.micpath.2011.08.005 (2012).
13. Saban, R. *et al*. Neurokinin-1 (NK-1) receptor is required in antigen-induced cystitis. *The American journal of pathology* **156**, 775–780, https://doi.org/10.1016/S0002-9440(10)64944-9 (2000).
14. Zhang, H. P. *et al*. The function of P2X3 receptor and NK1 receptor antagonists on cyclophosphamide-induced cystitis in rats. *World J Urol* **32**, 91–97, https://doi.org/10.1007/s00345-013-1098-z (2014).
15. Rudick, C. N. *et al*. Uropathogenic *Escherichia coli* induces chronic pelvic pain. *Infect Immun* **79**, 628–635, https://doi.org/10.1128/IAI.00910-10 (2011).
16. Rudick, C. N. *et al*. O-antigen modulates infection-induced pain states. *PloS one* **7**, e41273, https://doi.org/10.1371/journal.pone.0041273 (2012).
17. Rudick, C. N., Schaeffer, A. J. & Klumpp, D. J. Pharmacologic attenuation of pelvic pain in a murine model of interstitial cystitis. *BMC Urol* **9**, 16, https://doi.org/10.1186/1471-2490-9-16 (2009).
18. Meseguer, V. *et al*. TRPA1 channels mediate acute neurogenic inflammation and pain produced by bacterial endotoxins. *Nature communications* **5**, 3125, https://doi.org/10.1038/ncomms4125 (2014).
19. Yadav, M. *et al*. Inhibition of TIR domain signaling by TcpC: MyD88-dependent and independent effects on *Escherichia coli* virulence. *PLoS pathogens* **6**, e1001120, https://doi.org/10.1371/journal.ppat.1001120 (2010).
20. Ambite, I. *et al*. Molecular Basis of Acute Cystitis Reveals Susceptibility Genes and Immunotherapeutic Targets. *PLoS pathogens* **12**, https://doi.org/10.1371/journal.ppat.1005848 (2016).
21. Leffler, H., Lomberg, H. & Svanborg-Eden, C. In *Host Parasite Interactions in Urinary Tract Infections* (eds E. H. Kass & C. Svanborg-Eden) 93–99 (University of Chicago Press, Chicago, IL, 1989).
22. Poltorak, A. *et al*. Defective LPS signaling in C3H/HeJ and C57BL/10ScCr mice: mutations in Tlr4 gene. *Science* **282**, 2085–2088 (1998).
23. Oury-Donat, F. *et al*. SR 140333, a novel, selective, and potent nonpeptide antagonist of the NK1 tachykinin receptor: characterization on the U373MG cell line. *J Neurochem* **62**, 1399–1407 (1994).
24. Sunden, F., Hakansson, L., Ljunggren, E. & Wullt, B. *Escherichia coli* 83972 Bacteriuria Protects Against Recurrent Lower Urinary Tract Infections in Patients With Incomplete Bladder Emptying. *J Urology* **184**, 179–185, https://doi.org/10.1016/j.juro.2010.03.024 (2010).
25. Lundgren, O. Enteric nerves and diarrhoea. *Pharmacol Toxicol* **90**, 109–120 (2002).
26. Newton, M. *et al*. Oesophageal epithelial innervation in health and reflux oesophagitis. *Gut* **44**, 317–322 (1999).
27. Shanahan, F. Brain-gut axis and mucosal immunity: a perspective on mucosal psychoneuroimmunology. *Semin Gastrointest Dis* **10**, 8–13 (1999).
28. Suzuki, R. *et al*. Direct neurite-mast cell communication *in vitro* occurs via the neuropeptide substance P. *Journal of immunology* **163**, 2410–2415 (1999).
29. Birder, L. & Andersson, K. E. Urothelial signaling. *Physiol Rev* **93**, 653–680, https://doi.org/10.1152/physrev.00030.2012 (2013).
30. Girard, B. M., Malley, S. E., Braas, K. M., May, V. & Vizzard, M. A. PACAP/VIP and receptor characterization in micturition pathways in mice with overexpression of NGF in urothelium. *Journal of molecular neuroscience: MN* **42**, 378–389, https://doi.org/10.1007/s12031-010-9384-3 (2010).
31. Heng, Y. J., Saunders, C. I., Kunde, D. A. & Geraghty, D. P. TRPV1, NK1 receptor and substance P immunoreactivity and gene expression in the rat lumbosacral spinal cord and urinary bladder after systemic, low dose vanilloid administration. *Regul Pept* **167**, 250–258, https://doi.org/10.1016/j.regpep.2011.02.004 (2011).
32. Maggi, C. A., Santicioli, P., Giuliani, S., Regoli, D. & Meli, A. Activation of micturition reflex by substance P and substance K: indirect evidence for the existence of multiple tachykinin receptors in the rat urinary bladder. *J Pharmacol Exp Ther* **238**, 259–266 (1986).
33. Chien, C. T., Yu, H. J., Lin, T. B., Lai, M. K. & Hsu, S. M. Substance P via NK1 receptor facilitates hyperactive bladder afferent signaling via action of ROS. *American journal of physiology. Renal physiology* **284**, F840–851, https://doi.org/10.1152/ajprenal.00187.2002 (2003).
34. Dafny, N. *et al*. Lateral hypothalamus: Site involved in pain modulation. *Neuroscience* **70**, 449–460, https://doi.org/10.1016/0306-4522(95)00358-4 (1996).
35. Fowler, C. J., Griffiths, D. & de Groat, W. C. The neural control of micturition. *Nat Rev Neurosci* **9**, 453–466, https://doi.org/10.1038/nrn2401 (2008).
36. Abraham, S. N. & Miao, Y. The nature of immune responses to urinary tract infections. *Nat Rev Immunol* **15**, 655–663, https://doi.org/10.1038/nri3887 (2015).
37. Pang, X., Boucher, W., Triadafilopoulos, G., Sant, G. R. & Theoharides, T. C. Mast cell and substance P-positive nerve involvement in a patient with both irritable bowel syndrome and interstitial cystitis. *Urology* **47**, 436–438, https://doi.org/10.1016/S0090-4295(99)80469-5 (1996).
38. Saban, R. *et al*. Mast cells mediate substance P-induced bladder inflammation through an NK(1) receptor-independent mechanism. *American journal of physiology. Renal physiology* **283**, F616–629, https://doi.org/10.1152/ajprenal.00096.2002 (2002).
39. Wang, X. *et al*. Evidence for the Role of Mast Cells in Cystitis-Associated Lower Urinary Tract Dysfunction: A Multidisciplinary Approach to the Study of Chronic Pelvic Pain Research Network Animal Model Study. *PloS one* **11**, e0168772, https://doi.org/10.1371/journal.pone.0168772 (2016).
40. Xu, J., Xu, F. & Lin, Y. Cigarette smoke synergizes lipopolysaccharide-induced interleukin-1beta and tumor necrosis factor-alpha secretion from macrophages via substance P-mediated nuclear factor-kappaB activation. *American journal of respiratory cell and molecular biology* **44**, 302–308, https://doi.org/10.1165/rcmb.2009-0288OC (2011).
41. Chiu, I. M., von Hehn, C. A. & Woolf, C. J. Neurogenic inflammation and the peripheral nervous system in host defense and immunopathology. *Nature neuroscience* **15**, 1063–1067, https://doi.org/10.1038/nn.3144 (2012).
42. Guo, C. J. *et al*. Interleukin-1beta upregulates functional expression of neurokinin-1 receptor (NK-1R) via NF-kappaB in astrocytes. *Glia* **48**, 259–266, https://doi.org/10.1002/glia.20079 (2004).
43. Munoz, M. & Covenas, R. Involvement of substance P and the NK-1 receptor in human pathology. *Amino acids* **46**, 1727–1750, https://doi.org/10.1007/s00726-014-1736-9 (2014).
44. Wakabayashi, Y., Tomoyoshi, T., Fujimiya, M., Arai, R. & Maeda, T. Substance P-Containing Axon Terminals in the Mucosa of the Human Urinary-Bladder - Preembedding Immunohistochemistry Using Cryostat Sections for Electron-Microscopy. *Histochemistry* **100**, 401–407, https://doi.org/10.1007/Bf00267819 (1993).
45. Duell, B. L. *et al*. Innate transcriptional networks activated in bladder in response to uropathogenic *Escherichia coli* drive diverse biological pathways and rapid synthesis of IL-10 for defense against bacterial urinary tract infection. *Journal of immunology* **188**, 781–792, https://doi.org/10.4049/jimmunol.1101231 (2012).
46. Pennycuff, J. F. *et al*. Urinary neurotrophic peptides in postmenopausal women with and without overactive bladder. *Neurourology and urodynamics*, https://doi.org/10.1002/nau.23011 (2016).
47. Altuntas, S. C., Ipekci, T., Yakupoglu, G. & Erin, N. Changes in urine levels of substance P, vasoactive intestinal peptide and calcitonin-gene-related peptide in patients with urinary tract infections. *Peptides* **56**, 151–155, https://doi.org/10.1016/j.peptides.2014.04.003 (2014).
48. Kushner, L. *et al*. Urinary substance P concentration correlates with urinary frequency and urgency in interstitial cystitis patients treated with intravesical dimethyl sulfoxide and not intravesical anesthetic cocktail. *Urology* **57**, 129 (2001).

49. Campbell, D. J., Tenis, N., Rosamilia, A., Clements, J. A. & Dwyer, P. L. Urinary levels of substance P and its metabolites are not increased in interstitial cystitis. *BJU Int* **87**, 35–38 (2001).
50. Kamp, E. H., Beck, D. R. & Gebhart, G. F. Combinations of neurokinin receptor antagonists reduce visceral hyperalgesia. *J Pharmacol Exp Ther* **299**, 105–113 (2001).
51. Tillisch, K. *et al*. Neurokinin-1-receptor antagonism decreases anxiety and emotional arousal circuit response to noxious visceral distension in women with irritable bowel syndrome: a pilot study. *Aliment Pharmacol Ther* **35**, 360–367, https://doi.org/10.1111/j.1365-2036.2011.04958.x (2012).
52. Frenkl, T. L. *et al*. A multicenter, double-blind, randomized, placebo controlled trial of a neurokinin-1 receptor antagonist for overactive bladder. *The Journal of urology* **184**, 616–622, https://doi.org/10.1016/j.juro.2010.03.147 (2010).
53. Green, S. A. *et al*. Efficacy and safety of a neurokinin-1 receptor antagonist in postmenopausal women with overactive bladder with urge urinary incontinence. *The Journal of urology* **176**, 2535–2540; discussion 2540, https://doi.org/10.1016/j.juro.2006.08.018 (2006).
54. Haab, F. *et al*. Efficacy and safety of repeated dosing of netupitant, a neurokinin-1 receptor antagonist, in treating overactive bladder. *Neurourology and urodynamics* **33**, 335–340, https://doi.org/10.1002/nau.22406 (2014).
55. Hill, R. NK1 (substance P) receptor antagonists–why are they not analgesic in humans? *Trends Pharmacol Sci* **21**, 244–246 (2000).
56. Leffler, H. & Svanborg-Eden, C. Glycolipid receptors for uropathogenic *Escherichia coli* on human erythrocytes and uroepithelial cells. *Infect Immun* **34**, 920–929 (1981).
57. Caugant, D. A. *et al*. Genetic diversity in relation to serotype in *Escherichia coli*. *Infection and immunity* **49**, 407–413 (1985).
58. Mobley, H. L. *et al*. Pyelonephritogenic *Escherichia coli* and killing of cultured human renal proximal tubular epithelial cells: role of hemolysin in some strains. *Infection and immunity* **58**, 1281–1289 (1990).
59. Agace, W. W., Hedges, S. R., Ceska, M. & Svanborg, C. Interleukin-8 and the neutrophil response to mucosal gram-negative infection. *The Journal of clinical investigation* **92**, 780–785, https://doi.org/10.1172/JCI116650 (1993).
60. Lopes, F. M. *et al*. Comparison between proliferative and neuron-like SH-SY5Y cells as an *in vitro* model for Parkinson disease studies. *Brain Res* **1337**, 85–94, https://doi.org/10.1016/j.brainres.2010.03.102 (2010).
61. Olsson, L. M. *et al*. A single nucleotide polymorphism in the NCF1 gene leading to reduced oxidative burst is associated with systemic lupus erythematosus. *Ann Rheum Dis* **76**, 1607–1613, https://doi.org/10.1136/annrheumdis-2017-211287 (2017).
62. Horai, R. *et al*. Production of mice deficient in genes for interleukin (IL)-1alpha, IL-1beta, IL-1alpha/beta, and IL-1 receptor antagonist shows that IL-1beta is crucial in turpentine-induced fever development and glucocorticoid secretion. *The Journal of experimental medicine* **187**, 1463–1475 (1998).
63. Mariathasan, S. *et al*. Cryopyrin activates the inflammasome in response to toxins and ATP. *Nature* **440**, 228–232, https://doi.org/10.1038/nature04515 (2006).
64. Mariathasan, S. *et al*. Differential activation of the inflammasome by caspase-1 adaptors ASC and Ipaf. *Nature* **430**, 213–218, https://doi.org/10.1038/nature02664 (2004).
65. Rudick, C. N., Bryce, P. J., Guichelaar, L. A., Berry, R. E. & Klumpp, D. J. Mast cell-derived histamine mediates cystitis pain. *PloS one* **3**, e2096, https://doi.org/10.1371/journal.pone.0002096 (2008).
66. Chen, J., Bardes, E. E., Aronow, B. J. & Jegga, A. G. ToppGene Suite for gene list enrichment analysis and candidate gene prioritization. *Nucleic Acids Res* **37**, W305–311, https://doi.org/10.1093/nar/gkp427 (2009).
67. Bustin, S. A. *et al*. The MIQE guidelines: minimum information for publication of quantitative real-time PCR experiments. *Clinical chemistry* **55**, 611–622, https://doi.org/10.1373/clinchem.2008.112797 (2009).

Acknowledgements

We would gratefully acknowledge the assistance of Miss Arve, Miss Petersson and Mr. Schmidt for providing reagents and protocols for flow cytometry. Furthermore, we gratefully acknowledge the support of the Swedish Medical Research Council, Medical Faculty (Lund University), Swedish Cancer Society, the Sharon D Lund, Söderberg and Österlund Foundations, the Anna-Lisa and Sven-Erik Lundgren-, Maggie Stephens-, Inga-Britt and Arne Lundberg- and HJ Forssman Foundations and the Royal Physiographic Society. K.N. was supported by the European Urological Scholarship Program (EUSP/Scholarship S-03-2013).

Author Contributions

D.S.C.B., I.A. and M.P. planned, performed and analysed experiments and wrote the manuscript. C.C., A.A., A.N., N.F., H.T. and K.N. performed experiments and analysed data. B.W. provided the clinical material, K.E.-A. analysed data and wrote the manuscript. C.S. conceived the study, was responsible for clinical material, analysed data and wrote the manuscript.

Additional Information

Supplementary information accompanies this paper at https://doi.org/10.1038/s41598-018-28634-0.

Competing Interests: The findings are subject of a patent application where the rights are held by SelectImmune Pharma AB; a company that currently is inactive where CS is part of the scientific advisory board. No commercial funding has been received for this study.

Publisher's note: Springer Nature remains neutral with regard to jurisdictional claims in published maps and institutional affiliations.